Microbial Implication of Iron Oxide Nanoparticles

by

Kimberly Freeland Starr

A thesis submitted to the Graduate Faculty of
Auburn University
in partial fulfillment of the
requirements for the Degree of
Master of Science

Auburn, Alabama
August 9, 2010

Keywords: Magnetite, Nanoparticles, Iron oxide

Approved by

Yucheng Feng, Chair, Associate Professor of Agronomy and Soils
Mark Liles, Assistant Professor of Biological Sciences
Navin Twarakavi, Assistant Professor of Agronomy and Soils
Dongye Zhao, Associate Professor of Civil Engineering

Abstract

Magnetite nanoparticles (Fe_3O_4) designed for remediation will be intentionally released into the environment; however, little is known regarding their impact on bacterial populations. Research was conducted to 1) investigate the effect of Fe_3O_4 nanoparticles on bacterial growth in culture media and 2) evaluate the effect of Fe_3O_4 nanoparticles on bacterial survival in natural stream water. The effect of commercial and lab-prepared Fe_3O_4 nanoparticles was examined through growth experiments and observation of cell-nanoparticle interactions. Fe_3O_4 nanoparticles at 0.3, 0.6, and 1.0 g Fe/L were not inhibitory to the four organisms tested. Scanning electron microscopy was performed on precipitates formed in *E. coli* culture to examine the cell-nanoparticle interactions. Nanoparticles covered cell surfaces, but no damage to cell integrity was observed. Stabilized magnetite nanoparticles at 0.01 g Fe/L did not affect bacterial survival in stream water. Bacterial growth indicated by [^{3}H]thymidine incorporation, however, decreased in the presence of nanoparticle suspensions. Growth inhibition was attributed to background electrolytes and nanoparticles themselves. Overall, magnetite nanoparticles did not affect bacteria in culture media or natural waters enough to indicate significant risk. Our results suggest that stabilized magnetite nanoparticles interact with bacterial surfaces without causing damage sufficient to inhibit cell growth.

Acknowledgments

The author would like to express her sincere gratitude to Dr. Yucheng Feng for her guidance and encouragement during the course of her studies. Thanks are also extended to the members of her committee: Dr. Mark Liles, Dr. Dongye Zhao and Dr. Navin Twarakavi for their valuable knowledge, suggestions, and assistance. The author would also like to thank Dr. Joey Shaw, Julie Arriaga, and Dr. John Gorden for XRD analysis, and Dr. Michael Miller for assistance with electron microscopy work. Thanks are also extended to Cancan Zhao and Qiqi Liang for help developing experimental protocols. Michele Owsley and Jessica Bankos are also acknowledged for their assistance with data collection and sample preparation. This research was supported by the Alabama Agricultural Experiment Station Hatch and Multistate Funding program.

Table of Contents

List of Tables

List of Figures

I. Literature Review

As nanotechnology makes a greater appearance in the field of environmental remediation, the widespread use of nanoparticles will result in their release into aquatic and soil systems. Nanoparticles can make their way into the environment through various pathways. The release of different forms of nanoparticles will undoubtedly lead to effects on various scales. On the smallest scale, microorganisms make up the base of the food chain and are responsible for many of the ecological processes we depend on such as the nitrogen cycle. Different classes of bacteria exhibit different susceptibilities to nanoparticles (16), but the mechanisms controlling this toxicity are not yet well understood. This is partly due to the fact that all nanoparticles are different and there is no all encompassing model to govern their interaction with bacteria. Many factors such as synthesis, size, shape, chemical composition, addition of a stabilizer, and the method of nanoparticle addition can lead to different conclusions for very closely related nanosuspensions (66). The media for microbial growth, light source, cell density, ionic strength, and reaction vessel are other variables that must be considered. Due to the growing synthesis and use of nanoparticles, it is essential to understand the interactions taking place once they are released into the environment.

A. Background

Nanotechnology is defined as research and technology development at the atomic, molecular, or macromolecular levels using a length scale of one to one hundred nanometers in any dimension as well as the creation and use of structures, devices and systems that have novel

properties and functions because of their small size (65). This new technology has the opportunity to make better materials and products. Many of these products are already available in markets worldwide ranging from coatings and computer components to cosmetics and medical devices (46). Nanotechnology has the potential to also improve the environment by detecting, preventing, and removing pollutants such as arsenic and chromium (5). However, there is no definitive understanding of the risks posed by the release of these nanomaterials into human and environmental systems. Enhanced properties that make nanoparticles unique include greater catalytic efficiency, electrical conductivity, and improved hardness and strength due to their small size. These same properties that make nanoparticles so reactive and efficient are also the properties that may lead to deleterious effects to eukaryotic and prokaryotic cells (3, 45). Since the developmental stage of nanotechnology is ending and the testing stage is beginning, we need to assess any potential risks to the environment before the use of nanoparticles becomes widespread. Nanoparticles can be deposited into the environment unintentionally from manufacturing processes and intentionally through application as a remediation tool (3, 46). Once in the environment, nanoparticles will undergo changes that can affect their interaction with living cells. Complexation, aggregation, and sedimentation are a few of the processes that can prevent these highly reactive particles from interacting with living cells. Biodegradation and bioaccumulation of nanoparticles are also important processes that will control bioavailability (65).

Transport of nanoparticles occurs mainly through Brownian motion while Van der Waals and double layer forces are responsible for their attachment (5, 21). To understand the potential toxicity of nanoparticles *in vivo*, we must first understand the transport into and through cells. Nanoparticles can be taken into cells due to their small size leading to accumulation, but

nanoparticles can also build up on cell surfaces, limiting nutrients and interactions with the cell's environment. Because microorganisms are the building blocks of the ecosystem as well as a measure of soil health, nanoparticle-bacterium interaction must be understood to ensure the addition of nanoparticles will not exceed the ecological capabilities of microorganisms (68). Unlike some eukaryotic cells that can take in nanoparticles up to 100 nm (46), bacterial cells can only take up nanoparticles around 5 nm (32, 44). Antibacterial activity might involve direct contact of nanoparticles with cellular surfaces, meaning that surface chemistry, morphology, and oxidative stress could be influential to toxicity. Oxidation reactions can damage the cells, leaving them vulnerable to osmotic stress and reduced nutrient uptake. Various methods have been used in bacterial toxicity assays and nanoparticle characterization. The advantages and disadvantages of each method are listed in the table below:

Table 1.1 Benefits and disadvantages of various measurement techniques in nanotechnology

Measurement technique	Advantage	Disadvantage
Cells counts	Measures intact cells, color of solution does not interfere	Does not measure damaged cells or weakened membranes
Transmission electron microscopy (TEM)	Accurate particle size, shows electron rich nanoparticles, good resolution	Can only show one dimension, samples must be dried down
Scanning electron microscopy (SEM)	Shows surfaces and nanoparticle-bacterium interaction	Lower resolution than TEM, samples are dried down and artifacts are common
Atomic force microscopy (AFM)	High resolution	Difficult to interpret results
Enzyme activity	Measures cell function, rapid and colorimetric	Not suitable for soils or samples with color or turbidity

B. Reasons for concern

Few data are available concerning the unforeseen consequences of the release of nanomaterials into the environment and their effect on microorganisms (31). One area of concern is the bioavailability and toxicity of nanoparticles to bacteria, which are important for normal

ecosystem functions (68). Biochemical processes such as carbon and nitrogen cycling may be influenced by the addition of nanomaterials. Both metal and carbon nanoparticles cause toxicity to planktonic bacteria (46) and carbon based nanomaterials are shown to damage lung tissue of mice (5). However, most studies assume that nanoparticles and bacterial surfaces will be in close contact, similar to artificial laboratory conditions. In nature, however, nanomaterials can be greatly diluted and interact with organic matter and soil surfaces that will reduce the chance of nanoparticle-bacterium interactions. Because every class of nanoparticles has different chemical and morphological properties, it is difficult to estimate a model to describe a general pattern of toxicity towards bacteria. Thus, many different mechanisms of damage have been proposed and tested.

a. Mechanisms of damage

The first and most apparent mechanism of toxicity important to bacteria is damage to membrane integrity. Silver nanoparticles have been shown to disrupt membranes (47). ZnO, MgO, CeO_2, and carbon nanotubes have all been shown to damage architecture of bacterial cells (44). Nanoparticle size can affect damage to cell membranes and membrane transport as well as influence metal ion toxicity. Since bacteria are usually 1to 2 microns, there is an upper limit to the size of particles that can cross their membranes. However, there is some discrepancy concerning the size limit of nanoparticles that can enter cells (31). The smaller the nanoparticle, the more likely it can interact with and block membrane function. However, smaller nanoparticles are more reactive, and more likely to form aggregates. Once aggregated, the effective particle size is increased and this cluster cannot cross the membrane. Studies of the effect of antibacterial properties of silver nanoparticles on *E. coli* show that smaller nanoparticles

are more damaging than larger nanoparticles (38). Size alone is not the only variable. As size changes, the reactivity also changes which can be an unforeseen mechanism for toxicity. Nanoparticles may damage cell membranes through reactive oxygen species i.e., superoxide and hydroxyl radicals (44) or direct cell damage (25, 60).

In addition to nanoparticles, dissolved metal ions (i.e. iron) can enhance toxicity (34). Free ions can also facilitate cell wall damage, allowing nanoparticles access inside cells where they could not previously enter (44). For example, silver nanoparticles interact with cell membranes and subsequently release ions, which have an additional contribution to toxicity (42). Another study found that silver nanoparticles were more toxic than silver ions for *E. coli* (38).

Nanoparticles producing ROS (45) can lead to DNA, protein, and membrane damage (7), and nanoparticles have already demonstrated toxicity to bacteria and protozoa according to ecotoxicological studies (46). The toxicity of iron nanoparticles results from ROS production (5). Cell and nanoparticle interaction is an important factor for toxicity, determined by surface chemistry and reactivity (41). For metal oxide nanoparticles (i.e., ZnO, TiO_2, and Ag_2O), it is generally accepted that reactive oxygen species (ROS) (1, 20) and direct rupture of cell membranes can cause toxic effects on microorganisms (1, 29, 60, 73). Iron nanoparticles can also undergo Fenton-type reactions leading to the production of •OH radicals (5). In eukaryotic cells, lipid oxidation due to superoxide (O_2^-) and hydroxyl (•OH) radicals are mechanisms of damage (44). For silver nanoparticles, only individual particles (1 to10 nm), not aggregates, can attach to *E. coli* cell membranes and disturb respiration and membrane permeability (42). A study in 2009 showed carboxymethyl cellulose (CMC) coated nanoparticles grew into microparticles after cellulase degraded the CMC layer to glucose (48), which will ultimately limit their interaction with bacteria. Related inorganic nanoparticles such as ZnO can be internalized by bacteria (6)

and CeO_2 nanoparticles are adsorbed onto the *E. coli* cell wall (63). Nanoparticle shape also affects toxicity. Silver nanoparticles undergo a shape dependent interaction with *E. coli* based on active facets (47).

For one study, a higher concentration of gold nanoparticles was needed to rupture *E. coli* compared to red blood cells, suggesting bacteria are more resistant to nanoparticle toxicity compared to other cells. Protection was possibly provided by the cell wall (19). It was also demonstrated that gold nanoparticle toxicity is related to cell membrane interaction, and it is possible to ameliorate toxicity with nanoparticle surface modification (19). Another study found that silver nanoparticles disrupt important membrane activities and caused damage rather than cell death (47). Zn (6), Ag (60), Mg (61), Ce (63), and single-walled carbon nanotubes (25) have all shown damage to membrane stability.

Cell membranes can be compromised through physical battering as well as damage resulting from reactive oxygen species (ROS). Superoxide and hydroxyl radicals are two ROS that have been documented to cause cell damage (39). ROS can oxidize double bonds in phospholipids leading to increased membrane fluidity, which leaves cells more susceptible to osmotic stress. ROS can also damage iron-sulfur clusters that function as cofactors in enzymes (31). When superoxide dismutase (an enzyme for removing superoxide radicals) was added to silver nanoparticle suspensions, damage to *E. coli* membranes was reduced, supporting that ROS damage was responsible for damage (10). Metal ions released into the aqueous phase work in conjunction with ROS. For silver nanoparticles, only the oxidized form of silver is toxic to cells and reduced silver ions do not show toxicity to *E. coli* (38).

An important factor in ROS toxicity is the proximity between bacteria and nanoparticles. Charged groups on the particle surface and adsorption of ions can alter the charge on a

nanoparticle surface. Bacterial cell surfaces typically possess a negative charge. Nanoparticle charges can also be altered by the addition of a charged stabilizer or capping agent. We assume that positively charged nanoparticles will experience the greatest attraction to negatively charged bacterial surfaces. Biofilms stripped of extracellular polymeric substances (EPS), directly exposed to nanoparticles, were susceptible to membrane damage, while biofilms that produce extracellular materials were less susceptible (37, 44). Extracellular materials or polymers can either absorb ROS or prevent nanoparticles from coming into contact with bacterial surfaces (44).

Transport of nanoparticles across cell membranes can also cause damage in bacterial cells. Mg and Zn nanoparticles have been found inside damaged cells, suggesting they were transported across the cell membrane (61). Quantum dots smaller than 5 nm and silver nanoparticles smaller than 80 nm have been found inside bacterial cells (31). However it is difficult to discern whether nanoparticles were transported across healthy cell membranes or whether cells underwent damage and the nanoparticles made their way inside the cells through simple diffusion. Only the smallest nanoparticles (1 to 9 nm) would be able to be transported across cell membranes through various pores including protein-secreting pores (44). Pores are typically closed in everyday functions so nanoparticles could only migrate while the pores are open. It is unlikely that nanoparticles can cross into the cytoplasm until the membranes are damaged.

b. Oxidative damage and repair/defense mechanisms

Oxidative stress is unavoidable in an oxygen atmosphere. Reactive oxygen species (ROS) are generated as by-products of aerobic metabolism and through exposure to toxins (13).

Oxidative stress occurs when the concentration of ROS exceeds the cell's defenses (9, 40). Cells have multiple antioxidant defenses and repair mechanisms (13). The targets for oxygen species are DNA, RNA, proteins, and lipids. Modification of cellular components can lead to altered cell function and cell death (9). Lipids are a major target, and free radicals attack polyunsaturated fatty acids causing lipid peroxidation. The result is decreased membrane fluidity. Polyunsaturated fatty acids can also degrade into aldehydes and cause protein damage (9). Oxidation of proteins yields disulfide bonds, modification of metal clusters, and linkage or fragmentation of proteins (9, 13). In DNA, ROS attack the base and sugar causing strand breakage and cross-links of DNA to other molecules (9). UV light can also cause DNA damage including formation of pyrimidine dimers; however, this damage can be corrected through enzymatic repair. Photoreactivation splits the dimers in dark conditions, excision repair corrects damage using endonuclease II incision and repair via polymerase I, and postreplication repair connects daughter-strand segments providing continuity for replication (70).

Ferrous iron is required for growth of almost all living cells. Iron reacts in the Fenton reaction to produce •OH radicals (9, 15). Iron is controlled at the cell entrance by membrane-bound receptors and inside the cell by bacterioferritin and ferritin due to its potential for cell damage (9). In addition, superoxide dismutase (SOD) converts O_2^- to H_2O_2. Resulting hydrogen peroxide is broken down by catalase into molecular oxygen and water (40).

Repair of DNA damage (base modification, protein cross-links, and strand breakage) is possible through endonuclease IV (15), induced by oxidative stress, as well as exonuclease II, which is induced in stationary starving cells (9). Protein damage is corrected by hydrolysis by proteases (9) or catalysts that repair modified proteins. Finally, damaged lipids are corrected by peroxidases which decompose lipid peroxides and lipases which hydrolyze damaged lipids (13,

40). Even though nanoparticles containing iron can release ferrous iron to produce ROS, causing damage to membrane lipids, proteins, and DNA, cells naturally contain mechanisms to prevent or repair damage. Damage induced by nanoparticles differs with the properties of each nanoparticle.

c. Metal and carbon nanoparticles

Metal nanoparticles are of interest in bacterial toxicity because their dissolved ion forms show antibiotic properties. Iron particles are used for a variety of applications in the medical and environmental fields. Zero-valent iron is used in groundwater decontamination and magnetite nanoparticles are used in biomedicine and water treatment (68). Titanium dioxide, silicon dioxide and zinc oxide nanoparticles are common in paints, electronics, and semiconductors (1). Silver nanoparticles are used as antimicrobial agents in clothing and bandages. Carbon nanoparticles are used in many applications from cosmetics to electronics (4). These nanoparticles make their way into the environment through direct injection in the case of environmental cleanup or through disposal of nanoparticle-containing products when used by consumers. Carbon nanotubes are used in optical and energy storage devices. Carbon nanotubes have been proposed to cause damage to mammalian cells through oxidative stress, metal toxicity, and physical piercing (5). Carbon nanotubes also result in free radical formation, antioxidant depletion, accumulation of peroxidative products, and loss of cell viability in rodent epithelial cells (5). However, one study showed that carbon nanotubes exhibit strong antimicrobial activity to *E. coli* through direct cell/nanoparticle contact, resulting in outer membrane damage and release of cellular contents (25).

C. Toxicity studies involving pure cultures of bacteria

a. Titanium dioxide, silicon dioxide, and zinc oxide

Reports of different studies often give conflicting results due to the purity of nanoparticles used, bacterial strain and age, stabilizer differences, and the condition in which cells are exposed to nanoparticles. Titanium nanoparticles are reported to be toxic to both Gram-positive and Gram-negative bacteria, with *Bacillus* being less susceptible than *E. coli* due to spore formation (52). However, other studies have found Gram-positive bacteria to be more susceptible than Gram-negative bacteria (16). Zinc oxide is reported to be more toxic to Gram-positive *Bacillus* than Gram-negative *E. coli* (55). It is documented that these three nanomaterials produce ROS in the presence of UV light (72).

In a study comparing the toxic effects of these three types of commercial nanoparticles, toxicity increased with increasing nanoparticle concentration. Antibacterial activity increased from silicon, to titanium, to zinc. *B. subtilis* was more affected than *E. coli.* They also observed that the advertised particle size by the manufacturer did not equal actual particle size. When comparing small, medium, and large nanoparticles there was no difference in toxicity due to the fact that all particles formed aggregates about the same size. The presence of UV light increased toxicity under most conditions tested, but there was also toxicity observed under dark conditions (1).

Another study investigated the effect of particle size, concentration, and the use of dispersants on the antibacterial behavior of ZnO nanofluids on *E. coli*. The results showed the addition of zinc oxide nanoparticles caused damage to *E. coli* cell walls. Cells appeared shriveled and the membrane was compromised. Particle concentration was more important than particle

size since aggregation changes rapidly. Direct contact as well as ROS were suggested as mechanisms of cell damage (73).

b. Silver

It is well known that silver ions and silver compounds are very toxic to microorganisms (44, 59, 60). The goal of one study using silver nanoparticles was to study the interaction between bacteria and nanoparticles using scanning electron microscopy (SEM) and transmission electron microscopy (TEM). Silver nanoparticles were synthesized and excess silver ions were removed to eliminate ion toxicity. *E. coli* were grown in liquid media with nanoparticles and on agar plates supplemented with nanoparticles. In liquid media, increasing concentration of nanoparticles caused a decrease in cell growth. On agar plates, nanoparticle addition caused a growth delay proportional to concentration. SEM of bacteria exposed to nanosilver showed significant damage compared to the control. Smaller nanoparticles displayed more antimicrobial activity than larger nanoparticles (44). Pits were formed in the cell walls and chemical analysis showed that nanoparticles were incorporated into the membrane of treated cells. TEM images confirmed the presence of silver nanoparticles in the membrane as well as leaking intracellular contents and coagulation of particles on the bacterial surface (60).

c. Magnesium oxide

A study of magnesium oxide nanoparticles and their halogen adducts demonstrated biocidal activity towards *Bacillus* species, *E. coli*, as well as spores (61). Spores are more resistant to environmental stress due to their structure but they were still affected by nanoparticles. These magnesium oxide nanoparticles carry a high amount of active halogens making them toxic. Zeta potential measurements showed the positive charge carried by these

particles enhanced the interaction with negatively charged bacterial cells and spores. Confocal microscopy was used to show direct contact between bacteria and halogenated MgO particles. Atomic force microscopy (AFM) and TEM studies demonstrated the influence of nanoparticles on microorganisms and their membranes. AFM showed the cell envelope was significantly damaged and less smooth after 20 minutes of nanoparticle exposure. Formation of holes was the primary mechanism of damage to spores. TEM images displayed aggregates consisting of spores, bacteria, and nanoparticles. Both strains of bacteria formed large clumps that upon closer inspection consist of nanoparticles and bacteria. Nanoparticles were speculated to be the reason behind coagulation since bacteria were single cells in culture and nanoparticles were found inside aggregates. Electrostatic attraction, supported by zeta potential measurements, is the expected reason for mutual coagulation (61).

d. Iron oxide

Iron nanoparticles are considered to be less toxic than silver or gold nanoparticles. Their wide use in environmental applications makes them an ideal nanoparticle for in-depth research. In a recent study, the relationship between the redox state and toxicity of iron nanoparticles was examined. Zero-valent iron (ZVI), magnetite, and maghemite were used to study their toxicity to *E. coli* as well as a mutant strain of *E. coli* devoid of superoxide dismutase activity. In the wild type, toxicity increased with concentration for ZVI and magnetite, while maghemite showed no toxicity. Higher toxicity was observed in the mutant *E. coli*, suggesting superoxide dismutase helped decrease the effect of iron nanoparticles. The supernatant was also tested to ensure that toxicity was due to nanoparticles and not residue from synthesis. TEM showed a layer of nanoparticles adsorbed to the surface of cells. Cellular internalization was not seen. The structure

of maghemite was altered after incubation with *E. coli* from spherical to lamellar, while ZVI and magnetite did not change structure. It was concluded that concentration affected *E. coli* cell death, with ROS being the predominant mechanism (2). Iron nanoparticles generate hydroxyl radicals which are damaging to biological systems through the Fenton reaction (5). Several studies have evaluated the toxicity of iron oxide nanoparticles to eukaryotic cells. Although dextran-coated Fe_3O_4 has minimal *in vivo* toxicity in rats and humans (57), magnetite exhibits low neurotoxicity to rodent N27 neurons compared to ZVI due to its low "redox" activity (50) and causes a decrease in mitochondrial function in BRL2A rat liver cells (24). Maghemite (Fe_2O_3), which is considered less redox reactive than Fe_3O_4, has the highest toxicity to human mesothelioma cells among the seven nanoparticles tested (8). So far there are only a few published studies on cytotoxicity of Fe_3O_4 to bacteria.

D. Toxicity studies involving mixed cultures of bacteria

The easiest way to measure the toxicity of nanoparticles to bacteria is through pure culture conditions. Using a single well-studied organism provides known metabolic activity and well documented growth patterns. However, the environment is comprised of numerous species of bacteria, each filling a difference niche. Different bacterial species are not isolated. Species interact and often one species depends on the products produced by another species. If one member of this community is eliminated by the addition of nanoparticles, the effects could be compounded through the remaining members. Once released into soil, there will be breakdown, alteration, and aggregation of nanoparticles due to chemical changes (66). In the case of soil, a heterogeneous medium, there are aerobic as well as anaerobic microsites. Due to the heterogeneity of soil, the addition of nanoparticles will affect different spatial groups of bacteria

differently. Assuming that nanoparticles could access each community of bacteria equally, there are main differences between classes of bacteria with different susceptibility. Gram-positive bacteria have a thick cell wall that could be impenetrable to nanoparticles. Gram-negative bacteria have a thin cell wall but their lipopolysaccharide outer membrane may increase or reduce interaction with nanoparticles. A community-wide approach to assay the effects nanoparticles have on a microbial community is more representative of real world conditions than pure culture studies. However, community-wide tests can be difficult to interpret because of the high number of species present. Therefore it is important to employ several community assays to reach consistent conclusions.

Based on the suggested antibacterial activities of fullerene, one study investigated the effects of carbon nanoparticles on an aerobic bacterial community. Commercial fullerene was shown to have little effect on the structure or function of a soil microbial community. Total soil phospholipids were used to define the effects of fullerenes on the size of microbial biomass. Enzymatic activities were also measured as an indicator of microbial functions. The results of this study did not find any toxicity of fullerene nanoparticles. The proportion of Gram-negative bacteria was slightly higher than Gram-positive. DGGE analysis indicates that the introduction of nanomaterials had little effect on community structure. Their conclusions support the hypothesis that bioavailability of nanoparticles is one of the most important factors affecting bacterial toxicity. Nonetheless, the slight difference in numbers of Gram-positive and negative organisms suggests different mechanisms act on different classes of microbes (64). In eukaryotic cells, soluble fullerene formed superoxide anions responsible for membrane damage (56). Hydroxylated fullerols showed no toxicity to bacteria in the same study comparing solvents (56).

Due to the vast number of nanoparticles and different organisms they can interact with, there are still many gaps in our knowledge regarding nanotechnology's impact on biological organisms. Conflicting reports are a common occurrence due to the sheer number of nanoparticles and the number of ways to synthesize them. The method of synthesis alone can change the toxicity of nanoparticles, and there is no standard method for measuring toxicity. Several properties used to predict and understand toxicity include: particle identity (silver is usually considered antibacterial), particles size (only small particles can cross cell membranes while large aggregates cannot interact with bacteria surfaces), and particle charge (positively charged nanoparticles interact with negatively charged bacterial cells, while a stabilizer can prevent this attraction) (44, 66). While TEM and SEM are very powerful tools that allow us to examine nanoparticles in close contact with bacterial surfaces, there remains the problem of artifacts. Ideally, cells in liquid culture represent the closest analogue to nature. By drying down samples on grids or stubs, interactions can be seen that does not happen in liquid conditions. Drying down cells can also lead to nanoparticles covering bacteria that were not there prior. Cell counts can also be misleading especially if bacteria and nanoparticles attach to each other in liquid media. During dilution, very small aggregates of bacteria and nanoparticles can lead to higher cell counts than actually present. It is also not known why in some cases *E. coli* is affected more than *B. subtitis* and why sometimes the opposite is reported. Molecular approaches might offer some insight and provide a more robust method of measuring toxicity by eliminating many of the variables in growth experiments. A more consistent litany of tests should be suggested to measure toxicity.

E. Environmental conditions

In natural environments organic matter can coat nanoparticles (46) resulting in altered chemical properties. One type of iron nanoparticle, NZVI, was shown to be efficiently coated with humic acids altering aggregation patterns (17). Organic matter or stabilizer prevented adhesion between *E. coli* and ZVI, and lowered toxicity (36). Since changes in surface modification brought about by changes in environmental conditions such as light, pH, and ionic strength have not been studied thoroughly (46), it is difficult to predict the effect stabilized nanoparticles will have in a natural setting. Materials such as nanoparticles and their stabilizers undergo significant degradation, transformation, and aggregation in water (11), and association with natural colloids and salinity (41) could affect their bioavailability. Glucose, resulting from degradation of CMC and starch can be assimilated by microbes (48), which demonstrates the biocompatibility of these stabilizers.

As previously mentioned, aggregation of nanoparticles will limit mobility. Surface modification due to exposure to UV light or changing ionic strength can reduce the double layer surrounding nanoparticles, causing particles to bind together. The likelihood of bacteria coming into contact with a free unreacted nanoparticle is low in the environment. By the time nanoparticles come into contact with microbes, they could already be unreactive due to dissolution, reduction, or oxidation (3). Also, many studies are performed with high cell densities in well mixed systems, forcing interaction between cells and nanoparticles. In actuality, biofilms predominate in aqueous environments where only the surface layer of cells is free to interact with nanoparticles (49).

F. Magnetite

Magnetite (Fe_3O_4) is an iron oxide with a wide range of uses including magnetic resonance imaging, biomedicine, biosensors, immunoassays, and remediation due to its magnetic and optical properties (28, 58, 67). Magnetite has proven successful in removal of contaminants such as As (71), Cr (23), and Pb (12). Fe_3O_4 has an affinity for heavy metals and can adsorb Pb (II) and As (V) (12) while Fe^{2+} ions can act to reduce contaminants (Cr^{6+}) as well (67). Magnetite has a point of zero charge (PZC) ranging from 6 to 8 and can be oxidized to form other iron oxides. Magnetite has a cubic inverse spinel structure with Fe^{3+} occupying the octahedral and tetrahedral sites and Fe^{2+} occupying the octahedral sites (58, 62). A table listing physical and chemical properties of magnetite is provided below:

Table 1.2 Characteristics of magnetite

Physical characteristic	Chemical characteristic
Grayish black color	$Fe^{3+}{}_2Fe^{2+}O_4$
Density: 5.15 g/cm^3	Molecular Weight: 231.54 g/mol
Non fluorescent	72.36 % Iron

Magnetite is generally synthesized from three main procedures 1) coprecipitation of Fe^{2+}/Fe^{3+} in the presence of base (21), 2) thermal decomposition of an iron complex, and 3) a sonochemical approach. Chemical precipitation is the most popular approach which provides good control over yield, size, and morphology of nanoparticles (67). However, the large surface area of magnetite nanoparticles causes them to form large aggregates due to attractive forces. To overcome these forces (21), a polymer stabilizer can be used such as dextran (57), starch (28), or CMC (58). A polymer layer also prevents oxidation, affecting phase transformation (27). It has

also been shown that encapsulation of magnetite nanoparticles can alter surface reactivity and create a diffusion barrier (48). CMC has proven to be an effective stabilizer for ZVI nanoparticles, reducing particle size and increasing TCE degradation in a sandy soil (22), and starch has been used to stabilize magnetite nanoparticles for *in vivo* studies (27). This functionalization of magnetite nanoparticles has also been suggested to influence interactions with cellular membranes (33). Functionalization with an appropriate stabilizer has been shown to reduce toxicity in previous studies (36). In one study, gold nanoparticles coated with positively charged surface modifier were more toxic than those coated with negatively charged modifier (19), demonstrating the impact of electrostatic repulsion between negative charges of coated nanoparticles and bacteria. Lee et al. found no toxicity of Fe_3O_4 (9 mg/L) towards *E. coli* ATCC strain 8739 after 1 hour in a carbonate buffer (pH 8) (34). Oxidation state was correlated to toxicity in one study, with ZVI (Fe (0)) being more toxic than magnetite (Fe (III)/(II)), which is more toxic than maghemite (all Fe (III)). As ZVI ages, the magnetite shell grows thicker. Aged ZVI, which contains magnetite, was shown benign to bacteria (36). Since magnetite is less toxic than ZVI, perhaps ZVI toxicity can be considered the worst case scenario for magnetite.

G. Surface modifiers

Stabilizing agents such as CMC, starch, or dextran prevent particle coalescence during formation. Stabilizers are used often to produce small particle size and narrow particle size distribution. CMC is a carbohydrate consisting of glucose units which can be modified by replacing functional groups (35). Like starch, CMC is low-cost and environmentally friendly, whereas some organic stabilizers can cause harmful effects. Using a ‘green’ stabilizer will help

reduce the potential for toxicity (18, 22). Surface modification of ZVI nanoparticles appears to decrease toxicity to mammalian and prokaryotic cells (36, 50).

CMC, as the general case with natural polymers, is easily broken down in the environment. Carboxymethyl cellulose is broken down by cellulase enzymes. These enzymes are produced by bacteria as well as other microorganisms (69). The glycosidic bond can also be cleaved abiotically (14). The glucose units are cleaved before the side chains and glucose can be monitored to measure degradation (53). Lower degree of substitution results in more conversion to glucose compared to high degree of substitution (51). Endoglucanases cut the long cellulose chains at random points, exoglucanases cleave glucose or cellobiose units off the cellulose chains, and β-glucosidase converts cellobiose into glucose monomers (54). To determine the degradation of CMC, decline in viscosity can be measured as the polymer breaks down over time (35). UV absorbance can also be monitored to observe the CMC peak shift as the polymer is degraded (53). The presence of UV light can also increase the degradation of CMC which will be important under field conditions (51). CMC acts to keep particle size small and particles active. As CMC degrades, it is unknown how this will affect stabilized nanoparticle size, aggregation events, and particle reactivity. Enhanced degradation may prove potentially harmful if CMC or starch offers any protective action to keep bacteria and nanoparticles from interacting. Starch is structurally similar to CMC, meaning binding and toxicity are likely comparable as well. However due to the difference in charge, starch stabilizes nanoparticles slightly differently. Nonetheless, starch has been used successfully to stabilize magnetite nanoparticles for applications including hyperthermic thermoseed and magnetic resonance imaging (26, 27).

Polymers and polysaccharides play an important role as thickening agents. Polysaccharides have been demonstrated to play a role in free-radical scavenging for the

prevention of oxidative damage. Research shows that polysaccharides are able to absorb ROS and protect membranes from damage (44). CMC shows slight inhibitory effect on linoleic acid oxidation which increases with concentration and viscosity. Radical scavenging ability increased from pH 3 to7 with a maximum scavenging effect of 70% (30). As previously mentioned, CMC could act as a secreted polymer to prevent nanoparticle-bacterium interaction due to its negative charge, its steric hindrance, or its antioxidant properties (43). CMC and starch have been successfully used to control particle size of magnetite nanoparticles by changing the polymer concentration (58).

References

1. **Adams, L. K., D. Y. Lyon, and P. J. J. Alvarez.** 2006. Comparative eco-toxicity of nanoscale TiO_2, SiO_2, and ZnO water suspensions. Water Res. **40:**3527-3532.
2. **Auffan, M., W. Achouak, J. Rose, M.-A. Roncato, C. Chaneac, D. T. Waite, A. Masion, J. C. Woicik, M. R. Wiesner, and J.-Y. Bottero.** 2008. Relation between the redox state of iron-based nanoparticles and their cytotoxicity toward *Escherichia coli*. Environ. Sci. Technol. **42:**6730-6735.
3. **Auffan, M., J. Rose, J.-Y. Bottero, G. V. Lowry, J.-P. Jolivet, and M. R. Wiesner.** 2009. Towards a definition of inorganic nanoparticles from an environmental, health and safety perspective. Nat. Nanotechnol. **4:**634-641.
4. **Baughman, R. H., A. A. Zakhidov, and W. A. de Heer.** 2002. Carbon nanotubes-the route toward applications. Sci. **297:**787-792.
5. **Biswas, P., and C.-Y. Wu.** 2005. Nanoparticles and the environment. J. Air Waste Manage. **55:**708-746.
6. **Brayner, R., R. Ferrari-Iliou, N. Brivois, S. Djediat, M. F. Benedetti, and F. Fievet.** 2006. Toxicological impact studies based on *Escherichia coli* bacteria in ultrafine ZnO nanoparticles colloidal medium. Nano. Letters **6:**866-870.
7. **Brunet, L., D. Y. Lyon, E. M. Hotze, P. J. J. Alvarez, and M. R. Wiesner.** 2009. Comparative photoactivity and antibacterial properties of C_{60} fullerenes and titanium dioxide nanoparticles. Environ. Sci. Technol. **43:**4355-4360.
8. **Brunner, T. J., P. Wick, P. Manser, P. Spohn, R. N. Grass, L. K. Limbach, A. Bruinink, and W. J. Stark.** 2006. *In vitro* cytotoxicity of oxide nanoparticles:

Comparison to asbestos, silica, and the effect of particle solubility. Environ. Sci. Technol. **40:**4374-4381

9. **Cabiscol, E., J. Tamarit, and J. Ros.** 1999. Oxidative stress in bacteria and protein damage by reactive oxygen species. Int. Microbiol. **3:**3-8.

10. **Chang, Q., L. Yan, M. Chen, H. He, and J. Qu.** 2007. Bactericidal mechanism of Ag/Al_2O_3 against *Escherichia coli*. Langmuir **23:**11197–11199.

11. **Colvin, V. L.** 2003. The potential environmental impact of engineered nanomaterials. Nat. Biotech. **21:**1166-1170.

12. **D' Couto, H.** 2008. Development of a low-cost sustainable water filter: A study of the removal of water pollutants As (V) and Pb (II) using magnetite nanoparticles. J. US SJWP**:**32-45.

13. **Davies, K. J. A.** 2001. Oxidative stress, antioxidant defenses, and damage removal, repair, and replacement systems. IUBMB Life **50:**279 - 289.

14. **Eriksson, K.-E., and B. H. Hollmark.** 1969. Kinetic studies of the action of cellulase upon sodium carboxymethyl cellulose. Arch. Biochem. Biophys. **133:**233-237.

15. **Farr, S. B., and T. Kogoma.** 1991. Oxidative stress responses in *Escherichia coli* and *Salmonella typhimurium*. Microbiol. Mol. Biol. Rev. **55:**561-585.

16. **Fu, G., P. S. Vary, and C.-T. Lin.** 2005. Anatase TiO_2 nanocomposites for antimicrobial coatings. J. Phys. Chem. B **109:**8889–8898.

17. **Giasuddin, A. B. M., S. R. Kanel, and H. Choi.** 2007. Adsorption of humic acid onto nanoscale zerovalent iron and its effect on arsenic removal. Environ. Sci. Technol. **41:**2022-2027.

18. **Ginkel, C. G. v., and S. Gayton.** 1996. The biodegradability and nontoxicity of carboxymethyl cellulose (DS 0.7) and intermediates. Environ.Tox. Chem. **15:**270-274.

19. **Goodman, C. M., C. D. McCusker, T. Yilmaz, and V. M. Rotello.** 2004. Toxicity of gold nanoparticles functionalized with cationic and anionic side chains. Bioconjugate Chem. **15:**897-900.

20. **Grootveld, M., and C. J. Rhodes.** 1995. Methods for the detection and measurement of reactive radical species *in vivo* and *in vitro*. Academic Press Limited, London.

21. **Gupta, A. K., and M. Gupta.** 2005. Synthesis and surface engineering of iron oxide nanoparticles for biomedical applications. Biomaterials **26:**3995-4021.

22. **He, F., D. Zhao, J. Liu, and C. B. Roberts.** 2007. Stabilization of Fe-Pd nanoparticles with sodium carboxymethyl cellulose for enhanced transport and dechlorination of trichloroethylene in soil and groundwater. Ind. Eng. Chem. Res. **46:**29-34.

23. **Hu, J., I. Lo, and G. Chen.** 2004. Removal of Cr (VI) by magnetite nanoparticle. Water Sci. Technol. **50:**139-46.

24. **Hussain, S. M., K. L. Hess, J. M. Gearhart, K. T. Geiss, and J. J. Schlager.** 2005. *In vitro* toxicity of nanoparticles in BRL 3A rat liver cells. Toxicol. in Vitro **19:**975-983.

25. **Kang, S., M. Pinault, L. D. Pfefferle, and M. Elimelech.** 2007. Single-walled carbon nanotubes exhibit strong antimicrobial activity. Langmuir **23:**8670-8673.

26. **Kim, D.-H., K.-N. Kim, K.-M. Kim, and Y.-K. Lee.** 2009. Targeting to carcinoma cells with chitosan- and starch-coated magnetic nanoparticles for magnetic hyperthermia. J. Biomed. Mater. Res. A. **88A:**1-11.

27. **Kim, D. K., M. Mikhaylova, F. H. Wang, J. Kehr, B. Bjelke, Y. Zhang, T. Tsakalakos, and M. Muhammed.** 2003. Starch-coated superparamagnetic nanoparticles as MRI contrast agents. Chem. Mater. **15:**4343-4351.

28. **Kim, D. K., M. Mikhaylova, Y. Zhang, and M. Muhammed.** 2003. Protective coating of superparamagnetic iron oxide nanoparticles. Chem. mater. **15:**1617-1627.

29. **Kim, J. S., E. Kuk, K. N. Yu, J.-H. Kim, S. J. Park, H. J. Lee, S. H. Kim, Y. K. Park, Y. H. Park, C.-Y. Hwang, Y.-K. Kim, Y.-S. Lee, D. H. Jeong, and M.-H. Cho.** 2007. Antimicrobial effects of silver nanoparticles. Nanomed-nanotechnol. **3:**95-101.

30. **Kishk, Y. F. M., and H. M. A. Al-Sayed.** 2007. Free-radical scavenging and antioxidative activities of some polysaccharides in emulsions. Food Sci. Technol.-LEB **40:**270-277.

31. **Klaine, S. J., P. J. J. Alvarez, G. E. Batley, T. F. Fernandes, R. D. Handy, D. Y. Lyon, S. Mahendra, M. J. McLaughlin, and J. R. Lead.** 2008. Nanomaterials in the environment: Behavior, fate, bioavailability, and effects. Environ. Toxi. Chem. **27:**1825-1851.

32. **Kloepfer, J., R. Mielke, and J. Nadeau.** 2005. Uptake of CdSe and CdSe/ZnS quantum dots into bacteria via purine-dependent mechanisms. Appl. Environ. Microbiol. **71:**2548-2557.

33. **Koh, I., B. H. Cipriano, S. H. Ehrman, D. N. Williams, and T. R. Pulliam Holoman.** 2005. X-ray scattering study of the interactions between magnetic nanoparticles and living cell membranes. J. Appl. Phys. **97:**084310.

34. **Lee, C., J. Y. Kim, W. I. Lee, K. L. Nelson, J. Yoon, and D. L. Sedlak.** 2008. Bactericidal effect of zero-valent iron nanoparticles on *Escherichia coli*. Environ. Sci. Technol. **42:**4927-4933.

35. **Levinson, H. S., and E. T. Reese.** 1950. Enzymatic hydrolysis of soluble cellulose derivatives as measured by changes in viscosity. J. Gen. Physiol. **33:**601-628.

36. **Li, Z., K. Greden, P. J. J. Alvarez, K. B. Gregory, and G. V. Lowry.** 2010. Adsorbed polymer and NOM limits adhesion and toxicity of nano scale zerovalent iron to *E. coli*. Environ. Sci. Technol.**:**DOI:10.1021/es9031198.

37. **Liu, Y., J. Li, X. Qiu, and C. Burda.** 2007. Bactericidal activity of nitrogen-doped metal oxide nanocatalysts and the influence of bacterial extracellular polymeric substances. J. Photochem. Photobiol. A. Chem. **190:**94-100.

38. **Lok, C.-N., C.-M. Ho, R. Chen, Q.-Y. He, W.-Y. Yu, H. Sun, P. K.-H. Tam, J.-F. Chiu, and C.-M. Che.** 2006. Proteomic analysis of the mode of antibacterial action of silver nanoparticles. J. Proteome Res. **5:**916-924.

39. **Lovrić, J., S. Cho, F. Winnik, and D. Maysinger.** 2005. Unmodified cadmium telluride quantum dots induce reactive oxygen species formation leading to multiple organelle damage and cell death. Chem. Biol. **12:**1227-34.

40. **Lushchak, V. I.** 2001. Oxidative stress and mechanisms of protection against it in bacteria. Biochemistry Moscow **66:**476-489.

41. **Moore, M. N.** 2006. Do nanoparticles present ecotoxicological risks for the health of the aquatic environment? Environ. Int. **32:**967-976.

42. **Morones, J. R., J. L. Elechiguerra, A. Camacho, K. Holt, J. B. Kouri, J. T. Ramírez, and M. J. Yacaman.** 2005. The bactericidal effect of silver nanoparticles. Nanotechnol. **16:**2346-2353.

43. **Moseley, R., M. Walker, R. J. Waddington, and W. Y. J. Chen.** 2003. Comparison of the antioxidant properties of wound dressing materials-carboxymethylcellulose, hyaluronan benzyl ester and hyaluronan, towards polymorphonuclear leukocyte-derived reactive oxygen species. Biomaterials. **24:**1549-1557.

44. **Neal, A.** 2008. What can be inferred from bacterium–nanoparticle interactions about the potential consequences of environmental exposure to nanoparticles? Ecotoxicol. **17:**362-371.

45. **Nel, A., T. Xia, L. Madler, and N. Li.** 2006. Toxic potential of materials at the nanolevel. Sci. **311:**622-627.

46. **Nowack, B., and T. D. Bucheli.** 2007. Occurrence, behavior and effects of nanoparticles in the environment. Environ. Pollut. **150:**5-22.

47. **Pal, S., Y. K. Tak, and J. M. Song.** 2007. Does the antibacterial activity of silver nanoparticles depend on the shape of the nanoparticle? A study of the gram-negative bacterium *Escherichia coli*. Appl. Environ. Microbiol. **73:**1712-1720.

48. **Pan, G., L. Li, D. Zhao, and H. Chen.** 2009. Immobilization of non-point phosphorus using stabilized magnetite nanoparticles with enhanced transportability and reactivity in soils. Environ. Pollut. **1:**1-6.

49. **Pedersen, K.** 2001. Diversity and activity of microorganisms in deep igneous rock aquifers of the Fennoscandian shield. *In* J. Fredrickson and M. Fletcher (ed.), Subsurface Microbiology and Geochemistry. Wiley-Liss Inc., New York.

50. **Phenrat, T., T. C. Long, G. V. Lowry, and B. Veronesi.** 2009. Partial oxidation ("aging") and surface modification decrease the toxicity of nanosized zerovalent iron. Environ. Sci. Technol. **43:**195-200.

51. **Reese, E. T., R. Siu, and H. Levinson.** 1950. The biological degradation of soluble cellulose derivatives and its relationship to the mechanism of cellulose hydrolysis. J. Bacteriol. **59:**485-497.

52. **Rincon, A. G., and C. Pulgarin.** 2005. Use of coaxial photocatalytic reactor (CAPHORE) in the TiO_2 photo-assisted treatment of mixed *Escherichia coli* and *Bacillus subtilis* and the bacterial community present in wastewater. Catal. Today **101:**331–344.

53. **Saita, T.** 1983. Degradation of sodium-polymethacrylate and sodium carboxymethyl cellulose in dilute aqueous solution. Jpn. J. Appl. Phys. **23:**87-90.

54. **Saqib, A. A. N., and P. John Whitney.** 2006. Role of fragmentation activity in cellulose hydrolysis. Int. Biodeter. Biodegr. **58:**180-185.

55. **Sawai, H. I., A. Hashimoto, T. Kokugan, and M. Shimizu.** 1995. Effect of ceramic powders on spores of *Bacillus subtilis*. J. Chem. Eng. Japan **28:**288-293.

56. **Sayes, C. M., J. D. Fortner, W. Guo, D. Lyon, A. M. Boyd, K. D. Ausman, Y. J. Tao, B. Sitharaman, L. J. Wilson, J. B. Hughes, J. L. West, and V. L. Colvin.** 2004. The differential cytotoxicity of water-soluble fullerenes. Nano Letters **4:**1881-1887.

57. **Shaw, S. Y., E. C. Westly, M. J. Pittet, A. Subramanian, S. L. Schreiber, and R. Weissleder.** 2008. Perturbational profiling of nanomaterial biologic activity. Proc. Natl. Acad. Sci. USA **105:**7387-7392.

58. **Si, S., A. Kotal, T. K. Mandal, S. Giri, H. Nakamura, and T. Kohara.** 2004. Size-controlled synthesis of magnetite nanoparticles in the presence of polyelectrolytes. Chem. Mater. **16:**3489-3496.

59. **Slawson, R. M., M. I. V. Dyke, and H. L. J. T. Trevors.** 1992. Germanium and silver resistance, accumulation, and toxicity in microorganisms. Plasmid **27:**72-79

60. **Sondi, I., and B. Salopek-Sondi.** 2004. Silver nanoparticles as antimicrobial agent: a case study on *E. coli* as a model for Gram-negative bacteria. J. Colloid Interf. Sci. **275:**177-182.

61. **Stoimenov, P. K., R. L. Klinger, G. L. Marchin, and K. J. Klabunde.** 2002. Metal oxide nanoparticles as bactericidal agents. Langmuir **18:**6679-6686.

62. **Sun, S., and H. Zeng.** 2002. Size-controlled synthesis of magnetite nanoparticles. J. Am. Chem. Soc. **124:**8204-8205.

63. **Thill, A., O. Zeyons, O. Spalla, F. Chauvat, J. Rose, M. Auffan, and A. M. Flank.** 2006. Cytotoxicity of CeO_2 nanoparticles for *Escherichia coli*. Physico-chemical insight of the cytotoxicity mechanism. Environ. Sci. Technol. **40:**6151-6156.

64. **Tong, Z., M. Bischoff, L. Nies, B. Applegate, and R. F. Turco.** 2007. Impact of fullerene (C_{60}) on a soil microbial community. Environ. Sci. Technol. **41:**2985-2991.

65. **USEPA.** 2007. United States Environmental Protection Agency Nanotechnology White Paper. www.epa.gov/osa/nanotech.htm EPA/100/B-07/001.

66. **Warheit, D. B.** 2008. How meaningful are the results of nanotoxicity studies in the absence of adequate material characterization? Toxicol. Sci. **101:**183-185.

67. **Wei, X., and R. C. Viadero Jr.** 2007. Synthesis of magnetite nanoparticles with ferric iron recovered from acid mine drainage: Implications for environmental engineering. Colloid Surface A. **294:**280-286.

68. **Weisner, M. R., G. V. Lowry, P. Alvarez, D. Dionysiou, and P. Biswas.** 2006. Assessing the risks of manufactured nanomaterials. Environ. Sci. Technol. **40:**4336-4345.

69. **Wirth, S., and A. Ulrich.** 2002. Cellulose-degrading potentials and phylogenetic classification of carboxymethyl-cellulose decomposing bacteria isolated from soil. System Appl. Microbiol. **25:**584-591.

70. **Witkin, E. M.** 1976. Ultraviolet mutagenesis and inducible DNA repair in *Escherichia coli*. Bacteriol. Rev. **40:**869–907.

71. **Yean, S., L. Cong, and e. al.** 2005. Effect of magnetite particle size on adsorption and desorption of arsenite and arsenate. J. Mater. Res. **20:**3255-3264.

72. **Yeber, C. M., J. Rodriguez, J. Freer, N. Duran, and H. D. Mansilla.** 2000. Photocatalytic degradation of cellulose bleaching effluent by supported TiO_2 and ZnO. Chemosphere **41:**1193–1197.

73. **Zhang, L., Y. Jiang, Y. Ding, M. Povey, and D. York.** 2007. Investigation into the antibacterial behaviour of suspensions of ZnO nanoparticles (ZnO nanofluids). J. Nanopart. Res. **9:**479-489.

II. Implication of Carboxymethyl Cellulose Stabilized Magnetite Nanoparticles to Bacteria

Abstract

Stabilized iron oxide nanoparticles have potential for *in-situ* environmental remediation (31). However, little is known regarding the impact of these nanoparticles on microorganisms. To evaluate the possible microbial impact of iron nanoparticles, nanoscale Fe_3O_4 was prepared and evaluated for inhibition or toxicity to four bacteria: *Escherichia coli* and *Pseudomonas aeruginosa* were chosen to represent Gram-positive organisms while *Bacillus subtilis* and *Enterococcus faecalis* represented Gram-positive organisms. The effect of commercial and lab-prepared Fe_3O_4 nanoparticles was examined through growth experiments and observation of cell-nanoparticle interactions. The results show that Fe_3O_4 nanoparticles at concentrations of 0.3, 0.6, and 1.0 g Fe/L were neither toxic nor inhibitory to the four organisms tested. In some cases, growth stimulation was observed. After the addition of culture to nanoparticle suspensions, there was a loss of particle stability manifested by the formation of large precipitates. Scanning electron microscopy was performed on the precipitates formed in *E. coli* culture to examine the cell-nanoparticle interactions. Nanoparticles were found to cover cell surfaces and bridge cells together in clusters, but no damage to cell integrity was observed. *E. coli* cells blanketed by nanoparticles retained the shape of healthy cells. No cell damage or rupture was observed. Precipitates formed in the presence of bacteria consisted of nanoparticles and bacterial cells held in the nanoparticle matrix. CMC, the stabilizing agent, likely works as a radical scavenger (22) and provides a steric coating and electrostatic barrier between bacteria and Fe_3O_4. Our results

suggest that stabilized nanoparticles interact with bacterial surfaces without causing damage sufficient to inhibit cell growth. CMC not only improved dispersibility and mobility of Fe_3O_4 nanoparticles but also reduced toxicity to bacterial cells.

Introduction

Stabilized iron oxide nanoparticles have potential for *in-situ* environmental remediation (31). Specifically, magnetite (Fe_3O_4) nanoparticles can remove contaminants such as As (V), As (III) (54), Pb (7), and Cr (VI) (16) in groundwater and soil (7, 16, 25, 31, 32, 35). In addition to direct injection of magnetite nanoparticles into the ground, magnetite nanoparticles can enter the environment indirectly. Zero valent iron (ZVI), a more reactive iron nanoparticle, "ages" into magnetite after field injection (41). Van der Waals and magnetic forces cause these highly reactive magnetite nanoparticles to aggregate. The presence of a stabilizer limits the direct interactions of these forces between nanoparticles and allows these nanomaterials greater mobility at reaching the target pollutant. In addition, synthesizing iron nanoparticles in the presence of a polymer stabilizer produces smaller particles and often prevents coagulation leading to a more monodisperse suspension (12). CMC has been reported to be an effective stabilizer for ZVI nanoparticles, reducing particle size and increasing TCE degradation in a sandy soil (15).

New technologies designed for environmental application should be evaluated for unintended effects before their widespread implementation. Possible adverse effects could include harmful interactions of nanoparticles with living organisms in the environment. Nanoparticles may damage cell membranes through reactive oxygen species i.e., superoxide and hydroxyl radicals (37) or direct cell damage (19, 48). For metal oxide nanoparticles (i.e. ZnO,

TiO_2, and Ag_2O), it is generally accepted that reactive oxygen species (ROS) (1, 11) and direct rupture of cell membranes can cause toxic effects on microorganisms (1, 21, 48, 56). Iron nanoparticles can also undergo Fenton-type reactions leading to the production of •OH radicals (3). Limited information, however, is available concerning the effect Fe_3O_4 nanoparticles may have on living organisms. Several studies have evaluated the toxicity of iron oxide nanoparticles to eukaryotic cells. Although dextran-coated Fe_3O_4 has minimal *in vivo* toxicity in rats and humans (46), magnetite exhibits low neurotoxicity to rodent N27 neurons compared to ZVI due to its low "redox" activity (41) and causes a decrease in mitochondrial function in BRL2A rat liver cells (17). Maghemite (Fe_2O_3), which is considered less redox reactive than Fe_3O_4, has the highest toxicity to human mesothelioma cells among the seven nanoparticles tested (5). So far there are only a few published studies on cytotoxicity of Fe_3O_4 to bacteria. Auffan et al. demonstrated that Fe_3O_4 is toxic to *E. coli* strain Qc1301 in ultrapure water (pH 5–5.5) after 1 hour at concentrations higher than 700 mg/L and toxicity increased in the double mutant *sodA sodB* that is lacking iron and manganese superoxide dismutase activities (2). Lee et al. on the other hand found no toxicity of Fe_3O_4 (9 mg/L) towards *E. coli* ATCC strain 8739 after 1 hour in a carbonate buffer (pH 8) (23). Aged ZVI which contains magnetite was shown benign to bacteria (27). ZVI has also been shown to disrupt *E. coli* cell membranes leading to leakage of intracellular contents under deaerated conditions (23). Direct contact between nanoparticles and cells appears essential for toxicity due to ROS (37). Surface modification of ZVI nanoparticles appears to decrease toxicity to mammalian and prokaryotic cells (27, 41). The two previously mentioned studies involving *E. coli* used resting cells and bare nanoparticles for their toxicity assays. Instead of employing already stressed cells and bare nanoparticles, this study aimed to investigate the effects of stabilized Fe_3O_4 nanoparticles on four pure cultures of bacteria, i.e.,

Escherichia coli, *Pseudomonas aeruginosa*, *Bacillus subtilis*, and *Enterococcus faecalis* during growth phase in the presence of UV light to simulate natural conditions. We hypothesize that negatively charged surface coated nanoparticles will be less toxic to cells than bare nanoparticles.

Materials and Methods

Magnetite nanoparticles. Both laboratory-synthesized and commercial magnetite nanoparticles were used in this study. To prepare magnetite, ferric and ferrous salts purchased from Acros Organics (Fair Lawn, NJ) were added in a molar ratio of 2:1 to achieve a final iron concentration of 1.5 g Fe/L using a procedure modified after several protocols (12, 47, 51, 52). $FeCl_3 \cdot 6H_2O$ (0.018 M) and $FeSO_4 \cdot 7H_2O$ (0.009 M) solutions were prepared separately in distilled water purged with N_2. One percent of autoclaved carboxymethyl cellulose sodium salt (MW 90 kD, Acros Organics) was purged with N_2 gas for 30 minutes with continuous stirring. Ferrous and ferric iron solutions were added consecutively to the CMC solution and again purged with N_2 for 30 minutes. In one aliquot, 10 M NaOH was rapidly added to the suspension turning it black instantly and reaching a final pH of 11. The suspension was purged with N_2 for another 30 minutes, sealed with a rubber stopper, and allowed to age overnight. After 24 hours, the pH of the suspension was brought down to a biologically relevant pH of 7 with 5 M HCl. The final iron concentration was 1.5 g Fe/L with a corresponding CMC concentration of 0.5% (w/v). Sterile water was used in place of CMC for the synthesis of bare particles. After standing overnight and pH adjustment, the bare particles were washed three times with autoclaved N_2 purged water. Commercial Fe_3O_4 nanoparticles (20-30 nm) used in the studies were purchased from Nanostructured & Amorphous Materials, Inc. (Houston, TX). Magnetite powder (0.414 g,

corresponding to 1.5 g Fe/L) was sonicated in 200 mL of 0.5% autoclaved CMC for 1 hour at 60 W using a Misonix probe sonicator (Farmingdale, NY) pulsing off one minute for every 10 minute cycle. The sample vessel was placed in an ice bath to reduce heat resulting from the sonicating process.

Characterization of magnetite nanoparticles. Transmission electron microscopy (TEM) was performed on a Zeiss EM 10C 10CR Transmission Electron Microscope. Ten µL of sample was placed on a formvar/carbon coated copper grid and allowed to dry for 30 minutes, with excess liquid being wicked away with filter paper. Grids were stored in a dessicator prior to microscopic observation. Particle sizes of well dispersed samples were determined using an image processing software, ImageJ (http://rsbweb.nih.gov/ij/index.html). More aggregated samples were measured by hand. The average particle size was calculated based on a minimum of 300 particles for each treatment. X-ray diffraction (XRD) was performed on freeze-dried magnetite nanoparticles using a Bruker-AXS D8 Discover X-Ray Diffractometer with a GADDS area detector. Spectra were obtained for the 2θ range of 20 to 80 degrees. Zeta potential was measured on a Zetasizer Nano-ZS (Malvern Instruments, Worcestershire, UK). Viscosity was measured using a falling ball viscometer purchased from Gilmont Instruments (Barrington, IL). The surface areas of synthesized and commercial bare Fe_3O_4 were measured by N_2 adsorption at 77 K using a Micromeritics Gemini 2375 Surface Area Analyzer. The multi-point BET (Brunauer-Emmett-Teller) N_2 gas adsorption method was used to determine sample surface area. Since photocatalytical effectiveness of metal nanoparticles has been shown to correlate with cytotoxicity (45), the photocatalytic activity of bare Fe_3O_4 particles was measured using a standard method (10). In this assay, synthesized and commercial Fe_3O_4 were used to photodegrade the organic dye, Orange II, in the presence and absence of hydrogen peroxide. The

initial concentrations of Fe_3O_4 and Orange II were 0.5 g/L and 0.034 mM, respectively. The Fe_3O_4 suspensions were equilibrated with Orange II in darkness for 4 hours prior to hydrogen peroxide (6 mM) addition and UV light illumination. The disappearance of dye was monitored at 482 nm for 2 hours when dye concentration stopped decreasing.

Cell growth study. *E. coli* K-12 strain MG1655 and *E. faecalis* ATCC 19433 were purchased from the American Type Culture Collection (ATCC). *P. aeruginosa*, and *B. subtilis* were obtained from Auburn University Biological Sciences Microbiology culture collection. Glucose-MOPS medium (38) was used as a minimal medium with 0.01% yeast extract added to *Enterococcus* culture. Since iron is known to participate in Fenton-type reactions and UV promotes free radical formation, the first set of growth experiments was conducted to determine the effect of UV irradiation on bacterial growth. Cells were grown in borosilicate vials in the presence of commercial Fe_3O_4 at concentrations of 0.1 and 0.2 g Fe/L. Vials were placed on a flat platform partially immersed in a 37˚C shaking waterbath. UVA and UVB light was used to simulate solar UV radiation (290-400 nm). A 60 watt Mega-Ray UV lamp (Cedar Point, NC) was placed 30.5 cm away from the platform. The total UV irradiance (300-400 nm) monitored by a Solar Light radiometer (Glenside, PA) equipped with a UVA + UVB detector was 200 $\mu W/cm^2$. Borosilicate glass allowed UV light (>300 nm) to penetrate. One set of vials was exposed to UV light and the other set was kept in the dark by wrapping vials with aluminum foil. Vials were inoculated with cultures grown to early stationary phase. After 24 hours of growth 1 mL of cell suspension was removed and centrifuged. Harvested cells were then lysed using CelLytic B Plus Kit (Sigma); total protein, an indicator of cell growth, was determined using Sigma bicinchoninic acid (BCA) protein assay kit in a 96-well plate format.

The second set of growth experiments was conducted using synthesized and commercial magnetite nanoparticles at much higher concentrations (0.3, 0.6, and 1 g Fe/L) under UV light only. All four bacterial cultures were grown in 20-mL disposable borosilicate glass vials placed in a shaking waterbath as previously described. Each vial contained 0.33% of CMC by supplementing with different volumes of sterile stock solution. The vials were inoculated with bacterial cells in early stationary phase to obtain an initial cell density of 1-4 x 10^6 CFU/mL. After 6 hours of incubation, all four organisms reached log phase of growth and cells were enumerated using the Miles and Misra drop count technique (34).

To determine the effect of dissolved iron on bacterial growth, filtrate of magnetite suspension was used. The filtrate was collected as follows: magnetite suspension (1.5 g Fe/L, 0.5% CMC) aged for 24 hours was adjusted to pH 7 and filtered through an Amicon Ultra-15 centrifugal filter unit (100 KD molecular weight cutoff, Millipore, Billerica, MA) by centrifuging at 4000 x g for 1 hour. The filtrate was analyzed for CMC using 1% hexadecyltrimethylammonium bromide (Acros) (13), for total dissolved iron by atomic absorption spectrometry, and ferrous iron by spectroscopic determination using 1, 10-phenonthroline (6). This filtrate was added to culture media at volumes equal to the nanoparticle suspension.

Nanoparticle-bacterial cell interactions. Precipitates formed in *E. coli* cultures were separated from liquid media by brief centrifugation, fixed with 2% glutaraldehyde and 1% osmium tetroxide for 1 hour, and washed in 0.1 M phosphate buffer (pH 7). Samples were progressively dehydrated using a series of ethanol solutions (30%, 40%, 50%, 60%, 80%, 90%, and 95%; 15 minutes per step) followed by drying with dimethylsilizane. Healthy *E. coli* cells and nanoparticles serving as controls were prepared in the same manner. Dried samples were placed

onto stubs, gold sputter coated and examined with a Zeiss EVO 50VP Scanning Electron Microscope (SEM).

Additionally, TEM was used to examine whether Fe_3O_4 nanoparticles were present inside *E. coli* cells. TEM specimens were prepared after *E. coli* was grown in MOPS medium for 24 hours in the presence of CMC-stabilized Fe_3O_4 nanoparticles (0.6 g Fe/L). The samples were concentrated by brief centrifugation and washed twice with distilled water. Both the healthy cell control and treated cells were fixed in 2% glutaraldehyde and 0.1 M sodium cacodylate buffer (pH 7), followed by washing three times with 0.1 M sodium cacodylate buffer and postfixing with 1% osmium tetroxide in 0.1 M sodium cacodylate buffer for 1 hour in the dark. The cells were dehydrated with sequential treatment of 30, 50, 70, 80, 90, 95 and 100% (two times) ethanol for 15 minutes. The cells were then infiltrated and embedded in Embed 812 resin with propylene oxide (treatment with 3:1, 1:1, and 1:3 of propylene oxide/Embed 812 resin mixtures for 30 minutes each, and100% Embed 812 resin twice for 1 hour each). The samples, filled with resin, were cured overnight at 70°C to form sample blocks. The polymerized blocks were cut into ultrathin sections with a diamond knife on a Leica Ultracut T ultramicrotome (Leica Microsystems, Vienna, Austria), and sections were stained in 2% uranyl acetate and lead citrate and examined by TEM.

Radical quenching by CMC. Two assays were performed to assess the capability of CMC to quench free radicals. In the first assay, the radical scavenging activity of CMC was measured using stable 1,1-diphenyl-2-picrylhydrazyl (DPPH) radicals following the method of Lin and Chou (28) and Yamaguchi et al. (53) with minor modifications. Two mL of 400 µM DPPH• in methanol was mixed with 2 mL of CMC solution (0.5 % and 1 %). Absorbance was monitored over a 3-hour period. After 3 hours of incubation at room temperature (22 ± 1˚C), the

absorbance at 522 nm was measured using a Shimadzu UV- 1601 spectrophotometer. Ascorbic acid, a known radical scavenger, was used as a positive control. Scavenging effect was calculated with the following equation:

Scavenging effect (%) = [1-absorbance$_{sample}$/absorbance$_{control}$]x100.

In the second assay, hydrogen peroxide scavenging activity was measured using an existing method (28, 42, 43) with minor modifications. Briefly, 50 µl of CMC (0.5% and 1%) was added to 50 µl of 5.3 mM H_2O_2 in a 96 well plate. Samples were incubated in the dark for 30 minutes at room temperature (22˚C). Then 100 µl of phenol red solution (PRS) was added. The PRS solution consisted of 1.12 mM phenol red in 0.1 M phosphate buffer pH 7 and 226 µg/mL (19U/mL) horseradish peroxidase (Sigma). After addition of PRS solution, the 96 well plate was incubated for an additional 10 minutes before the addition of 10 µl of 1 M NaOH to each well to raise the pH to 12.5. After waiting one minute for color change to reach completion, the absorbance was read at 610 nm using a uQuant Microplate reader (Biotek, Winooski, VT). Actual concentration of H_2O_2 from the stock solution (30-35%) was calculated using the extinction coefficient of 43.6 $M^{-1}cm^{-1}$ at 240 nm (39). Scavenging effectiveness was calculated using the equation previously mentioned.

Statistical analysis. All growth experiments were prepared in triplicate and repeated three times. Error bars showing the standard error of the mean are included in the figures. Data were analyzed for statistical significance using pairwise comparison. Statistical significance relative to the controls was determined at $p < 0.05$, $p < 0.01$, and $p < 0.001$.

Results

Characterization of magnetite. Figure 2.1 shows the TEM images of synthesized and commercial Fe_3O_4 nanoparticles. CMC-stabilized Fe_3O_4 nanoparticles (Fig. 2.1A) were spherical with an average diameter of 6.58 ± 3.93 nm; the polydispersity was the lowest of the four types of nanoparticles analyzed. In the liquid suspension, these nanoparticles were stable for over two weeks. Bare Fe_3O_4 nanoparticles synthesized in the absence of CMC were larger and cubical (Fig. 2.1B), with an average particle size of 22.0 ± 11.2 nm. Without the stabilizer, the particle size was less uniform and larger aggregates were formed. In fact, synthesized bare Fe_3O_4 particles had the greatest size range of all four particle types examined. Similar to synthesized bare Fe_3O_4, commercial Fe_3O_4 particles were larger and cubical with rounded corners. Commercial magnetite resuspended with 0.5% CMC (Fig. 2.1C) had an average particle size of 22.1 ± 8.2 nm whereas those suspended in water (Fig. 2.1D) had an average size of 23.3 ± 8.5 nm. In liquid suspensions, commercial Fe_3O_4 stabilized with CMC were stable for one day whereas those without stabilizer settled within minutes. XRD analyses confirmed that the synthesized crystals were magnetite as shown in Figure 2.2. Peak positions consistent with Fe_3O_4 (24, 47) were present in all three nanoparticle samples; however, presence of CMC reduced peak intensity and increased peak broadness.

Zeta potentials of synthesized and commercial Fe_3O_4 stabilized with CMC at pH 7 were –67.0 and –52.6 mV, respectively, according to DLS measurements (Table 2.1). The suspensions of non-stabilized Fe_3O_4 were not stable and thus their zeta potentials could not be measured by DLS. The point of zero charge (PZC) for Fe_3O_4, however, has been reported to be in the range of pH 6 to 8 (2, 8, 30, 51, 55). At pH 7 bare Fe_3O_4 particles have a mostly neutral charge (51). As expected the synthesized bare particles had a greater surface area (129.8 m^2/g) than the

commercial particles (40.7 m^2/g). The higher surface area suggests that the synthesized particles are more reactive than the commercial particles. In regard to photocatalytic activity, neither synthesized nor commercial Fe_3O_4 resulted in photodegradation of Orange II in the absence of H_2O_2. With the addition of hydrogen peroxide (6 mM), both types of particles brought about degradation of Orange II to a similar extent (Table 2.1).

Cell growth. Table 2.2 shows selected characteristics of bacteria used in the study. Since UV light promotes the formation of reactive oxygen species and may potentially exert more oxidative stress to bacteria, effects of Fe_3O_4 nanoparticles on bacterial growth were first examined under both light and dark conditions. Only non-stabilized Fe_3O_4 were used in these experiments. Fig. 2.3 shows that cell growth under UVA+ UVB was similar to that in the dark for all four organisms. After a 24 hour period in the dark, all four organisms showed a significant growth increase ($P<0.05$) compared to the corresponding controls in the presence of Fe_3O_4 at 0.2 g Fe/L (Fig. 2.3). Significant growth increase ($P<0.01$) occurred for *P. aeruginosa* under both UV light and dark conditions for both iron concentrations (Fig. 2.3B). Growth of *E. coli*, *B. subtilis*, and *E. faecalis* under UV light, however, were not significantly different from growth in the corresponding controls. For *E. coli* and *E. faecalis*, protein contents were numerically lower than the controls at 0.1 g Fe/L (Fig. 2.3A and 2.3D) under UV irradiation, but the difference was not statistically significant. Since the growth differences between UV light and dark conditions were small for all four organisms, the rest of the experiments were conducted under UV light to simulate the natural conditions bacteria may experience in the aquatic environment.

Synthesized Fe_3O_4 nanoparticles with and without CMC as well as CMC-stabilized commercial Fe_3O_4 were used to further examine the impact of nanoparticles on bacteria under UV irradiation. Increasing concentrations of synthesized magnetite stabilized with 0.5% CMC

resulted in stimulation of growth for all organisms although the increases were statistically significant only for *E. coli* at 1.0 g Fe/L and *E. faecalis* at all three concentrations (Fig. 2.4A). The addition of bare particles resulted in different trends for the four organisms. There was a slight but significant reduction of growth for *E. coli*, but there was not a dose dependent effect. *B. subtilis* showed a significant growth increase at 0.6 g Fe/L and *E. faecalis* at both 0.6 and 1.0 g Fe/L (Fig. 2.4B).The cell counts for *P. aeruginosa* after 6 hours of growth were numerically higher than the control at all three magnetite concentrations. The increases, however, were not statistically significant (Fig. 2.4B). All organisms exhibited significantly increased growth with the addition of CMC stabilized commercial Fe_3O_4 at one or more concentrations (Fig. 2.4C).

Since the background electrolytes and CMC may be the cause of the growth stimulation, experiments were conducted to examine the effect of the filtrate from the synthesized magnetite suspension on the growth of all four organisms. The clear filtrate contained approximately 0.05% of CMC, 0.260 mg/L of total dissolved iron, and 0.247 mg/L of ferrous iron. Only 10% of the initial CMC remained in the filtrate, indicating most of the CMC was either bound to nanoparticles or retained by the membrane filter. With the addition of the filtrate, we did not observe stimulation of growth consistent with the nanoparticle suspension (Fig. 2.4D). In fact, as the volume of filtrate increased there was a decrease in growth for *E. coli*. Unlike the synthesized Fe_3O_4 suspension, the resuspended commercial Fe_3O_4 did not contain dissolved iron and other salts derived from the synthesis process. The experiment using MOPS supplemented with 0.5% CMC did not show significant changes in cell growth compared to the MOPS medium control (Fig. 2.4D). Growth was even reduced in two cases perhaps due to limiting oxygen diffusion (Fig. 2.4D). Thus, the presence of free CMC was not likely responsible for the observed growth stimulation.

Nanoparticle-bacterial cell interactions. During the 6-hour growth period, large precipitates formed in the vials containing bacteria. The precipitates, however, were not observed in the medium control containing sterile stabilized nanoparticles, suggesting nanoparticle-bacterium interaction is the mechanism behind large precipitate formation, as opposed to purely nanoparticle-nanoparticle interaction. Precipitates formed from the stabilized synthesized Fe_3O_4 were much smaller than those from the commercial and non-stabilized Fe_3O_4 and could easily be broken up by simply inverting the sample vial, suggesting weak interactions between cells and CMC-stabilized Fe_3O_4 nanoparticles. To observe constituents of these precipitates, SEM was performed using samples from *E. coli* culture. Broken cells observed in some of the images could have resulted from the sample preparation process. Fig. 2.5A shows the SEM image of a precipitate formed in *E. coli* culture in the presence of CMC-stabilized synthesized Fe_3O_4 nanoparticles. These nanoparticles appeared to be very fine and packed together closely; nanoparticle-nanoparticle interactions were prevalent. *E. coli* cells were coated with nanoparticles that were barely visible (Fig. 2.5A). TEM of ultrathin-sectioned cells incubated with nanoparticles showed that these Fe_3O_4 nanoparticles did not enter the cell or disrupt the cell wall. Nanoparticles were found aggregated on the cell surface and to each other (Fig. 2.5A inset). Fig. 2.5B shows precipitates consisted mostly of bacteria and nanoparticles in the presence of non-stabilized synthesized magnetite. The particles were not as small and dispersed as stabilized samples and nanoparticles bound to bacterial surfaces. Precipitates were tightly packed with bacteria covered in nanoparticles. Cells were seen bridging the gap between nanoparticle aggregates. Cells were covered in nanoparticles and nanoparticles were covered in cells. Neither interaction appeared predominant. Fig. 2.5C shows loose aggregates of *E. coli* cells and nanoparticles in CMC-stabilized commercial magnetite. Nanoparticles were loosely associated

with the cell surface but cells were covered in nanoparticles despite the weak interaction. Precipitates consisted of nanoparticles and bacteria bound to each other. Nanoparticles were capable of bridging two cells together and nanoparticles were bound together by cells. Fig. 2.5D shows healthy cells grown in MOPS media that underwent the dehydration process for SEM and TEM (Fig. 2.5D inset). Cells appear whole with a healthy morphology and demonstrate an intact cell wall.

Radical quenching by CMC. DPPH has been used to determine scavenging activities of antioxidants for hydrogen radicals (4). Since CMC is considered a mild antioxidant, its radical scavenging activity was measured using the DPPH assay. Ascorbic acid, a known radical scavenger, reacted quickly with $DPPH^{\bullet}$ and the scavenging activity reached 41 ± 6% within one minute. CMC, however, reacted with $DPPH^{\bullet}$ more slowly compared to ascorbic acid. After 3 hours 0.5% and 1% of CMC showed scavenging effects of 41±6 % and 27 ± 2%, respectively. CMC was capable of quenching the $DPPH^{\bullet}$ radical although increased CMC concentration did not result in an increase of scavenging effectiveness.

Since hydrogen peroxide is a precursor of hydroxyl radical, the phenol red assay was used to determine hydrogen peroxide scavenging activity by CMC. Ascorbic acid, the positive control, showed the highest scavenging effect at 25 ± 4% followed by 1% CMC at 21 ± 2% and 0.5% CMC at 15 ± 6%. Ascorbic had the greatest ability to scavenge H_2O_2 but both concentrations of CMC followed closely behind. The higher concentration of CMC was more effective at scavenging peroxide than the lower concentration.

Discussion

Our data showed that bare and CMC-stabilized Fe_3O_4 nanoparticles did not inhibit the growth of four bacteria used in the study, in fact growth increase was observed in some cases. Further evidence supporting the absence of toxicity was provided by TEM images showing intact cells; even the smallest nanoparticles were not capable of entering *E. coli* cells, only aggregating on the surface. Since there is the possibility of phosphate passivating magnetite surfaces (8), we determined the effect of magnetite on *E. coli* in phosphate buffer, carbonate buffer, and water. Growth differences at the concentration used in our growth media (0.001M) were not observed (data not shown); therefore we could rule out phosphate passivating Fe_3O_4, reducing particle reactivity, and diminishing toxicity. Additionally, growth increase observed in the study cannot be attributed to CMC or dissolved iron in the media (Fig. 2.4D). Causes of growth increase observed in this study should be further investigated. Interpretation of surface effects on microbial activity is rather complex; the presence of a solid can stimulate, inhibit, or have no effect on biodegradation of a target chemical (33). *P. putida* undergoes structural and metabolic changes following adhesion to a surface (44). There is a consensus that surfaces (including glass beads) affect bacterial metabolism; however, there is no general explanation for the increase or decrease in cell numbers, only proposed hypotheses including nutrient accumulation (50). It should also be noted that as nanoparticle concentration increased we did not observe a consistent decrease in growth. This is consistent with a previous study that found toxicity of magnetite to *E. coli* in ultrapure water did not always increase with concentration (2). Thus, concentration is not the only variable important in Fe_3O_4 nanoparticle toxicity. As nanoparticle concentration increases, aggregation between nanoparticles likely increases as well (9), leading to less free particles able to interact with cell surfaces.

There are several explanations for lack of growth inhibition. First of all, Fe_3O_4 is not very toxic to bacteria. Photocatalytic activities of nanoparticles have been related to cytotoxicity (45). Fe_3O_4 is far less photoreactive compared with other transition-metal oxide nanoparticles, such as TiO_2 (10). Our data showed that bare Fe_3O_4 nanoparticles catalyzed the photodegradation of Orange II only in the presence of hydrogen peroxide under UV irradiation similar to natural sunlight. Second, bacteria may overcome or repair the damage caused by nanoscale Fe_3O_4 during growth. A previous study reported Fe_3O_4 toxicity to *E. coli* strain Qc1301 and its double mutant *sod*A *sod*B Qc2472 was conducted under non-growing conditions in water (pH 5-5.5) within one-hour contact period (2). In our study, actively growing cells in a nutrient medium were employed. Perhaps the lack of toxicity was due to the favorable conditions in which our cells encountered the nanoparticle suspension. Growing cells were more likely to repair damage caused by nanoparticles due to the abundance of nutrients. Similarly, cells were more resistant to copper during logarithmic growth phase compared to stationary phase due to the ATP produced during rapid growth, contributing to the efflux pump mechanism for heavy metal resistance (49). Additionally, bacteria in our study were exposed to Fe_3O_4 under aerobic conditions in the presence of CMC. Perhaps oxygen diminished the bactericidal effect of the Fe (II) ion as suggested for iron compounds (23, 26). Third, presence of nanoparticles could limit UV penetration, thus cells grown with Fe_3O_4 might exhibit more growth compared to controls. Fourth, CMC may render protection to cells when stabilized nanoparticles are used. CMC increases stability and dispersibility of Fe_3O_4 nanoparticles by preventing particle-particle interaction sterically and electrostatically. CMC can also create a diffusion barrier around nanoparticles, reducing ROS or nanoparticles interaction with cells (40). Steric hindrance and electrostatic repulsion also likely limit nanoparticle and bacterium interaction (9) and radical

scavenging properties of the stabilizer diminish toxicity resulting from reactive oxygen species. CMC has been shown to scavenge superoxide and hydroxyl radicals at a concentration of 5 g/L (36). The antioxidant properties of CMC were similar to a low concentration of ascorbic acid, a known antioxidant, at scavenging DPPH radicals as well as H_2O_2. Most likely the protective action of CMC acts primarily through electrostatic repulsion, keeping nanoparticles from intercting with bacteria. Secondarily, the mild antioxidative properties and diffusion layer act to prevent oxidative damage and reduce potential toxicity. In nature, exopolymers secreted by biofilms absorb reactive oxygen species and prevent nanoparticles from contacting cell surfaces (37). It is likely CMC, like other polymers, forms a viscous pericellular network around cells that prevents ROS movement in close proximity with cells (36).

The use of CMC as a stabilizer resulted in changes in size and surface charge of Fe_3O_4 nanoparticles. When added during synthesis, the CMC stabilizer can adequately act as a capping agent to create small, uniform shaped particles as well as prevent interactions between nanoparticles. Particles without stabilizer were much larger, making them less reactive than stabilized particles. For commercial powders, CMC was added after nanoparticle synthesis and kept particles separated to a lesser extent. Since nanoparticles were already aggregated in the dry powder form, CMC could not surround each individual particle and was only capable of surrounding smaller aggregates. XRD analysis supports our TEM evidence that CMC effectively reduces particle size when added during synthesis. Figure 2.2 shows narrow peaks associated with both the commercial Fe_3O_4 as well as synthesized bare Fe_3O_4, suggesting a larger particle size compared to Fe_3O_4 synthesized with CMC, which shows broader peaks. The decrease in intensity seen with the Fe_3O_4 synthesized with CMC also shows a decrease in crystallinity (47). Because surface area/size plays a large role in toxicity to cells through reactivity and

nanoparticle-cell surface interactions, it is difficult to compare stabilized versus non stabilized particles due to the size difference between the two treatments.

Magnetite nanoparticles (synthesized and commercial) interacted with cell surfaces less in the presence of CMC stabilizer. When comparing stabilized synthesized and commercial nanoparticles, commercial nanoparticles formed larger precipitates in the presence of cells. CMC worked well at preventing aggregation of nanoparticles from forming precipitates and preventing small nanoparticles from interacting with cell surfaces through its negatively charged functional groups. Non stabilized nanoparticles were not stable in suspension and formed large precipitates with cells. However, even in the absence of the stabilizer, magnetite nanoparticles were not toxic or inhibitory to the four organisms tested in terms of growth. Aged ZVI which contains magnetite was benign to *E. coli* in a previous study (27). When bare synthesized Fe_3O_4 nanoparticles were compared to CMC stabilized synthesized particles, we hypothesize there was less stimulation of growth observed with the stabilized particles due to their small diameter, and increased reactivity. Comparing bare synthesized particles and commercial stabilized particles more growth was observed with the stabilized particles. A recent study showed nanoparticles Al_2O_3, SiO_2 and ZnO nanoparticles had a greater tendency to attach to bacteria than to aggregate together. Flocculation between bacterial cells (*P. fluorescens*, *B. subtilis*, and *E. coli*) and nanoparticles, similar to the phenomenon seen in our study, was also reported (9, 18). They concluded the zeta potentials of bacterial cells and nanoparticles are helpful to understand the attachment or repulsion between nanoparticles and bacteria. In our study we reached the same conclusion that the negative zeta potential conveyed by our stabilizer will reduce the interaction between cells and nanoparticles (27).

Examination of cultures containing Fe_3O_4 nanoparticles revealed that vials containing bare magnetite nanoparticles resulted in many more large precipitates than vials containing stabilized nanoparticles. Adhesion of bacteria has been shown to increase during exponential growth, explaining the precipitation observed over the course of the experiment (50). Non-stabilized particles in bacterial culture packed much looser together due to their size and inability to fit closely together. However, the interactions between non-stabilized particles (both synthetic and commercial) were much stronger, characterized by the difficulty in disrupting aggregates after formation. While stabilized nanoparticles could fit together closely, they formed smaller precipitates than non stabilized particles. Bare particles, exhibiting the strongest interactions, also had the strongest interactions with cell surfaces. Synthesized nanoparticles with CMC loaded on the surface formed the smallest precipitates with cells, but it should be noted that this was the only treatment that exhibited a noticeable change in cell morphology.

Stabilized aggregates were loosely held together and formed more slowly than non-stabilized particles. Since aggregates of substantial size were not observed in the sterile nanoparticles samples, two scenarios arose 1) precipitates consisted of live, intact bacteria coated in nanoparticles that collected together through adhesion until larger and larger aggregates formed or 2) precipitates were made entirely of nanoparticles held together with cell components or compromised cells. Aggregates observed in liquid culture consisted of smaller looser precipitates made up of intact bacteria covered in a layer of nanoparticles which could interact with other cells via their free surface not already bound to a cell. While nanoparticles appear to be loosely associated with cells, the interaction was strong enough to create large aggregates that appeared to precipitate nanoparticles out of solution. This effect was less noticeable in stabilized treatments due to the negatively charged stabilizer creating electrostatic repulsion between cells

and nanoparticles. The presence of *E. coli* enhances the structural transformation (oxidation) of iron oxide surfaces, leading to less stable suspensions according to Auffan et al. (2). *B. subtilis* was shown to mediate the oxidation of Fe^{2+} to Fe^{3+}, forming flocs (9). CMC and other stabilizers could potentially reduce the interaction between cells and nanoparticles and therefore reduce this transformation. According to SEM, synthesized particles interacted with cells less than commercial particles and stabilized particles interacted with cells less than non stabilized particles. The presence of CMC and aggregate size affected the interaction between nanoparticles and cell surfaces. The different treatments each showed different aggregation patterns and cells were coated with nanoparticles to different extents. However, aggregates were easily broken up in liquid culture and SEM images of nanoparticles loosely bound to cells supports the significant yet overall weak interaction between bacteria and nanoparticles. Zeta potential measurements supported visual observations that stabilized synthesized magnetite nanoparticles were more stable than commercial powder suspended in CMC. The polymer could better surround particles during synthesis leading to higher negative repulsive forces between particles. Greater negative charge in addition to better coverage repels particles away from negative bacterial surfaces. Bare particles do not carry this negative charge and are attracted to bacterial surfaces to a greater extent. This stronger attraction is the reason the bacteria-nanoparticle aggregates were difficult to break apart. The presence of a stabilizer, particle size, particle concentration, and aggregate morphology all likely play a role to the extent at which nanoparticles interact with bacterial surfaces. This interaction needs more research to understand how bacteria degrade stabilizers, precipitate nanoparticles, and transform particle surfaces.

This study showed the charge carried by a stabilizer and effective particle size gives a good approximation of the likelihood of nanoparticles interacting with cell surfaces. Even with

nanoparticles resulting in complete coverage of bacteria surfaces there was no observable toxicity or decrease in protein, and the effect was not always dose dependent. Only bare nanoparticles reduced growth in *E. coli*, while the smaller, more reactive stabilized particles did not decrease cell growth due to the polymer layer. As concern rises in regard to the lifetime and dispersability of nanoparticles into the environment, it is important to remember that bacteria will interact with and transform these nanoparticles, reducing their longevity. This study showed the apparent non-toxic interaction between bacteria and nanoparticles and the subsequent loss of nanoparticle stability once introduced into a biological system. This study also showed that magnetite nanoparticles aggregate on cell surfaces but do not make it inside the cell walls via cellular uptake or through destruction of membrane integrity. Aggregation and precipitation of iron nanoparticles in a biological setting is a multistep process consisting of oxidation of particle surfaces and bridging via cells. As concentration varies, the preferential binding pattern of nanoparticle-nanoparticle and nanoparticle-bacterium needs further investigation to understand the potential for these nanoparticles to interact with biological surfaces. It seems apparent these interactions are dependent on the charge of the particle (affected by stabilizer), particle size, and presence of bacteria. Microbial degradation of stabilizing polymers needs further research since bacteria in the environment will likely enhance the breakdown of stabilizer, limiting the mobility and reactivity of the nanoparticles themselves.

The lack of toxicity for synthesized and commercial particles with and without stabilizer is encouraging for the prospect of releasing these nanomaterials into the environment. Not only were bare particles not toxic, but the added stabilizer has properties that can potentially reduce interactions between cells and nanoparticles. The layer of stabilizer not only makes particles more mobile through soil, but is also an added layer of protection around nanoparticles.

Acknowledgements

The authors thank Dr. Joey Shaw, Julie Arriaga, and Dr. John Gorden for XRD analysis, and Dr. Michael Miller for assistance with electron microscopy work. This research was supported by the Alabama Agricultural Experiment Station Hatch and Multistate Funding program.

References

1. **Adams, L. K., D. Y. Lyon, and P. J. J. Alvarez.** 2006. Comparative eco-toxicity of nanoscale TiO_2, SiO_2, and ZnO water suspensions. Water Res. **40:**3527-3532.
2. **Auffan, M., W. Achouak, J. Rose, M.-A. Roncato, C. Chaneac, D. T. Waite, A. Masion, J. C. Woicik, M. R. Wiesner, and J.-Y. Bottero.** 2008. Relation between the redox state of iron-based nanoparticles and their cytotoxicity toward *Escherichia coli*. Environ. Sci. Technol. **42:**6730-6735.
3. **Biswas, P., and C.-Y. Wu.** 2005. Nanoparticles and the environment. J. Air Waste Manage. **55:**708-746.
4. **Brand-Williams, W., M. E. Cuvelier, and C. Berset.** 1995. Use of a free radical method to evaluate antioxidant activity. Food Sci. Technol. -LEB **28:**25-30.
5. **Brunner, T. J., P. Wick, P. Manser, P. Spohn, R. N. Grass, L. K. Limbach, A. Bruinink, and W. J. Stark.** 2006. *In vitro* cytotoxicity of oxide nanoparticles: Comparison to asbestos, silica, and the effect of particle solubility. Environ. Sci. Technol. **40:**4374-4381
6. **Christian, G. D.** 1977. Analytical Chemistry, p. 723-724, 5th ed. Wiley.
7. **D' Couto, H.** 2008. Development of a low-cost sustainable water filter: A study of the removal of water pollutants As (V) and Pb (II) using magnetite nanoparticles. J. US SJWP**:**32-45.
8. **Daou, T. J., S. Begin-Colin, J. M. Greneche, F. Thomas, A. Derory, P. Bernhardt, P. Legare, and G. Pourroy.** 2007. Phosphate adsorption properties of magnetite-based nanoparticles. Chem. Mater. **19:**4494-4505.

9. **Diao, M., and M. Yao.** 2009. Use of zero-valent iron nanoparticles in inactivating microbes. Water Res. **43:**5243-5251.

10. **Du, W., Y. Xu, and Y. Wang.** 2008. Photoinduced degradation of orange II on different iron (hydr)oxides in aqueous suspension: Rate enhancement on addition of hydrogen peroxide, silver nitrate, and sodium fluoride. Langmuir **24:**175-181.

11. **Grootveld, M., and C. J. Rhodes.** 1995. Methods for the detection and measurement of reactive radical species *in vivo* and *in vitro*. Academic Press Limited, London.

12. **Gupta, A. K., and M. Gupta.** 2005. Synthesis and surface engineering of iron oxide nanoparticles for biomedical applications. Biomaterials **26:**3995-4021.

13. **Hankin, L., and S. L. Anagnostakis.** 1977. Solid media containing carboxymethylcellulose to detect Cx cellulase activity of micro-organisms. J. Gen. Microbiol. **98:**109-115.

14. **He, F., and D. Zhao.** 2005. Preparation and characterization of a new class of starch-stabilized bimetallic nanoparticles for degradation of chlorinated hydrocarbons in water. Environ. Sci. Technol. **39:**3314-3320.

15. **He, F., D. Zhao, J. Liu, and C. B. Roberts.** 2007. Stabilization of Fe-Pd nanoparticles with sodium carboxymethyl cellulose for enhanced transport and dechlorination of trichloroethylene in soil and groundwater. Ind. Eng. Chem. Res. **46:**29-34.

16. **Hu, J., I. Lo, and G. Chen.** 2004. Removal of Cr (VI) by magnetite nanoparticle. Water Sci. Technol. **50:**139-46.

17. **Hussain, S. M., K. L. Hess, J. M. Gearhart, K. T. Geiss, and J. J. Schlager.** 2005. *In vitro* toxicity of nanoparticles in BRL 3A rat liver cells. Toxicol. in Vitro **19:**975-983.

18. **Jiang, W., H. Mashayekhi, and B. Xing.** 2009. Bacterial toxicity comparison between nano- and micro-scaled oxide particles. Environ. Pollut. **157:**1619-1625.

19. **Kang, S., M. Pinault, L. D. Pfefferle, and M. Elimelech.** 2007. Single-walled carbon nanotubes exhibit strong antimicrobial activity. Langmuir **23:**8670-8673.

20. **Kecskes, L. J., R. H. Woodman, S. F. Trevino, B. R. Klotz, S. G. Hirsch, and B. L. Gersten.** 2003. Characterization of a nanosized iron powder by comparative methods. KONA **21:**143-150.

21. **Kim, J. S., E. Kuk, K. N. Yu, J.-H. Kim, S. J. Park, H. J. Lee, S. H. Kim, Y. K. Park, Y. H. Park, C.-Y. Hwang, Y.-K. Kim, Y.-S. Lee, D. H. Jeong, and M.-H. Cho.** 2007. Antimicrobial effects of silver nanoparticles. Nanomed-nanotechnol. **3:**95-101.

22. **Kishk, Y. F. M., and H. M. A. Al-Sayed.** 2007. Free-radical scavenging and antioxidative activities of some polysaccharides in emulsions. Food Sci. Technol.-LEB **40:**270-277.

23. **Lee, C., J. Y. Kim, W. I. Lee, K. L. Nelson, J. Yoon, and D. L. Sedlak.** 2008. Bactericidal effect of zero-valent iron nanoparticles on *Escherichia coli*. Environ. Sci. Technol. **42:**4927-4933.

24. **Lee, J., T. Isobe, and M. Senna.** 1996. Preparation of ultrafine Fe_3O_4 particles by precipitation in the presence of PVA at high pH. J. Colloid Interf. Sci. **177:**490-494.

25. **Leun, D., and A. K. SenGupta.** 2000. Preparation and characterization of magnetically active polymeric particles (MAPPs) for complex environmental separations. Environ. Sci. Technol. **34:**3276-3282.

26. **Li, X.-q., D. W. Elliot, and W.-x. Zhang.** 2006. Zero-valent iron nanoparticles for abatement of environmental pollutants: Materials and engineering aspects. Crit. Rev. Solid State **31:**111-122.

27. **Li, Z., K. Greden, P. J. J. Alvarez, K. B. Gregory, and G. V. Lowry.** 2010. Adsorbed polymer and NOM limits adhesion and toxicity of nano scale zerovalent iron to *E. coli*. Environ. Sci. Technol.**:**DOI:10.1021/es9031198.

28. **Lin, H.-Y., and C.-C. Chou.** 2004. Antioxidative activities of water-soluble disaccharide chitosan derivatives. Food Res. Int. **37:**883-889.

29. **Mark, H., B. F., NM., and e. al.** 1986. Encyclopedia of Polymer Science and Engineering., vol. 3. Wiley-Interscience Publication., New York.

30. **Marmier, N., A. Delisée, and F. Fromage.** 1999. Surface complexation modeling of Yb(III), Ni(II), and Cs(I) sorption on magnetite. J. Colloid Interf. Sci. **211:**54-60.

31. **Masciagngioli, T., and W. X. Zhang.** 2003. Environmental technologies at the nanoscale. Environ. Sci. Technol. **37:**102-108.

32. **Mayo, J. T., C. Yavuz, S. Yean, L. Cong, H. Shipley, W. Yu, J. Falkner, A. Kan, M. Tomson, and V. L. Colvin.** 2007. The effect of nanocrystalline magnetite size on arsenic removal. Sci. Technol. Adv. Mat. **8:**71-75.

33. **Mihelcic, J. R., D. R. Lueking, R. J. Mitzel, and J. M. Stapleton.** 1993. Bioavailability of sorbed- and separate-phase chemicals. Biodegradation **4:**141-153.

34. **Miles, A. A., and S. S. Misra.** 1938. The estimation of the bactericidal power of the blood. J. Hyg.-Cambridge **38:**732-749.

35. **Moeser, G. D., K. A. Roach, W. H. Green, P. E. Laibinis, and T. A. Hatton.** 2002. Water-based magnetic fluids as extractants for synthetic organic compounds. Ind. Eng. Chem. Res. **41:**4739-4749.

36. **Moseley, R., M. Walker, R. J. Waddington, and W. Y. J. Chen.** 2003. Comparison of the antioxidant properties of wound dressing materials-carboxymethylcellulose, hyaluronan benzyl ester and hyaluronan, towards polymorphonuclear leukocyte-derived reactive oxygen species. Biomaterials. **24:**1549-1557.

37. **Neal, A.** 2008. What can be inferred from bacterium–nanoparticle interactions about the potential consequences of environmental exposure to nanoparticles? Ecotoxicol. **17:**362-371.

38. **Neidhardt, F. C., P. L. Bloch, and D. F. Smith.** 1974. Culture medium for enterobacteria. J. Bacteriol. **119:**736-747.

39. **Noble, R., and Q. Gibson.** 1970. The reaction of ferrous horseradish peroxidase with hydrogen peroxide J. Biol. Chem. **243:**2409-2413.

40. **Pan, G., L. Li, D. Zhao, and H. Chen.** 2009. Immobilization of non-point phosphorus using stabilized magnetite nanoparticles with enhanced transportability and reactivity in soils. Environ. Pollut. **1:**1-6.

41. **Phenrat, T., T. C. Long, G. V. Lowry, and B. Veronesi.** 2009. Partial oxidation ("aging") and surface modification decrease the toxicity of nanosized zerovalent iron. Environ. Sci. Technol. **43:**195-200.

42. **Pick, E., and Y. Keisari.** 1980. A simple colorimetric method for the measurement of hydrogen peroxide produced by cells in culture. J. Immunol. Methods. **38:**161-170.

43. **Pick, E., and D. Mizel.** 1981. Rapid microassays for the measurement of superoxide and hydrogen peroxide production by macrophages in culture using an automatic enzyme immunoassay reader. J. Immunol. Methods **46:**211-226.

44. **Sauer, K., and A. K. Camper.** 2001. Characterization of phenotypic changes in *Pseudomonas putida* in response to surface-associated growth. J. Bacteriol. **183:**6579–6589.

45. **Sayes, C. M., R. Wahi, P. A. Kurian, Y. Liu, J. L. West, K. D. Ausman, D. B. Warheit, and V. L. Colvin.** 2006. Correlating nanoscale titania structure with toxicity: A cytotoxicity and inflammatory response study with human dermal fibroblasts and human lung epithelial cells. Toxicol. Sci. **92:**174-185.

46. **Shaw, S. Y., E. C. Westly, M. J. Pittet, A. Subramanian, S. L. Schreiber, and R. Weissleder.** 2008. Perturbational profiling of nanomaterial biologic activity. Proc. Natl. Acad. Sci. USA **105:**7387-7392.

47. **Si, S., A. Kotal, T. K. Mandal, S. Giri, H. Nakamura, and T. Kohara.** 2004. Size-controlled synthesis of magnetite nanoparticles in the presence of polyelectrolytes. Chem. Mater. **16:**3489-3496.

48. **Sondi, I., and B. Salopek-Sondi.** 2004. Silver nanoparticles as antimicrobial agent: a case study on *E. coli* as a model for Gram-negative bacteria. J. Colloid Interf. Sci. **275:**177-182.

49. **Teitzel, G. M., and M. R. Parsek.** 2003. Heavy metal resistance of biofilm and planktonic *Pseudomonas aeruginosa*. Appl. Environ. Microbiol. **69:**2313-2320.

50. **van Loosdrecht, M. C., J. Lyklema, W. Norde, and A. J. Zehnder.** 1990. Influence of interfaces on microbial activity. Microbiol. Mol. Biol. Rev. **54:**75-87.

51. **Vayssières, L., C. Chanéac, E. Tronc, and J. P. Jolivet.** 1998. Size tailoring of magnetite particles formed by aqueous precipitation: An example of thermodynamic stability of nanometric oxide particles. J. Colloid Interf. Sci. **205:**205-212.

52. **Wei, X., and R. C. Viadero Jr.** 2007. Synthesis of magnetite nanoparticles with ferric iron recovered from acid mine drainage: Implications for environmental engineering. Colloid Surface A. **294:**280-286.

53. **Yamaguchi, T., H. Takamura, T. Matoba, and J. Terao.** 1998. HPLC method for evaluation of the free radical-scavenging activity of foods by using 1,1-Diphenyl-2-picrylhydrazyl. Biosci. Biotech. Bioch. **62:**1201-1204.

54. **Yean, S., L. Cong, and e. al.** 2005. Effect of magnetite particle size on adsorption and desorption of arsenite and arsenate. J. Mater. Res. **20:**3255-3264.

55. **Yuan, P., M. Fan, D. Yang, H. He, D. Liu, A. Yuan, J. Zhu, and T. Chen.** 2009. Montmorillonite-supported magnetite nanoparticles for the removal of hexavalent chromium [Cr(VI)] from aqueous solutions. J. Hazard. Mater. **166:**821-829.

56. **Zhang, L., Y. Jiang, Y. Ding, M. Povey, and D. York.** 2007. Investigation into the antibacterial behaviour of suspensions of ZnO nanoparticles (ZnO nanofluids). J. Nanopart. Res. **9:**479-489.

Table 2.1. Summary of characteristics of magnetite nanoparticles

	Particle size[a] (29)	Surface area (m^2/g)	Zeta potential[a] (mV @ pH 7)	Photocatalytic rate (Abs/min)	Aggregation
Synthesized Fe_3O_4 with CMC	6.58 ± 3.93	176.0[b]	-67.0 ± 4.2	ND	None
Synthesized Fe_3O_4	22.0 ± 11.2	129.8	~0	-0.0007	Severe
Commercial Fe_3O_4 with CMC	22.1 ± 8.2	52.4[b]	-52.6 ± 6.7	ND	Mild
Commercial Fe_3O_4	23.3 ± 8.5	40.7	~0	-0.0007	Severe

[a] Mean ± standard deviation

[b] Calculated based on the equation from Kecskes et al. (2003) (20) and He and Zhao (2005) (14).

Table 2.2. Selected characteristics of bacteria used in the study

Organism	**Gram stain**	**First-order rate constant (h^{-1})**	**Doubling time (h)**	**Zeta Potential (mV)**
Escherichia coli	Negative	0.26	2.56	-18.5 ± 1.0
Pseudomonas aeruginosa	Negative	0.29	2.36	-15.9 ± 0.7
Bacillus subtilis	Positive	0.76	0.90	-22.4 ± 1.2
Enterococcus faecalis	Positive	0.44	1.56	-18.0 ± 0.3

Figure Legends

FIG. 2.1. TEM images of Fe_3O_4 nanoparticles. (A) Synthesized CMC stabilized Fe_3O_4, (B) Synthesized non-stabilized Fe_3O_4, (C) Commercial Fe_3O_4 powder resuspended in 0.5% CMC, and (D) Commercial Fe_3O_4 powder resuspended in water.

FIG. 2.2. XRD spectra of (A) Commercial Fe_3O_4 nanoparticles, (B) Synthesized Fe_3O_4, and (C) Synthesized Fe_3O_4 stabilized with CMC.

FIG. 2.3. Effects of UV light and commercial magnetite nanoparticles on cell growth as indicated by protein production: (A) *E. coli*, (B) *P. aeruginosa*, (C) *B. subtilis*, and (D) *E. faecalis*. Statistical significance: *, $p< 0.05$; **, $P< 0.01$; ***, $p< 0.001$. Error bars represent standard errors of three repeated experiments.

FIG. 2.4. Stimulating effect of magnetite suspensions on bacteria as a function of iron concentration. (A) Synthesized magnetite stabilized with 0.5% CMC, (B) Fe_3O_4 nanoparticles synthesized without stabilizer, (C) Commercial nanoparticles stabilized with 0.5% CMC, and (D) Filtrate collected from synthesized magnetite stabilized with 0.5% CMC. Statistical significance: *, $p< 0.05$; **, $P< 0.01$; ***, $p< 0.001$. Error bars represent standard errors of three repeated experiments.

FIG. 2.5. SEM images of *E. coli* in the presence of (A) Synthesized magnetite with 0.5% CMC stabilizer, (B) Synthesized magnetite without stabilizer, (C) Commercial magnetite powder resuspended in 0.5% CMC, and (D) MOPS medium only. Insets for (A) and (B) are TEM images for the respective treatment.

Starr et al. Fig. 2.1.

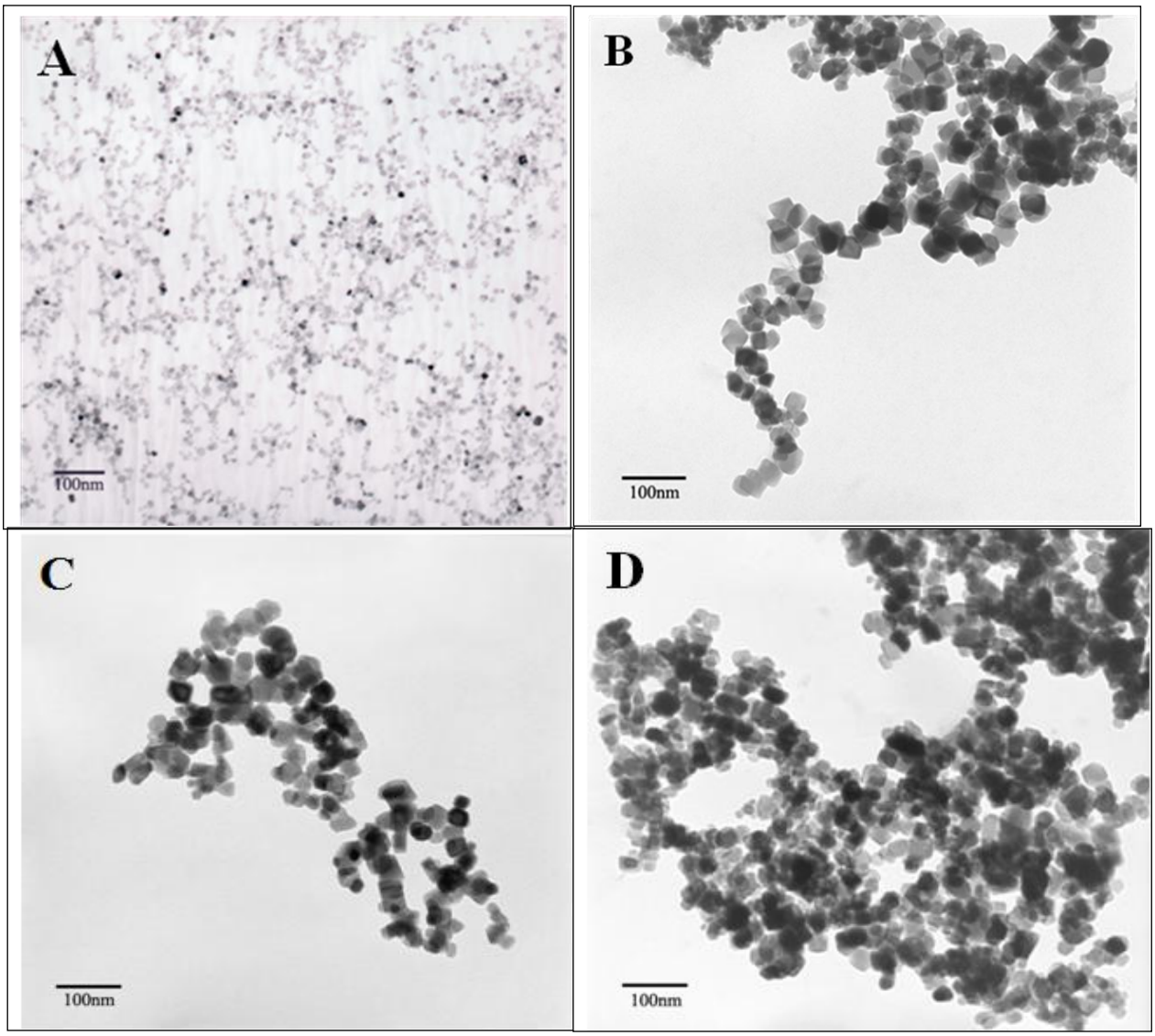

Starr et al. Fig. 2.2.

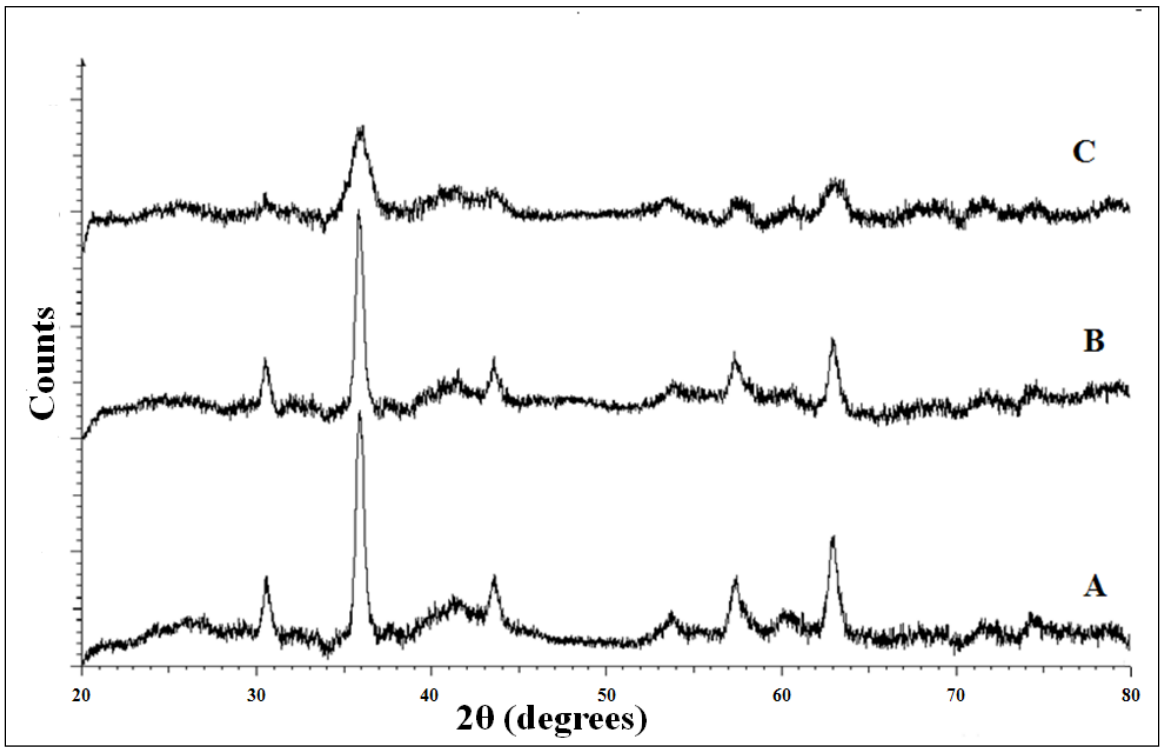

Starr et al. Fig. 2.3.

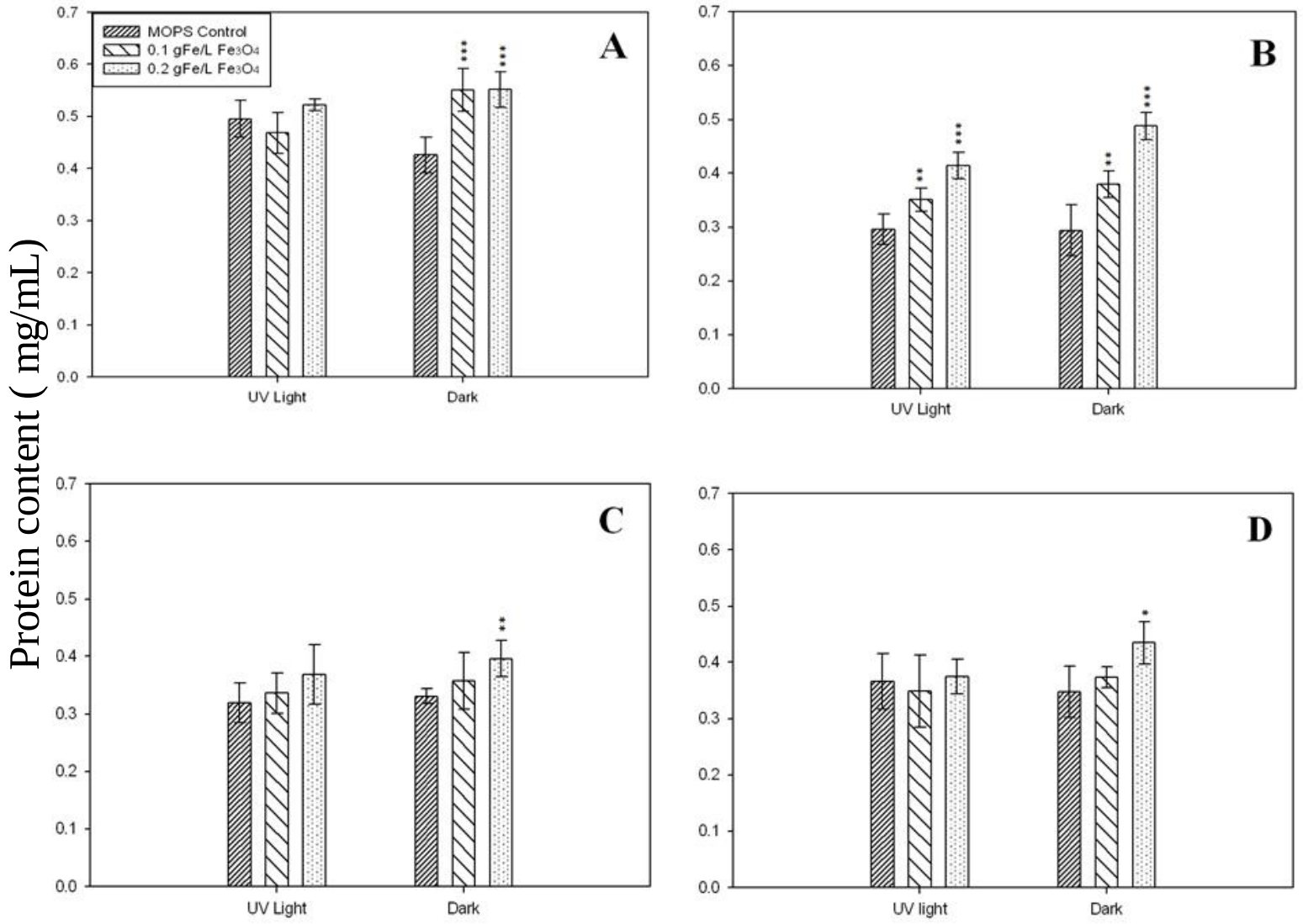

Starr et al. Fig. 2.4.

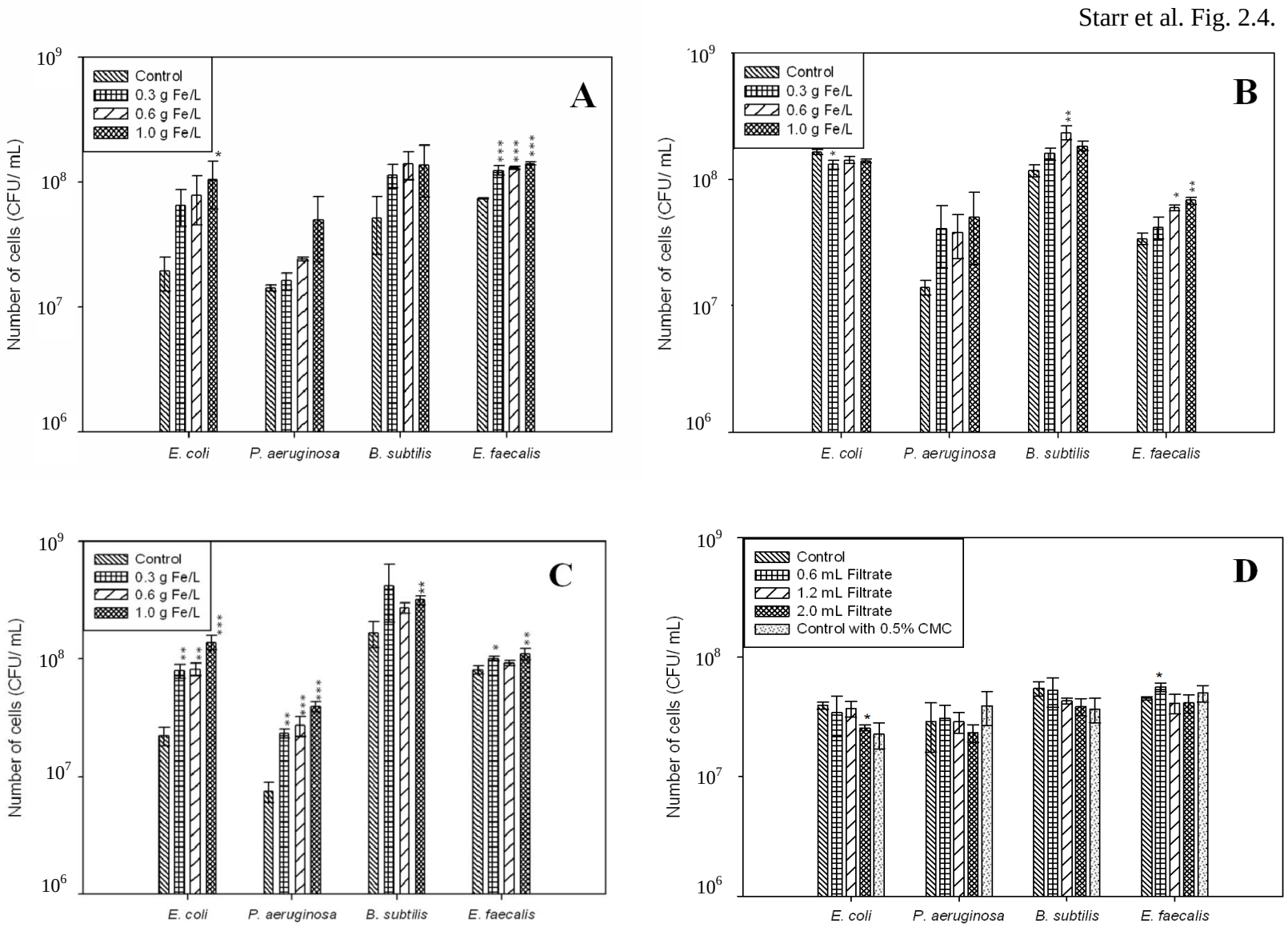

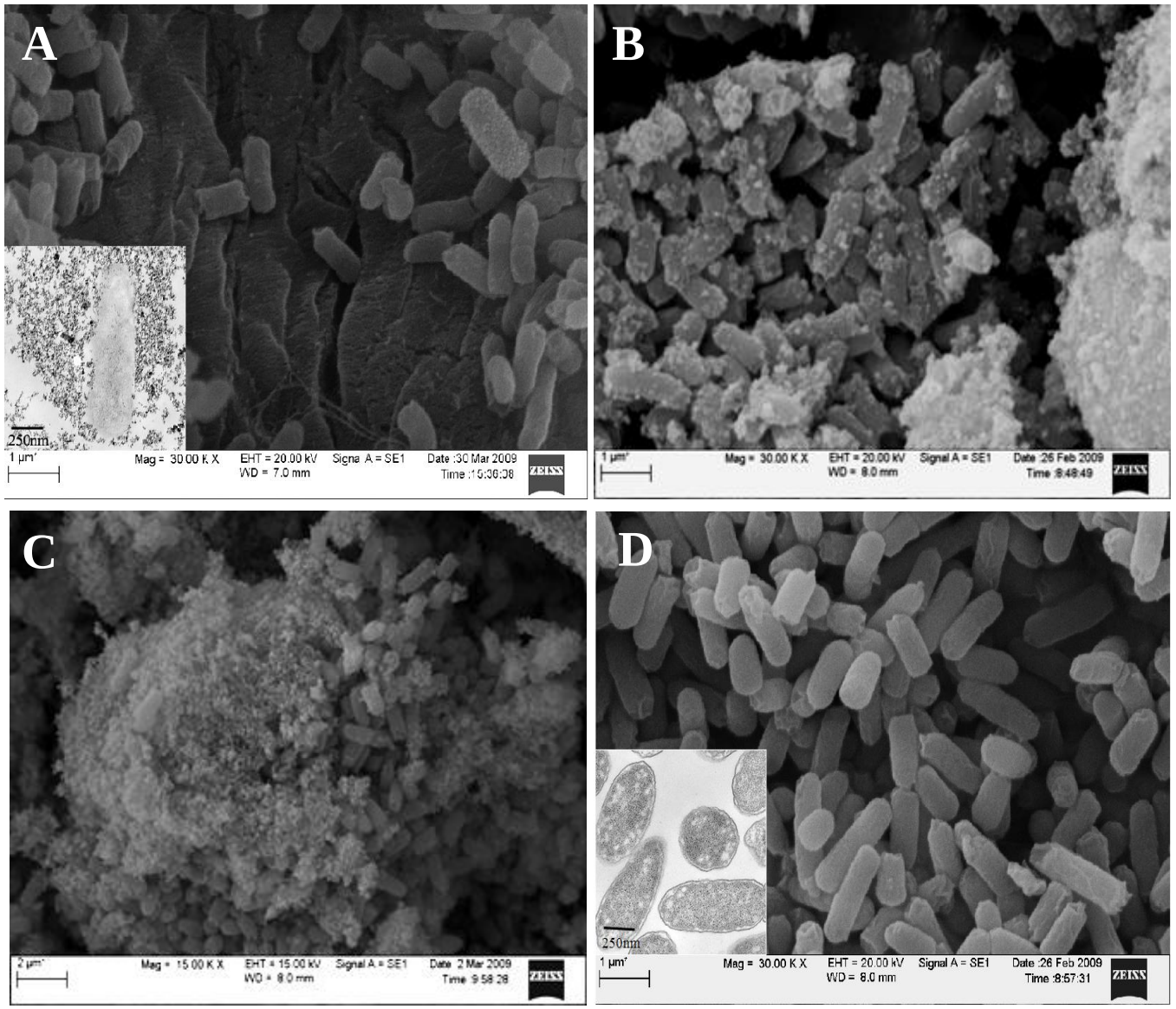

Starr et al. Fig. 2.5.

III. Effects of CMC- and Starch-Stabilized Fe_3O_4 Nanoparticles on Bacteria in Natural Water

Abstract

Stabilized magnetite nanoparticles for environmental remediation will be released directly to the environment. However, little is known regarding the impact of these nanoparticles on bacterial populations. Two stabilizers were compared on their stabilizing capabilities and inhibition of cell growth in simulated natural conditions. Use of starch as a stabilizer resulted in smaller nanoparticles but CMC lead to the formation of more uniform and stable nanoparticle suspensions over time. To evaluate possible microbial impact, suspensions of Fe_3O_4 were evaluated for toxicity toward four bacteria in stream water. The effect of commercial and lab-prepared Fe_3O_4 nanoparticles stabilized with CMC or starch was examined through cell viability experiments and thymidine uptake into cells. Results showed no toxicity when stabilized particles were used at a concentration of 0.01 g Fe/L, a realistic concentration cells would experience in water bodies. CMC-stabilized nanoparticles in ultrapure water showed the least masking of cell surface charge (zeta potential), indicating minimal interaction between cells and nanoparticles. Starch-stabilized nanoparticles demonstrated lower negative zeta potential, indicative of lower stability and greater interaction with cells. Thymidine studies of four nanoparticle treatments showed a dose dependent relationship between concentration and thymidine uptake in natural pond water. The majority of the Fe_3O_4 suspension's effect on cells was due to background electrolytes and nanoparticles themselves. Stabilized particles showed

greater inhibition of thymidine compared to bare particles. These results conclude that stabilized magnetite nanoparticles are not lethally toxic to bacteria in natural settings.

Introduction

Metal oxides are among the most used nanoparticles and have already entered the commercial market (2). Specifically, stabilized magnetite nanoparticles have potential for use in *in-situ* environmental remediation. Magnetite (Fe_3O_4) nanoparticles can remove contaminants such as As (V), As (III) (50), Pb (12), and Cr (VI) (20) in groundwater and soil. In addition to remediation which leads to the direct release of nanoparticles in the environment, magnetite nanoparticles will also enter water bodies through improper disposal of wastes (5). Van der Waals and magnetic forces cause these highly reactive magnetite nanoparticles to aggregate, an undesirable property for remediation. Synthesizing iron nanoparticles in the presence of a polymer stabilizer produces smaller particles and often prevents aggregation leading to a more monodisperse and stable suspension (17). A polymer layer also prevents oxidation affecting phase transformation according to Kim et al. (23). It has also been shown that encapsulation of magnetite nanoparticles can alter surface reactivity and create a diffusion barrier (43). CMC has proven to be an effective stabilizer for ZVI nanoparticles, reducing particle size and increasing TCE degradation in a sandy soil (19) and starch has been used to stabilize magnetite nanoparticles for *in vivo* studies (23). This surface modification of magnetite nanoparticles has also been suggested to influence interactions with cellular membranes (27). In the environment nanoparticles can be affected by light, oxidation, or microorganisms which can lead to chemical modification or functionalization of nanoparticles (40). Like all new technologies designed for

environmental application we must evaluate potential toxicity before its widespread implementation.

Much attention has been focused on health implication of nanoparticles, while ecotoxicology and behavior in the environment have not been well studied (40). There is little consensus concerning the effect Fe_3O_4 nanoparticles may have on bacteria after their release into water bodies, and very few studies have examined the effect of nanoparticles on bacterial cells (38). Lee et al. found no toxicity of Fe_3O_4 (9 mg/L) towards *E. coli* after one hour in buffer and increased toxicity of ZVI in anaerobic compared to aerobic conditions (28). Auffan et al. demonstrated that Fe_3O_4 was toxic to *E. coli* in ultrapure water after one hour for doses higher than 700 mg/L and toxicity increased in the double mutant *sodA sodB* that is lacking antioxidant enzymes (3), supporting the assumption that ROS are responsible for cell damage (38). Using five nanoparticle types, one study compared ROS production in pure water and media. More superoxide was produced in media and more singlet oxygen was produced in pure water (9). In natural environments organic matter can lead to coated nanoparticles (40), resulting in altered surface properties. Nanoscale zero-valent iron (NZVI) was shown to be efficiently coated with humic acids altering aggregation patterns (14). Organic matter or stabilizer prevented adhesion between *E. coli* and ZVI and lowered toxicity (30). Since changes in surface properties brought about by changes in environmental conditions such as light, pH, and ionic strength have not been studied thoroughly (40), it is difficult to predict the effect stabilized nanoparticles will have in a natural setting. Another aspect in need of study is the effect of surface modification on nanomaterials' interaction with microorganisms. Surface modification with an appropriate stabilizer has been shown to reduce toxicity in previous studies (30). In one study, gold nanoparticles coated with positively charged surface modifier were more toxic than those coated

with negatively charged modifier (16), showing the impact of electrostatic repulsion between negative charges of coated nanoparticles and bacteria. In the environment, nanoparticles and their stabilizers undergo significant degradation, transformation, and aggregation in water (11) and natural colloids and salinity affect their bioavailability (34). Glucose, resulting from degradation of CMC and starch can be assimilated by microbes (43), which demonstrates the biocompatibility of these stabilizers.

ROS producing nanoparticles can lead to DNA, protein, and membrane damage (9) and its toxicity to bacteria and protozoa has been demonstrated by ecotoxicological studies (40). Cell and nanoparticle interaction is an important factor for toxicity determined by surface chemistry and reactivity (34). For silver nanoparticles, only individual particles (1 to 10 nm), not aggregates, can attach to *E. coli* cell membranes and disturb respiration and membrane permeability (36). A study in 2009 showed CMC coated nanoparticles grew into microparticles after cellulase degraded the CMC layer to glucose (43), which will ultimately limit their interaction with bacteria due to increased size. Related inorganic nanoparticles such as ZnO can be internalized by bacteria (7) and CeO_2 nanoparticles are adsorbed onto the *E. coli* cell wall (47). Nanoparticle size and shape are also parameters affecting toxicity since silver nanoparticles undergo a shape dependent interaction with *E. coli* based on active facets (42). For one study, a higher concentration of gold nanoparticles (2-3 fold) was needed to rupture *E. coli* compared to red blood cells, suggesting bacteria are more resistant to nanoparticle toxicity. Protection was suggested to be provided by the outer membrane and cell wall (16). It was also demonstrated that gold nanoparticle toxicity is related to cell membrane interaction and it is possible to ameliorate toxicity with nanoparticle surface modification as previously mentioned (16).

In addition to a nanoparticle effect, toxicity may result from dissolved metal ions (i.e. Fe) (28). Free ions can also facilitate cell wall damage, allowing nanoparticles access inside cells where they could not previously enter (38). For example, silver nanoparticles interact with cell membranes and subsequently release ions which have an additional contribution to toxicity (36). Likewise, another study found that nano Ag is more toxic than silver ions for *E. coli* (32).

The objectives of this study were to 1) compare starch and CMC for their stabilizing ability, 2) determine the effects of stabilized Fe_3O_4 nanoparticles on the survival of four pure cultures of bacteria in stream water, and 3) determine the impact of stabilized Fe_3O_4 nanoparticles on the indigenous bacterial population in pond water. Since nanoparticles are likely to be diluted in the environment, we used lower concentrations of nanoparticle suspensions in this study for bacterial exposure. Using zeta potential we also hoped to gain insight into nanoparticle stability under biotic conditions, since zeta potential has been used successfully to predict interaction between bacteria and various surfaces (29). We hypothesize that negatively charged CMC coated nanoparticles will be less toxic to bacteria than starch coated nanoparticles due to electrostatic and electrosteric interactions.

Materials and Methods

Nanoparticle synthesis and characterization. Magnetite nanoparticles were synthesized as previously described (see Chapter II) to obtain a concentration of 0.5 g Fe/L in 0.2% stabilizer. CMC and starch were dissolved in ultrapure water and autoclaved prior to use. Freshly prepared nanoparticle stocks were kept overnight in airtight screw-cap glass vials with no airspace permitted until pH was adjusted just prior to the start of an experiment. TEM was carried out to determine size and aggregation state of nanoparticles stabilized with CMC and starch,

respectively. TEM was performed on a Zeiss EM 10C 10CR Transmission Electron Microscope. Ten µl of sample was placed on a formvar/carbon coated copper grid and allowed to dry down for 30 minutes, wicking away excess liquid. Grids were stored in a dessicator prior to microscopic observation. All nanoparticles suspensions were adjusted to pH 7 prior to TEM observation. Particle size of stabilized nanoparticles was determined using ImageJ (1). The average particle size was calculated based on greater than three representative images for each treatment with a minimum of 300 total particles counted. X-ray diffraction (XRD) was performed on freeze-dried magnetite nanoparticles using a D8 Discover X-Ray Diffractometer by Bruker-AXS with a GADDS area detector. Spectra were obtained for the 2θ range of 20 to 80 degrees. The filtrate was collected as follows: magnetite suspension aged for 24 hours was adjusted to pH 7 and filtered through an Amicon Ultra-15 centrifugal filter unit (100 KD molecular weight cutoff, Millipore, Billerica, MA) by centrifuging at 4000 x g for 1 hour. Dissolved iron present in nanoparticle filtrate was measured using a Varian Liberty Series II ICP-AES. Fourier-transform infrared spectroscopy (FTIR) was carried out to confirm the interaction between each stabilizer and Fe_3O_4 surface. Nanoparticle suspensions (0.5 g Fe/L with 0.2% stabilizer) were adjusted to pH 7 and centrifuged at 13,000 rpm for one hour until a small pellet was visible. Supernatant was decanted and the pellet was dried overnight in a VirTis Freeze Mobile Freeze dryer (Gardiner, New York). FTIR spectra were obtained for the stabilizer-coated nanoparticles by mixing nanoparticle powder with KBr for measurement in a Shimadzu IR Prestige-21 spectrometer.

Water samples. Water was collected at Parkerson Mill Creek in Auburn, Alabama in 2009 and 2010. Nitrogen, pH, and EC were determined on unfiltered samples. Prior to other analyses, the sample was filtered through a 0.45 µm filter. Nitrate and NH_4-N were determined

colorimetrically using a microplate reader (46). Phosphate was determined colorimetrically (37). Total N was determined by the Kjeldahl method (8). Total K, Ca, Mg, Mn, Na, Al, Fe, Zn were determined by Inductively Coupled Argon Plasma Spectroscopy (ICAP) (SPECTRO CIROS CCD, side-on plasma. Germany). Total organic carbon was measured on a Shimadzu TOC/TON analyzer. *E. coli* present in water samples was quantified using a Colilert Quanti-Tray (IDEXX , Westbrook, Maine) and pH and turbidity were measured using an Accumet 950 pH/ion meter (Fisher Norcross, GA) and a 2100N Turbidimeter (Hach, Loveland, Colorado), respectively. Direct counts of pond water were performed using a standard procedure (6). Number of bacteria dividing per hour ($N\ h^{-1}$) and specific growth rate was calculated using a well established calculation (35).

Nanoparticle stability in natural water. Stock suspensions of CMC-stabilized and starch-stabilzed Fe_3O_4 were prepared as before and diluted to reach final concentration of 0.01 g Fe/L in filtered natural stream water and ultrapure water. A final volume of 10 mL in 45-mL borosilicate glass vials was placed on a platform shaker in a manner described below. Zeta potential was determined on a Zetasizer Nano-ZS (Malvern Instruments, Worcestershire, UK) to measure change in overall charge. Viscosity was measured using a falling ball viscometer (Gilmont Instruments, Barrington, IL). To compare biotic and abiotic nanoparticle suspensions in stream water, an initial inoculum size corresponding to 10^5 cell/mL for each organism was added prior to zeta potential measurement.

Effect of nanoparticle suspensions on bacterial survival in natural water. *E. coli* K-12 strain MG1655 and *E. faecalis* ATCC 19433 were purchased from the American Type Culture Collection (ATCC). *P. aeruginosa*, and *B. subtilis* were obtained from Auburn University Biological Sciences Microbiology culture collection. Natural stream water was filter sterilized

through a 0.2 μM filter. In the case of commercial magnetite powder, 20 mL disposable borosilicate glass vials were used to incubate cultures for 24 hours. During the first six hours vials were exposed to UV light and then covered with aluminum foil for the remaining 18 hours. Commercial magnetite was sonicated as previously mentioned prior to the beginning of the experiment and diluted to a final concentration of 0.1 g Fe/L.

For the comparison of CMC-stabilized and starch-stabilized nanoparticles 20 mL vials were used to incubate cultures for 6 hours. Stock suspensions of 0.5 g Fe/L with 0.2% stabilizer were diluted to reach a final concentration of 0.01 g Fe/L for stabilized magnetite suspensions. Borosilicate glass allowed UV light (>300 nm) to penetrate the vials and reach the nanoparticles, simulating natural UV exposure of aqueous environments. The 60 watt Mega-Ray UV lamp (Cedar Point, NC) was placed 30.5 cm away from the vial platform, which was partially immersed in a 37˚C shaking waterbath. The total UV irradiance (300-400 nm) monitored by a Solar Light radiometer (Glenside, PA) equipped with a UVA + UVB detector was 200 $\mu W/cm^2$. Cells were incubated overnight in glucose MOPS media (39) prior to inoculation. The initial inoculum corresponded to 10^7 for the evaluation of commercial magnetite on cell viability and 10^5 CFU/ mL for CMC- and starch-stabilized nanoparticle experiments. Cells were counted using the Miles and Misra drop count technique (33).

Effect of CMC stabilized nanoparticle suspensions on bacterial function. Bacterial growth was measured by measuring the incorporation of [^{3}H] thymidine into cells following a modified procedure (26). The overall experiment was conducted on two separate occasions to ensure trend consistency. Triplicate 1.5 mL pond water samples and controls were placed into sterile 2-mL microcentrifuge tubes. Blanks were prepared by adding 75 μL of trichloroacetic acid solution (TCA) prior to the addition of [^{3}H] thymidine. Nanoparticles treatments (synthesized bare Fe_3O_4,

commercial Fe_3O_4, and synthesized Fe_3O_4 with CMC or starch) were added to reach a final concentration of 0.01 and 0.05 g Fe/L and allowed to equilibrate for 10 minutes prior to incubation with 50 nM [^{3}H]thymidine (25Ci/mmol, Moravek Biochemicals, Brea, California) for 40 minutes, a time chosen based on prior time course experiments. Samples were inverted once every ten minutes to ensure adequate mixing. The incubation was terminated by the addition of 75 uL ice-cold TCA and samples were kept refrigerated for one hour. Samples were then centrifuged at 12,000 rpm for 15 minutes (Eppendorf Centrifuge 5415D) and the supernatant was decanted carefully. Next, samples were treated with 1.5 mL ice-cold TCA and 80% ethanol sequentially. After each addition the samples were centrifuged and the supernatant decanted. Finally, 1.2 mL scintillation cocktail (Scintisafe Econo1) was added to the residue remaining in the 2 mL tubes and radioactivity was determined with a multi-purpose scintillation counter (LS 6500 Liquid Scintillation Counter, Beckman Coulter, USA). [^{3}H]thymidine taken up by the bacteria in unamended water samples and nanoparticle amended samples was calculated by subtracting the corresponding blanks and calculating the percent decrease. Since temperature, pH, turbidity variation from day to day lead to differing specific growth rates, percent decrease was calculated to allow comparison of treatments performed on different days. This experiment was also carried out with nanoparticle filtrates collected from nanoparticle suspensions to rule out effects due to dissolved compounds. Statistical significance was determined by mean comparison performed at alpha = .05 and 0.1.

Results

Nanoparticle synthesis and characterization. After aging overnight, the nanoparticle suspensions prepared with CMC retained its black color even after pH was adjusted from 11 to 7.

However, starch-stabilized particles began to change from black to brown shortly after pH adjustment. Starch acted as a more effective stabilizer for controlling size, producing an average particle diameter of 3.82 ± 2 nm (Fig. 3.1B). Using CMC as a stabilizing agent produced an average particle size of 5.05 ± 3 nm (Fig. 3.1A). It should be noted that CMC-stabilized particles also displayed a more uniform shape than starch-stabilized particles. It was clear from the spatial arrangement of magnetite nanoparticles seen in TEM images as well as visual observation of the suspension itself that while starch produced a smaller particle size, CMC produced a more stable and well dispersed suspension. Data obtained from centrifuged filtrates showed that more dissolved iron remained in solution when starch was the stabilizing agent compared to CMC. The filtrate from starch-stabilized suspension contained 0.528 ppm of dissolved iron, whereas CMC-stabilized suspension had 0.007 ppm of dissolved iron in the filtrate. TOC present in the filtrate was 635 ppm and 793 ppm for CMC- and starch-stabilized suspensions, respectively. The filtrate collected from nanoparticles synthesized with starch contained more iron and carbon that could potentially influence observable toxicity compared to CMC. Supernatants from washed bare synthesized nanoparticles were also collected after the first and third washes and analyzed for dissolved iron. The first bare nanoparticle wash contained 2.47 ppm Fe and the third wash with ultrapure water contained 0.099 ppm Fe. XRD analysis (Fig. 3.2) confirmed that synthesized products were magnetite. XRD analysis also showed that particle size decreased with the use of stabilizers, as supported by TEM.

FTIR spectra obtained from commercial Fe_3O_4, bare synthesized Fe_3O_4, as well as synthesized Fe_3O_4 with CMC and starch were consistent with spectra obtained from previous studies (19, 48). When comparing the spectra of CMC synthesized particles, CMC only, and CMC added to particles post synthesis, the peaks were not identical. Similar differences were

noticeable between starch stabilized particles, starch only, and starch added to particles post synthesis (Fig. 3.3). Characteristic bands/peaks were present for bare magnetite (15, 31, 48, 52), starch (18, 22-24), and CMC (19, 45, 51), supporting XRD and TEM evidence that the stabilizer was in fact interacting with the surface of Fe_3O_4 nanoparticles. Using the equation provided by He et al. (19):

$\Delta\nu = \Delta(\text{asym}) - \Delta(\text{sym})$

The binding between an iron nanoparticle surface and CMC was calculated to be bidentate by subtracting the symmetric COO- band value from COO-asymmetric band value. Our $\Delta\nu$ was determined to be 176 cm^{-1} (1595-1419 cm^{-1}), suggesting our particles also demonstrate bidentate binding (45). Comparing the spectra of synthesized bare particles and commercial powder provided more supporting evidence that our particles are magnetite (Fig. 3.3C).

Nanoparticle stability in natural water. Ultrapure water has lower ionic strength than stream water, and has fewer constituents to interact/interfere with charged surfaces. Bacteria had lower zeta potentials in stream water compared to ultrapure water for all four organisms (Fig. 3.4). The measurable decrease in zeta potential in stream water suggests charge neutralization due to environmental compounds. We expected negatively charged bacteria to interact with starch-stabilized particles to a greater extent than CMC-stabilized particles due to the charge repulsion between bacteria and CMC. CMC's greater negative charge compared to starch should result in bacteria interacting with starch coatings preferentially over CMC coatings. For all four treatments (combination of stabilizers and water types) there was little difference between the zeta potential of the sterile water control and the samples containing bacteria (Fig. 3.4), suggesting charge neutralization between nanoparticles and bacteria. The largest difference between the sterile control and biotic samples was seen in ultrapure water containing CMC-

stabilized particles. For ultrapure water with CMC-stabilized nanoparticles, it was also observed that zeta potentials for biotic samples remained more stable over time compared to the abiotic control. For both water types, zeta potentials were higher when CMC was used to stabilize nanoparticles compared to starch. This result is likely due to CMC carrying more negative charge than starch and the cell's surface charge coming into play. After measurement of bacterial zeta potential (Fig. 3.4), there was a greater loss of negative charge after addition of starch coated particles compared to CMC coated particles (Fig. 3.5), correlating to a decrease in stability.

Effect of commercial magnetite on bacterial survival in natural water. Characterization of stream water is shown in Table 3.1. In the control containing only bacteria and stream water, cells were allowed to die off at a natural rate. Assuming Fe_3O_4 nanoparticles physically damage bacteria (i.e. shrinking, shriveling, pit formation), cells would die off at an increased rate due to the induced stress in the dark samples. If UV light enhanced the toxicity of ROS production we would expect a discernable increase in the rate of cell death in the samples under UV light.

After 6 hours, cells died off steadily in the presence of UV light, but this die off was not accelerated by the presence of Fe_3O_4 nanoparticles. After 18 hours of subsequent darkness, the cells died off at a slower rate, but there was still no increase of cell death with Fe_3O_4 to suggest these nanoparticles were toxic in light or dark conditions (Fig. 3.6). At 0.1 g, Fe/L Fe_3O_4 did not increase cell death due to ROS in the presence of UV light or cell damage in dark conditions.

Effect of synthesized nanoparticle suspensions on bacterial survival in natural water. At a nanoparticle concentration of 0.01 g Fe/L there was no significant reduction in bacterial survival under UV light (Fig. 3.7) compared to the controls at 1 and 6 hours. CMC-stabilized nanoparticles as well as starch-stabilized nanoparticles did not interact with bacteria strongly

enough to produce a decrease in viable bacteria measurable in cell counts. CMC and starch alone did not affect cell viability, showing that these stabilizers are safe for delivering nanoparticles during remediation.

Effect of CMC stabilized nanoparticle suspensions on bacterial function. Characteristics of pond water samples for the analysis period are listed in Tables 3.1 and 3.2. Data from the days with closest temperatures was averaged. Commercial and bare synthesized nanoparticles resulted in lower thymidine uptake compared to the pond water control for both 0.01 and 0.05 g Fe/L (Fig. 3.8). Synthesized nanoparticle suspensions stabilized with CMC and starch lead to the formation of smaller and better dispersed nanoparticles, thus these stabilized nanoparticle suspensions reduced the amount of thymidine uptake more than the non-stabilized nanoparticle suspensions. For all four nanoparticle suspensions tested, as concentration increased, the percent decrease of thymidine uptake also increased, showing a dose-dependent relationship between nanoparticle suspension concentration and thymidine uptake (Fig. 3.8). The decrease in thymidine uptake caused by the CMC-stabilized nanoparticle suspension was attributed to background electrolytes and nanoparticles when applied at 0.05 g Fe/L ($\alpha = 0.05$). For starch-stabilized nanoparticles this same trend was observed. Stabilizer did not decrease thymidine uptake. Synthesized bare nanoparticles dispersed in ultrapure water had statistically the same effect on thymidine uptake as the electrolytes in the third wash collected from washed particles, suggesting the effect of synthesized bare nanoparticles on cells was mostly due to the dissolved salts and change in ionic strength, not a unique nanoparticle effect. Commercial bare nanoparticles effected thymidine uptake despite simply being dispersed in ultrapure water.

Discussion

Starch-stabilized nanoparticles appeared more susceptible to oxidation and dissolution compared to CMC-stabilized nanoparticles based on particle size and observable color change. Both TEM and XRD data showed decreases in size and crystallinity of magnetite with the addition of stabilizer during synthesis. Since starch produced smaller particles yet CMC produced more stable suspensions, there is a clear trade off to consider when comparing these two stabilizers. The fact that more dissolved iron was found in starch-stabilized suspensions compared to CMC-stabilized suspensions has implications for toxicity studies. It is proposed that the addition of a polymer layer on magnetite can prevent oxidation (23) but this protective action is likely different for each stabilizer. The biological impact of iron can be completely changed by its oxidation state since controlling oxidation can control ion release (4, 5). For metal nanoparticles, toxicity can result from metal dissolution as well as the nanoparticle effect. For toxicity studies where dissolved iron could be a cause of toxicity (28), this should be noted when choosing an appropriate stabilizer. There are two possibilities that could have led to higher dissolved iron detected in starch stabilized suspensions: (1) starch was less efficient at capturing iron during the formation of nanoparticles, allowing only a fraction of the iron nuclei to form and the remaining iron to remain dissolved or (2) smaller starch-stabilized nanoparticles dissolved more than CMC-stabilized nanoparticles. CMC kept nanoparticles physically separated as shown by TEM, and even at lower pH, CMC was capable of maintaining good nanoparticle coverage to yield a more stable suspension over time. Nanoparticles synthesized with starch and CMC consist of glucose which is biocompatible, nontoxic, and biodegradable (22, 43). It is likely both stabilizers will break down easily in the environment.

FTIR data support the binding of CMC and starch with the particle's surface. Differences between peaks observed for stabilizer bound to nanoparticle surfaces and peaks observed for powdered stabilizer added to particles post synthesis supports the visual observation of nanoparticle-stabilizer interaction observed in TEM images. After pH was reduced 11 to 7, the interaction between nanoparticle and stabilizer persisted. However, the bond can be easily broken down by enzymes present in the environment. CMC is a beneficial stabilizer not only due to its stabilizing properties but also its ease of biodegradation. The practical application of stabilized magnetite nanoparticles was described as "feasible and safe" since there are many bacteria in soils that produce cellulase capable of degrading CMC into glucose, a compound easily assimilated by microbes (43). Dextran, another stabilizer, can easily be desorbed which can lead to direct contact of organisms with nanoparticles after release into the environment. CMC, on the other hand, may exist on particles for months without desorption (25). More research is needed to characterize and compare the degradation of CMC and starch in order to select an appropriate stabilizer for the task at hand.

Studying the effect of stabilizer on nanoparticle-cell interaction through zeta potential is important for understanding nanoparticle toxicity (38). Zeta potential is a measure of the particle/bacterium surface charge, and ultimately its stability. Zeta potential measurements were also used to predict interaction between charged species. This method of analysis has been shown capable of predicting interaction between bacteria and surfaces previously (29). The high zeta potential of bacterial cells decreased the most after the addition of starch-stabilized Fe_3O_4 in both water types. This reduction of zeta potential suggests a loss of stability and charge neutralization. Zeta potential data after Fe_3O_4 addition showed there was little difference between treatments except for the treatment with CMC coated nanoparticles in ultrapure water. The sterile

control became less stable over time compared to the suspensions with bacteria present. This treatment (Fig. 3.5C) also retained the highest zeta potential after the interaction between bacteria and nanoparticle surfaces. This suggests minimal interaction between these two surfaces (cells and CMC coated surfaces) in ultrapure water. If nanoparticles were attached heavily on the bacterial surface, there would be a masking or neutralization of the cell's negative charge, shown by zeta potential decrease which was not seen. For the other treatment using CMC coated particles, the compounds present in stream water could mask the cell's charge and promote aggregation between cells and nanoparticles by reducing electrostatic repulsion, indicated by a decrease in zeta potential. Contrarily, the presence of organic matter can reduce cell-nanoparticle interaction and reduce toxicity (30). For Cu nanoparticles, toxicity increased with increasing DOC and decreased with ionic strength, while for silver nanoparticles, toxicity decreased with an increase of DOC and ionic strength indicated with a MetPLATE assay (13). Clearly DOC and ionic strength are components of natural water systems that can drastically change nanoparticle aggregation and ultimately toxicity. Regardless of water type, both starch treatments were unstable indicated by a low negative zeta potential. Stream water compounds and nanoparticles are capable of masking the cell's surface charge in stream water, while only nanoparticles can mask surface chare in ultrapure water. At a certain ionic strength particle/bacterial charge can become completely masked (13), altering interactions. Based on zeta potential measurements, there appeared to be less interaction between cell surfaces and CMC coated nanoparticle surfaces in ultrapure water compared to other treatments. The electrostatic repulsion of CMC molecules in ultrapure water likely reduced interaction between nanoparticles and cells. However, in stream water, there was more interaction with cell surfaces, due to lack of electrostatic repulsion between starch molecules. Surface reactions, adsorption,

and redox state affect nanoparticle fate in the environment (4). In both water types, CMC was more capable than starch at preventing cell and nanoparticle interaction. The negative charge and steric hindrance resulting from CMC is likely the reason for this phenomenon (30). A previous study supporting this hypothesis showed that there was more interaction with L929 cells (64%) when using starch coated magnetic particles compared chitosan coated particles (positive charged) (73%) (22). Tailoring the separation of cells and nanoparticles by stabilizer could be essential to preventing toxicity, since direct contact between cells and nanoparticles is essential for ROS damage (38, 47).

In cell viability assays we compared bare particles as well as CMC- and starch-stabilized particles for toxicity. However, there was no toxicity observed so we set out to find an explanation. Since ROS formation occurs in rich growth media (44), we used stream water for this reason as well as to mimic natural conditions. It is also understood that the use of media or ultrapure water alone does not accurately micic the chemistry, reactivity and dispersion of nanoparticles in the environment (13). Given our organisms did not demonstrate slowed cell death in the presence of commercial nanoparticles, there must be a mechanism explaining this cell viability. Under UV light, there is a possibility that the dark nature of nanoparticle aggregates provide some reprieve from UV damage. However *E. coli* experienced some protective action under both dark and light conditions. Given the interaction observed with the naked eye as well as TEM images, it is likely the aggregates between bacteria and nanoparticle can exert some protective action. Cells involved in nanoparticle interaction are no longer free floating and perhaps some sort of biofilm-like benefits are being conferred (38, 41). These commercial nanoparticles are also much larger than freshly synthesized particles and are therefore less likely to coat bacterial surfaces strongly or exhibit strong reactivity. Nanoparticles

released into water bodies will likely oxidize quickly, making them less damaging than more reduced forms over time (5), since fully oxidized maghemite is very stable in biological media. In the case of ZVI, stronger bactericidal effects were seen under anaerobic conditions (28) suggesting as particles oxidize they will lose their toxicity over time.

Starch-stabilized nanoparticles were hypothesized to be more toxic than CMC-stabilized nanoparticles based on 1) their interaction with cells based on zeta potential, 2) higher concentration of dissolved iron due to their instability, and 3) the negative charge carried by CMC. For Fe_3O_4 nanoparticles coated with CMC or starch, there were no inhibitory effects observed. It is likely that despite no measurable differences between viable bacteria in the presence and absence of nanoparticle suspensions, nanoparticles themselves or stabilizer was coated on the cell surface. On a population scale there was no effect seen due to the addition of stabilized nanoparticles at a concentration of 0.01 g Fe/L. Likewise, aged ZVI particles (containing magnetite) were previously shown to be benign to bacteria (30). Another study using fibroblasts found >89% cell viability after addition of starch coated magnetite particles (22). One possibility is that bacteria are actually benefiting by the presence of stabilizer coated nanoparticles, which are reducing the UV light the cells experience. It is also proposed that surface coatings can mitigate UV induced reactive oxidants (49). Using 0.2% CMC stabilizer, hydroxyl radicals were reduced almost fifty percent, demonstrating the beneficial properties of CMC (21). The lowered surface reactivity of polymer coated nanoparticles could also prevent toxicity (43). In the presence of cellulase, CMC coated nanoparticles quickly aggregate over time, which could lead to limited interaction with bacteria in natural water based on size and settling (43). These results are encouraging since this study simulated the lower concentration of nanoparticles bacteria will encounter in a natural setting.

Since no toxicity or inhibition was observed in viability assays, thymidine uptake was measured with different nanoparticle treatments and controls to look for alternative stresses to the cell. Controls were performed to examine the effect ionic strength and stabilizer had on the overall nanoparticle suspension's effect to cells. Commercial nanoparticles lacked dissolved salts and stabilizer, yet still reduced thymidine uptake by indigenous organisms in pond water. For all nanoparticle treatments there was a concentration dependent effect observed. However, dissolved salts contributing to background electrolytes and nanoparticles themselves accounted for most of reduction in thymidine uptake at higher magnetite concentration. At lower magnetite concentration, the nanoparticle effect was more significantly different from background electrolytes. Nanoparticle controls were included to eliminate any quenching effect of nanoparticles during scintillation counting. While there was some quenching, the percent decrease from the control was much smaller than the percent decrease in the samples. We concluded the effects were due to the interactions between cells and nanoparticles and not due to any interaction between nanoparticles and thymidine. No decrease was observed in prior survival experiments measuring total cell numbers in media/stream water, yet thymidine uptake was reduced. Previous SEM results also demonstrated interaction between cells and nanoparticles with no observable detrimental effects to cells. Based on previous TEM images showing the heavy coating of nanoparticles on *E. coli* surfaces without visible cell damage, this uptake data supports the theory that even at high concentration magnetite nanoparticles are only slightly inhibitory to bacteria. Cells used in this study were mature cells grown under the minimal nutrient conditions of pond water. Nutrient availability is a proposed reason for the inhibition seen here compared to previous studies. CeO_2 nanoparticles toxicity was prevented when nanoparticles were put into contact with bacteria in growth medium (47). Under rich nutrient

conditions cells may show less inhibition, which is not detectable by plate count. Clearly there was some nanoparticle effect seen in the thymidine uptake study not observed using previous plate count methods. It has been shown that encapsulation of magnetite nanoparticles can alter surface reactivity and result in a diffusion barrier toward contaminants (43). One possibility is that during bacterial coating with nanoparticles a diffusion barrier is created which lowers nanoparticle reactivity and limits diffusion around the cell. We did not observe a nanoparticle effect significantly different from the dissolved iron effect at higher concentration, unlike the study comparing CdSe quantum dots to dissolved cadmium (44). Another study using eukaryotic cells showed a toxicity of iron oxide nanoparticles that could not be explained due to dissolved iron species and suggested a nanoparticle dependent toxicity (10), which we observed at lower concentration. The discrepancy between growth/survival studies and this cell function study demonstrates the need for further research into what processes if any are reduced, amplified, or shut down in bacteria in the presence of magnetite nanoparticles.

Combining the results in this study we concluded commercial magnetite nanoparticles as well as magnetite synthesized with CMC and starch was not significantly toxic to reduce viable cell numbers in stream water under UV light or darkness. There were no harmful effects seen in stream water, the likely medium where bacteria will encounter nanoparticles. However, results from thymidine studies suggest nanoparticles may cause more subtle impacts on cells that require further investigation. Lethal toxicity was not observed when Fe_3O_4 nanoparticle suspensions were added to bacteria, yet statistically significant non-lethal toxicity was observed in natural pond water. It is clear from the discrepancy between cell function and viability assay results that a myriad of tests examining several aspects of cell health are necessary to understand a nanoparticle's effect on bacteria.

References

1. **Abramoff, M. D., P. J. Magelhaes, and S. J. Ram.** 2004. Image processing with ImageJ. Biophotonics **11:**36-42.
2. **Aitken, R. J., M. Q. Chaudhry, A. B. Boxall, and M. Hull.** 2006. Manufacture and use of nanomaterials: current status in the UK and global trends. Occup. Med. **56:**300-306.
3. **Auffan, M., W. Achouak, J. Rose, M.-A. Roncato, C. Chaneac, D. T. Waite, A. Masion, J. C. Woicik, M. R. Wiesner, and J.-Y. Bottero.** 2008. Relation between the redox state of iron-based nanoparticles and their cytotoxicity toward *Escherichia coli*. Environ. Sci. Technol. **42:**6730-6735.
4. **Auffan, M., J. Rose, J.-Y. Bottero, G. V. Lowry, J.-P. Jolivet, and M. R. Wiesner.** 2009. Towards a definition of inorganic nanoparticles from an environmental, health and safety perspective. Nat. Nanotechnol. **4:**634-641.
5. **Auffan, M., J. Rose, M. R. Wiesner, and J.-Y. Bottero.** 2009. Chemical stability of metallic nanoparticles: A parameter controlling their potential cellular toxicity in vitro. Environ. Pollut. **157:**1127-1133.
6. **Bloem, J.** 1994. Direct microscopy counts for bacteria using soil smears and DTAF, p. 162-170. *In* K. Alef and P. Nannipieri (ed.), Methods in Applied Soil Microbiology and Biochemistry. Academic Press, New York.
7. **Brayner, R., R. Ferrari-Iliou, N. Brivois, S. Djediat, M. F. Benedetti, and F. Fievet.** 2006. Toxicological impact studies based on *Escherichia coli* bacteria in ultrafine ZnO nanoparticles colloidal medium. Nano. Letters **6:**866-870.
8. **Bremner, J. M.** 1965. Total nitrogen, p. 1149-1178. *In* C. A. Black (ed.), Methods of soil analysis, Part 2, vol. 9. Am. Soc. Agron., Inc., Madison, WI. .

9. **Brunet, L., D. Y. Lyon, E. M. Hotze, P. J. J. Alvarez, and M. R. Wiesner.** 2009. Comparative photoactivity and antibacterial properties of C_{60} fullerenes and titanium dioxide nanoparticles. Environ. Sci. Technol. **43:**4355-4360.

10. **Brunner, T. J., P. Wick, P. Manser, P. Spohn, R. N. Grass, L. K. Limbach, A. Bruinink, and W. J. Stark.** 2006. *In vitro* cytotoxicity of oxide nanoparticles: Comparison to asbestos, silica, and the effect of particle solubility. Environ. Sci. Technol. **40:**4374-4381

11. **Colvin, V. L.** 2003. The potential environmental impact of engineered nanomaterials. Nat. Biotech. **21:**1166-1170.

12. **D' Couto, H.** 2008. Development of a low-cost sustainable water filter: A study of the removal of water pollutants As (V) and Pb (II) using magnetite nanoparticles. J. US SJWP**:**32-45.

13. **Gao, J., S. Youn, A. Hovsepyan, V. Llaneza, Y. Wang, G. Bitton, and J. Bonzongo.** 2009. Dispersion and toxicity of selected manufactured nanomaterials in natural river water samples: Effects of water chemical composition. Environ. Sci.Technol. **43:**3322-3328.

14. **Giasuddin, A. B. M., S. R. Kanel, and H. Choi.** 2007. Adsorption of humic acid onto nanoscale zerovalent iron and its effect on arsenic removal. Environ. Sci. Technol. **41:**2022-2027.

15. **Giri, J., S. Guha Thakurta, J. Bellare, A. Kumar Nigam, and D. Bahadur.** 2005. Preparation and characterization of phospholipid stabilized uniform sized magnetite nanoparticles. J. Magn. Magn. Mater. **293:**62-68.

16. **Goodman, C. M., C. D. McCusker, T. Yilmaz, and V. M. Rotello.** 2004. Toxicity of gold nanoparticles functionalized with cationic and anionic side chains. Bioconjugate Chem. **15:**897-900.

17. **Gupta, A. K., and M. Gupta.** 2005. Synthesis and surface engineering of iron oxide nanoparticles for biomedical applications. Biomaterials **26:**3995-4021.

18. **Hai, T. H., L. H. Phuc, D. T. K. Dung, and N. T. l. Huyen.** 2008. Iron oxide nanoparticles with biocompatible starch and dextran coatings for biomedicine applications. Adv. Nat. Sci. **9:**87-92.

19. **He, F., D. Zhao, J. Liu, and C. B. Roberts.** 2007. Stabilization of Fe-Pd nanoparticles with sodium carboxymethyl cellulose for enhanced transport and dechlorination of trichloroethylene in soil and groundwater. Ind. Eng. Chem. Res. **46:**29-34.

20. **Hu, J., I. Lo, and G. Chen.** 2004. Removal of Cr (VI) by magnetite nanoparticle. Water Sci. Technol. **50:**139-46.

21. **Joo, S. H., and D. Zhao.** 2008. Destruction of lindane and atrazine using stabilized iron nanoparticles under aerobic and anaerobic conditions: Effects of catalyst and stabilizer. Chemosphere **70:**418-425.

22. **Kim, D.-H., K.-N. Kim, K.-M. Kim, and Y.-K. Lee.** 2009. Targeting to carcinoma cells with chitosan- and starch-coated magnetic nanoparticles for magnetic hyperthermia. J. Biomed. Mater. Res. A. **88A:**1-11.

23. **Kim, D. K., M. Mikhaylova, F. H. Wang, J. Kehr, B. Bjelke, Y. Zhang, T. Tsakalakos, and M. Muhammed.** 2003. Starch-coated superparamagnetic nanoparticles as MRI contrast agents. Chem. Mater. **15:**4343-4351.

24. **Kim, D. K., M. Mikhaylova, Y. Zhang, and M. Muhammed.** 2003. Protective coating of superparamagnetic iron oxide nanoparticles. Chem. mater. **15:**1617-1627.

25. **Kim, H.-J., T. Phenrat, R. D. Tilton, and G. V. Lowry.** 2009. Fe^0 Nanoparticles remain mobile in porous media after aging due to slow desorption of polymeric surface modifiers. Environ. Sci. Technol. **43:**3824-3830.

26. **Kirschner, A. K. T., and B. Velimirov.** 1999. Modification of the ^{3}H-leucine centrifugation method for determining bacterial protein synthesis in freshwater samples. Aquat. Microb. Ecol. **17:**201-206.

27. **Koh, I., B. H. Cipriano, S. H. Ehrman, D. N. Williams, and T. R. Pulliam Holoman.** 2005. X-ray scattering study of the interactions between magnetic nanoparticles and living cell membranes. J. Appl. Phys. **97:**084310.

28. **Lee, C., J. Y. Kim, W. I. Lee, K. L. Nelson, J. Yoon, and D. L. Sedlak.** 2008. Bactericidal effect of zero-valent iron nanoparticles on *Escherichia coli*. Environ. Sci. Technol. **42:**4927-4933.

29. **Li, B., and B. E. Logan.** 2004. Bacterial adhesion to glass and metal-oxide surfaces. Colloid Surface B. **36:**81-90.

30. **Li, Z., K. Greden, P. J. J. Alvarez, K. B. Gregory, and G. V. Lowry.** 2010. Adsorbed polymer and NOM limits adhesion and toxicity of nano scale zerovalent iron to *E. coli*. Environ. Sci. Technol.**:**DOI:10.1021/es9031198.

31. **Liu, Z. L., X. Wang, K. L. Yao, G. H. Du, Q. H. Lu, Z. H. Ding, J. Tao, Q. Ning, X. P. Luo, D. Y. Tian, and D. Xi.** 2004. Synthesis of magnetite nanoparticles in W/O microemulsion. J. Mater. Sci. **39:**2633-2636.

32. **Lok, C.-N., C.-M. Ho, R. Chen, Q.-Y. He, W.-Y. Yu, H. Sun, P. K.-H. Tam, J.-F. Chiu, and C.-M. Che.** 2006. Proteomic analysis of the mode of antibacterial action of silver nanoparticles. J. Proteome Res. **5:**916-924.

33. **Miles, A. A., and S. S. Misra.** 1938. The estimation of the bactericidal power of the blood. J. Hyg.-Cambridge **38:**732-749.

34. **Moore, M. N.** 2006. Do nanoparticles present ecotoxicological risks for the health of the aquatic environment? Environ. Int. **32:**967-976.

35. **Moriarty, D. J. W.** 1990. Techniques for estimating bacterial growth rates and production of biomass in aquatic environments, p. 211-234. *In* R. Grigorova and J. R. Norris (ed.), Methods in Microbiology, vol. 22. Academic Press.

36. **Morones, J. R., J. L. Elechiguerra, A. Camacho, K. Holt, J. B. Kouri, J. T. Ramírez, and M. J. Yacaman.** 2005. The bactericidal effect of silver nanoparticles. Nanotechnol. **16:**2346-2353.

37. **Murphy, J., and J. P. Riley.** 1962. A modified single solution method for determining phosphate in natural waters. Anal. Chim. Acta. **27:**31-36.

38. **Neal, A.** 2008. What can be inferred from bacterium–nanoparticle interactions about the potential consequences of environmental exposure to nanoparticles? Ecotoxicol. **17:**362-371.

39. **Neidhardt, F. C., P. L. Bloch, and D. F. Smith.** 1974. Culture medium for enterobacteria. J. Bacteriol. **119:**736-747.

40. **Nowack, B., and T. D. Bucheli.** 2007. Occurrence, behavior and effects of nanoparticles in the environment. Environ. Pollut. **150:**5-22.

41. **Olson, M. E., H. Ceri, D. W. Morck, A. G. Buret, and R. R. Read.** 2002. Biofilm bacteria: Formation and comparative susceptibility to antibiotics. Can. J. Vet. Res. **66:**86-92.

42. **Pal, S., Y. K. Tak, and J. M. Song.** 2007. Does the antibacterial activity of silver nanoparticles depend on the shape of the nanoparticle? A study of the gram-negative bacterium *Escherichia coli*. Appl. Environ. Microbiol. **73:**1712-1720.

43. **Pan, G., L. Li, D. Zhao, and H. Chen.** 2009. Immobilization of non-point phosphorus using stabilized magnetite nanoparticles with enhanced transportability and reactivity in soils. Environ. Pollut. **1:**1-6.

44. **Priester, J., P. Stoimenov, R. Mielke, S. Webb, C. Ehrhardt, J. Zhang, G. Stucky, and P. Holden.** 2009. Effects of soluble cadmium salts versus CdSe quantum dots on the growth of planktonic *Pseudomonas aeruginosa*. Environ. Sci. Technol. **43:**2589-2594.

45. **Si, S., A. Kotal, T. K. Mandal, S. Giri, H. Nakamura, and T. Kohara.** 2004. Size-controlled synthesis of magnetite nanoparticles in the presence of polyelectrolytes. Chem. Mater. **16:**3489-3496.

46. **Sims, G. K., T. R. Ellsworth, and R. L. Mulvaney.** 1995. Microscale determination of inorgainc nitrogen in water and soil extracts. Commun. Soil Sci. Plant Anal. **26:**303-316.

47. **Thill, A., O. Zeyons, O. Spalla, F. Chauvat, J. Rose, M. Auffan, and A. M. Flank.** 2006. Cytotoxicity of CeO_2 nanoparticles for *Escherichia coli*. Physico-chemical insight of the cytotoxicity mechanism Environ. Sci. Technol. **40:**6151-6156.

48. **Wang, L., J. Bao, L. Wang, F. Zhang, and Y. Li.** 2006. One-pot synthesis and bioapplication of amine-functionalized magnetite nanoparticles and hollow nanospheres. Chem. Eur. J. **12:**6341-6347.

49. **Warheit, D. B.** 2008. How meaningful are the results of nanotoxicity studies in the absence of adequate material characterization? Toxicol. Sci. **101:**183-185.

50. **Yean, S., L. Cong, and e. al.** 2005. Effect of magnetite particle size on adsorption and desorption of arsenite and arsenate. J. Mater. Res. **20:**3255-3264.

51. **Zaleska, H., P. Tomasik, and C. Lii.** 2002. formation of carboxymethyl cellulose-casein complexes by electrosynthesis. Food Hydrocolloid. **16:**215-224.

52. **Zhang, Y., C. Sun, N. Kohler, and M. Zhang.** 2004. Self-assembled coatings on individual monodisperse magnetite nanoparticles for efficient intracellular uptake. Biomed. Microdevices **6:**33-40.

Table 3.1. Selected chemical characteristics for stream and pond water used in this study.

	pH	EC S/m	NO3-N mg/L	NH4-N mg/L	Ca mg/L	Fe mg/L	Mg mg/L	P mg/L	TOC mg/L
Stream	7.5	0.002	0.581	0.169	19.35	0	11.23	0.039	21.12
Pond	6.3	0.1	0.717	0.095	10.916	0	4.769	0	20.9

Table 3.2. Characteristics of pond water samples collected over the study period.

Date	Temp (˚C)	pH	Turbidity (NTU)	*E. coli* cells/100 mL	Number of bacteria dividing per hour ($N\ h^{-1}$)	Specific growth rate (μ)
12/8/2009	11.5	6.658	12.8	1732.9	1.35E+05	----------
12/11/2009	10	7.666	15.9	575.4	1.99E+05	----------
12/17/2009	12	6.634	18.45	344.8	1.71E+05	----------
1/6/2010	4	6.958	14.8	52.9	2.25E+04	----------
1/7/2010	3.5	6.728	11.3	179.3	1.55E+04	0.12
1/12/2010	3.5	6.689	10.4	50.4	1.55E+04	0.14
1/25/2010	12	6.508	76.97	816.4	3.74E+04	----------
1/26/2010	10.5	6.604	49.4	290.9	3.92E+04	----------

Figure legends

Fig. 3.1. TEM images of Fe_3O_4 nanoparticles stabilized with (A) CMC and (B) starch.

Fig. 3.2. XRD spectra of (A) Commercial Fe_3O_4 nanoparticles, (B) Synthesized starch-stabilized Fe_3O_4, and (C) Synthesized CMC-stabilized Fe_3O_4.

Fig. 3.3. FTIR spectra for treatments of Fe_3O_4 nanoparticles: (A) Spectra for (I) CMC mixed with nanoparticle powder 1:1, (II) CMC powder control, and (III) Fe_3O_4 nanoparticles (0.5 g Fe/L) synthesized in the presence of CMC (0.2%). (B) Spectra for (I) starch mixed with nanoparticle powder 1:1, (II) Starch powder control, and (III) Fe_3O_4 nanoparticles (0.5 g Fe/L) synthesized in the presence of starch (0.2%). (C) Spectra of (I) Commercial Fe_3O_4 nanoparticles and (II) synthesized bare Fe_3O_4 nanoparticles.

Fig. 3.4. Zeta potential measurements over time of (A) *P. aeruginosa* and *E. faecalis* and (B) *E. coli* and *B. subtilis* in stream water and ultrapure water respectively.

Fig. 3.5. Zeta potential measurements over time in the presence of *E. coli*, *P. aeruginosa*, *B. subtilis*, and *E. faecalis* as a function of the combination of stabilizing agent and water type. (A) CMC-stabilized Fe_3O_4 in stream water, (B) Starch-stabilized Fe_3O_4 in stream water, (C) CMC-stabilized Fe_3O_4 in ultrapure water, and (D) Starch-stabilized Fe_3O_4 in ultrapure water.

Fig. 3.6. Bacterial survival in stream water after 6 hours of UV exposure and 18 hours of subsequent dark period. (A) *E. coli*, (B) *P. aeruginosa*, (C) *B. subtilis*, and (D) *E. faecalis*. Dashed line represents 0.1 g Fe/L of commercial bare particles and solid line represents stream water control.

Fig. 3.7. Bacterial survival in stream water after 1 and 6 hours of UV light exposure in the presence of CMC- and starch-stabilized synthesized Fe_3O_4 nanoparticles at 0.01 g Fe/L. (A) *E. coli*, (B) *P. aeruginosa*, (C) *B. subtilis*, and (D) *E. faecalis*.

Fig. 3.8. Percent decrease of [^{3}H] thymidine uptake by indigenous bacteria in pond water as a function of nanoparticle treatment and concentration. Statistical significance: *, alpha = .05.

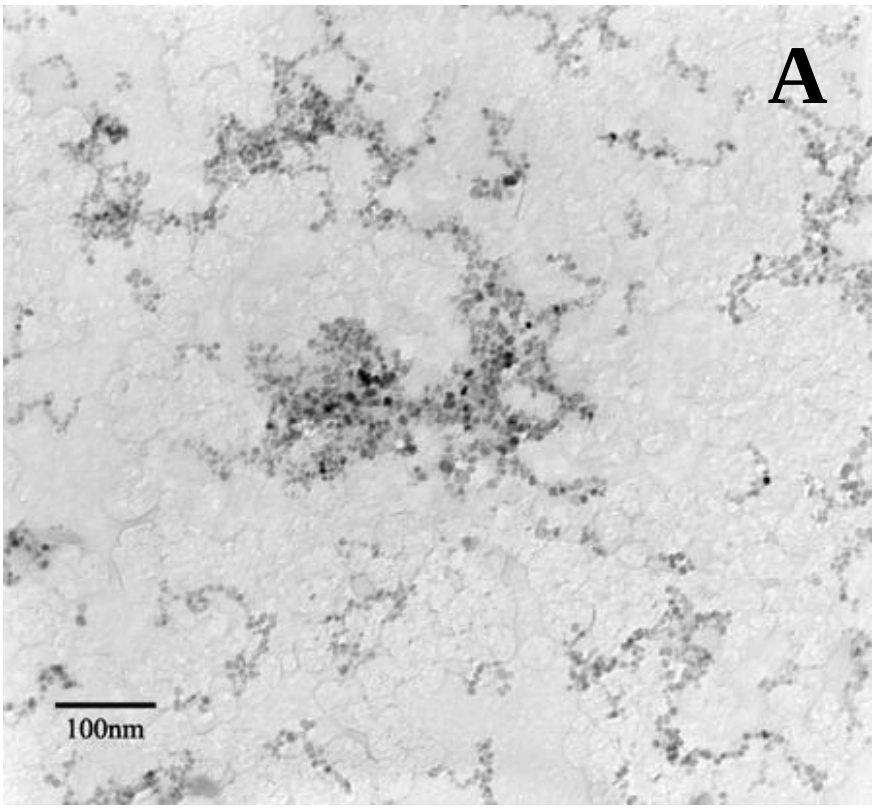

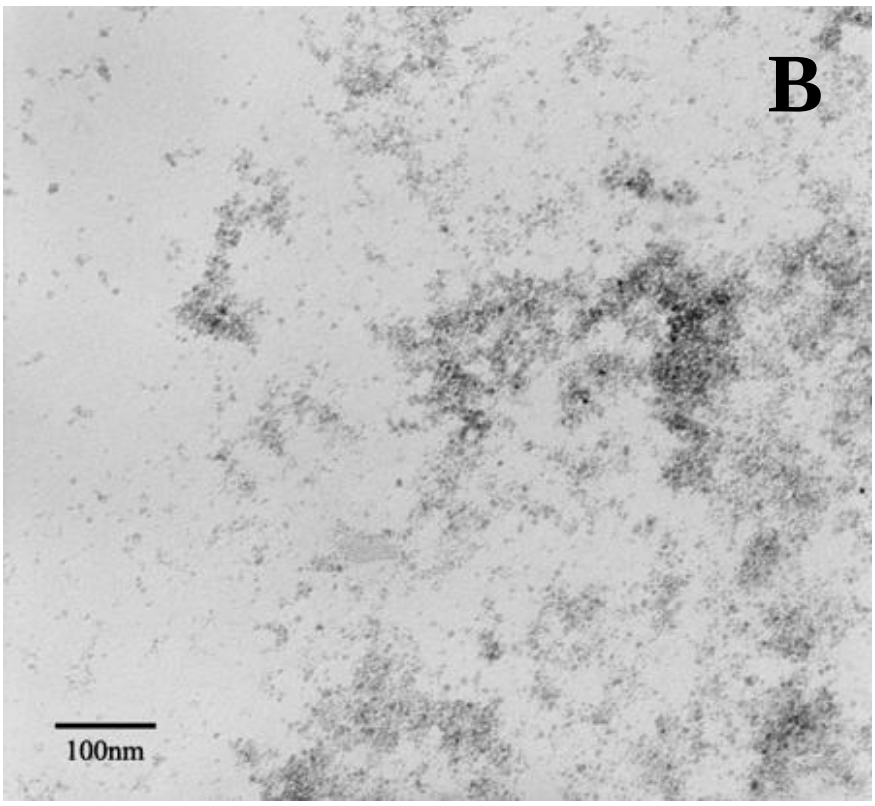

Starr et al. Fig. 3.1

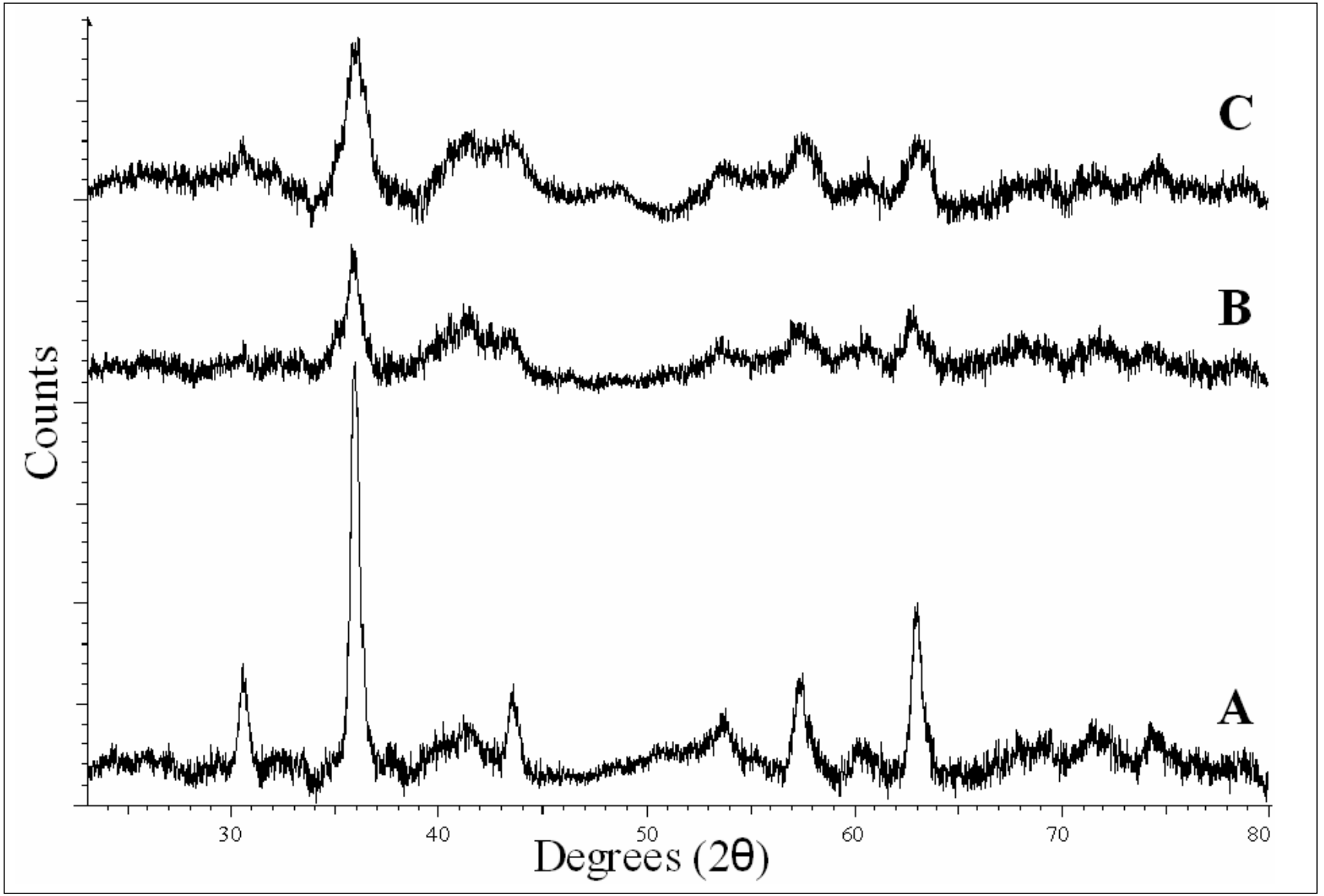
C
B
A
Counts
30
40
50
60
70
80
Degrees (2θ)

Starr et al. Fig. 3.3

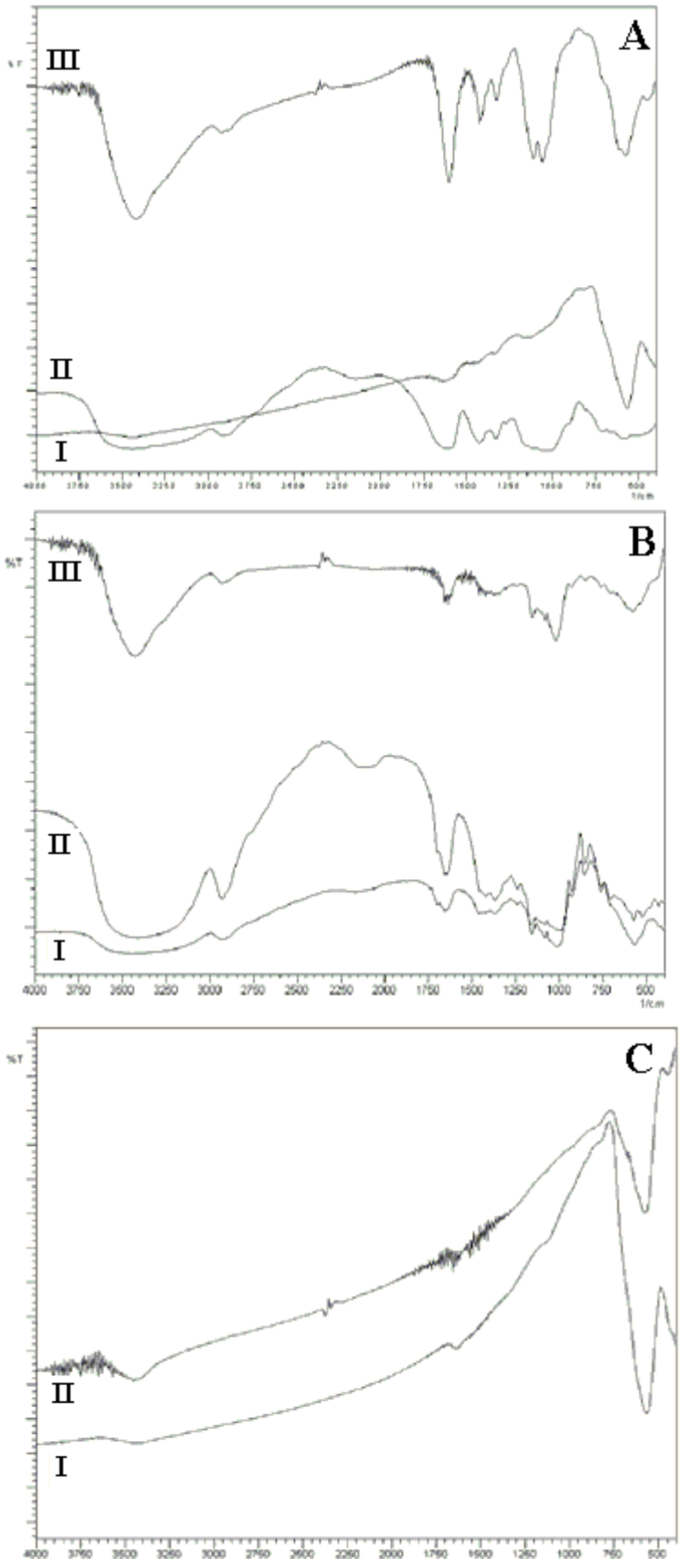

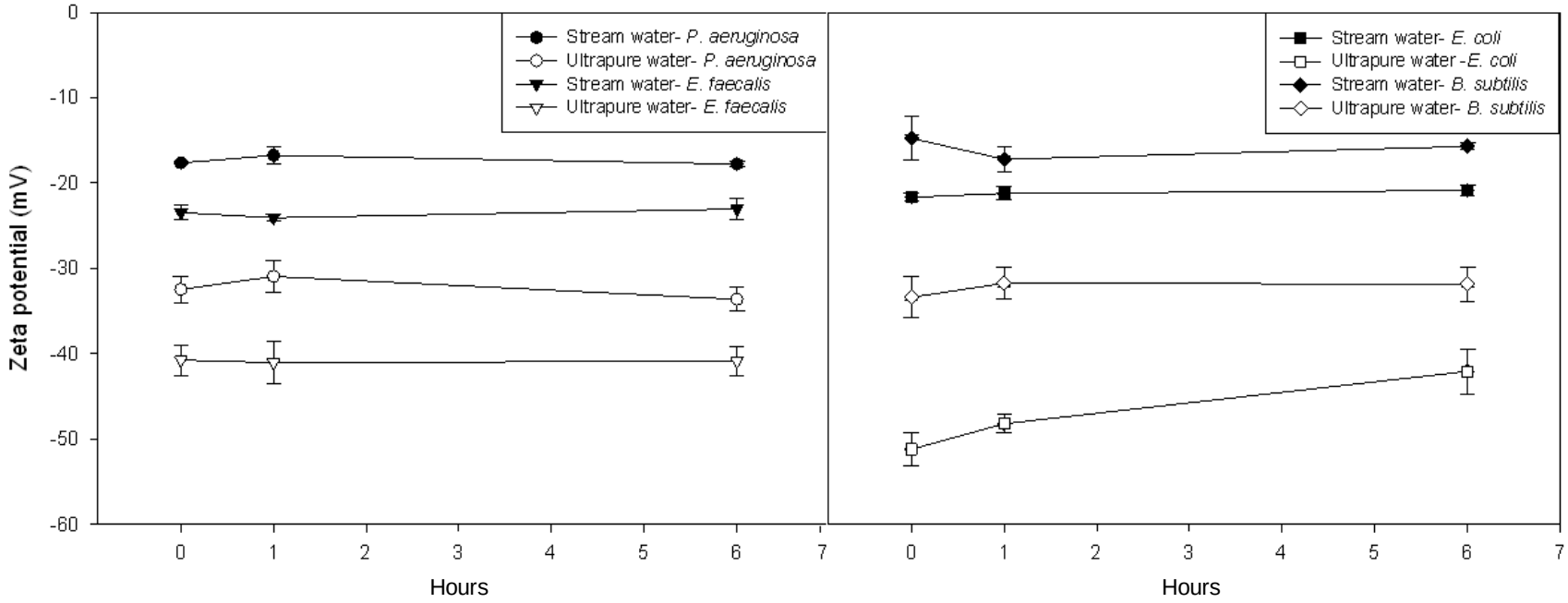
Zeta potential (mV)
0
-10
-20
-30
-40
-50
-60
0
1
2
3
4
5
6
7
Hours
Stream water- P. aeruginosa
Ultrapure water- P. aeruginosa
Stream water- E. faecalis
Ultrapure water- E. faecalis
Stream water- E. coli
Ultrapure water -E. coli
Stream water- B. subtilis
Ultrapure water- B. subtilis

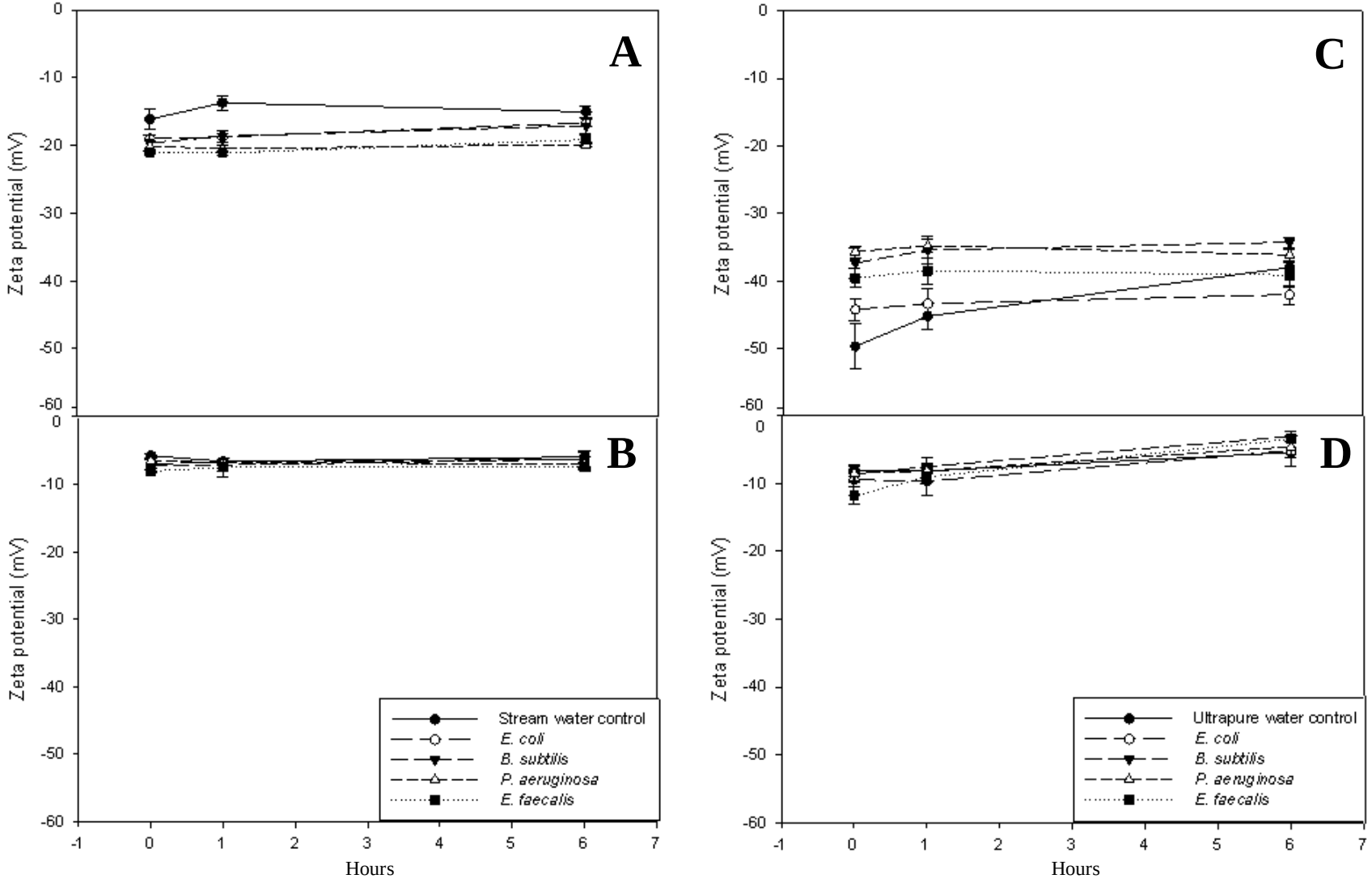
A
B
C
D
Zeta potential (mV)
Hours
Stream water control
Ultrapure water control
E. coli
B. subtilis
P. aeruginosa
E. faecalis

102

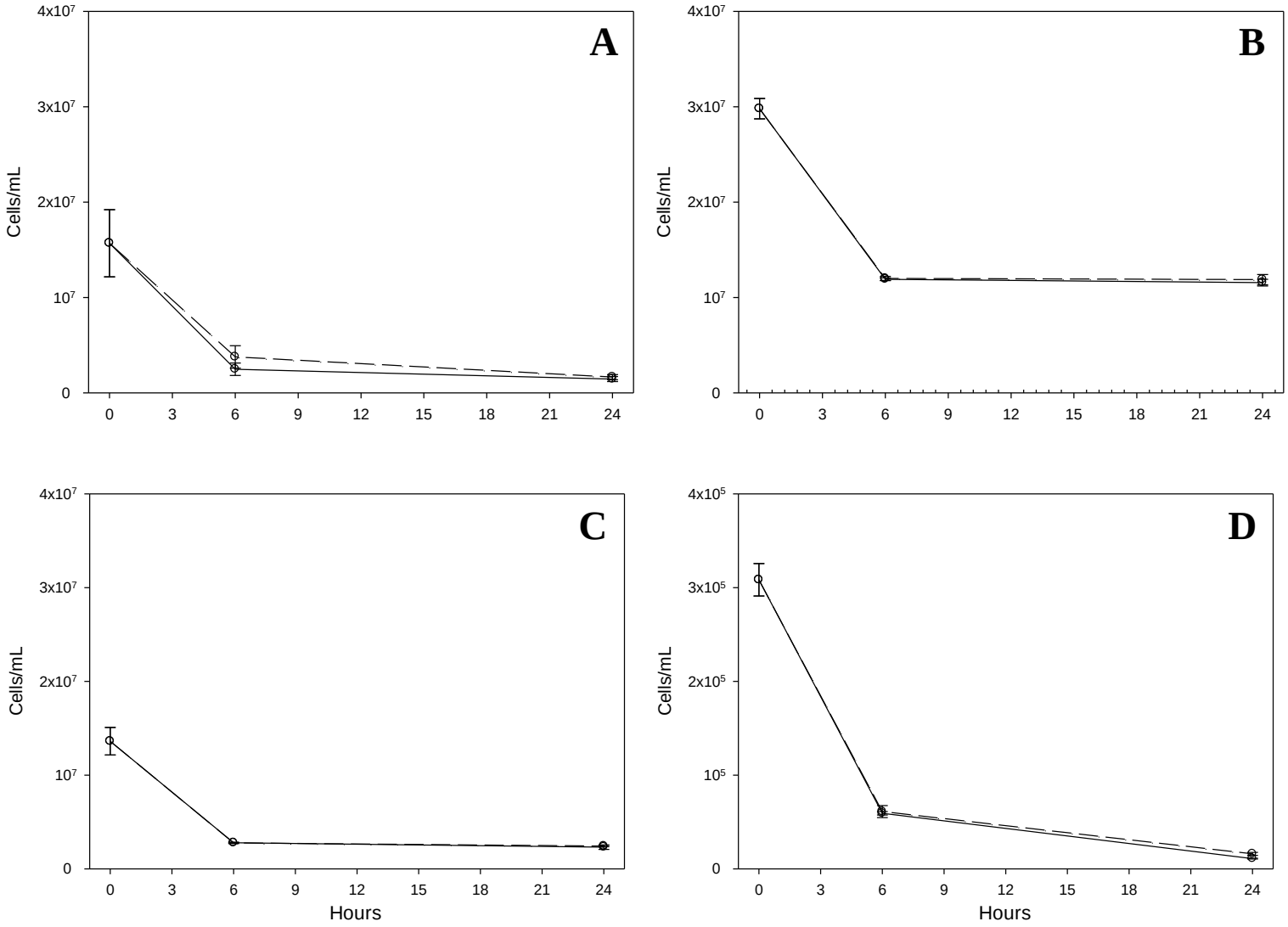
A
B
C
D
Cells/mL
Hours
4x10^7
3x10^7
2x10^7
10^7
0
4x10^5
3x10^5
2x10^5
10^5
0 3 6 9 12 15 18 21 24

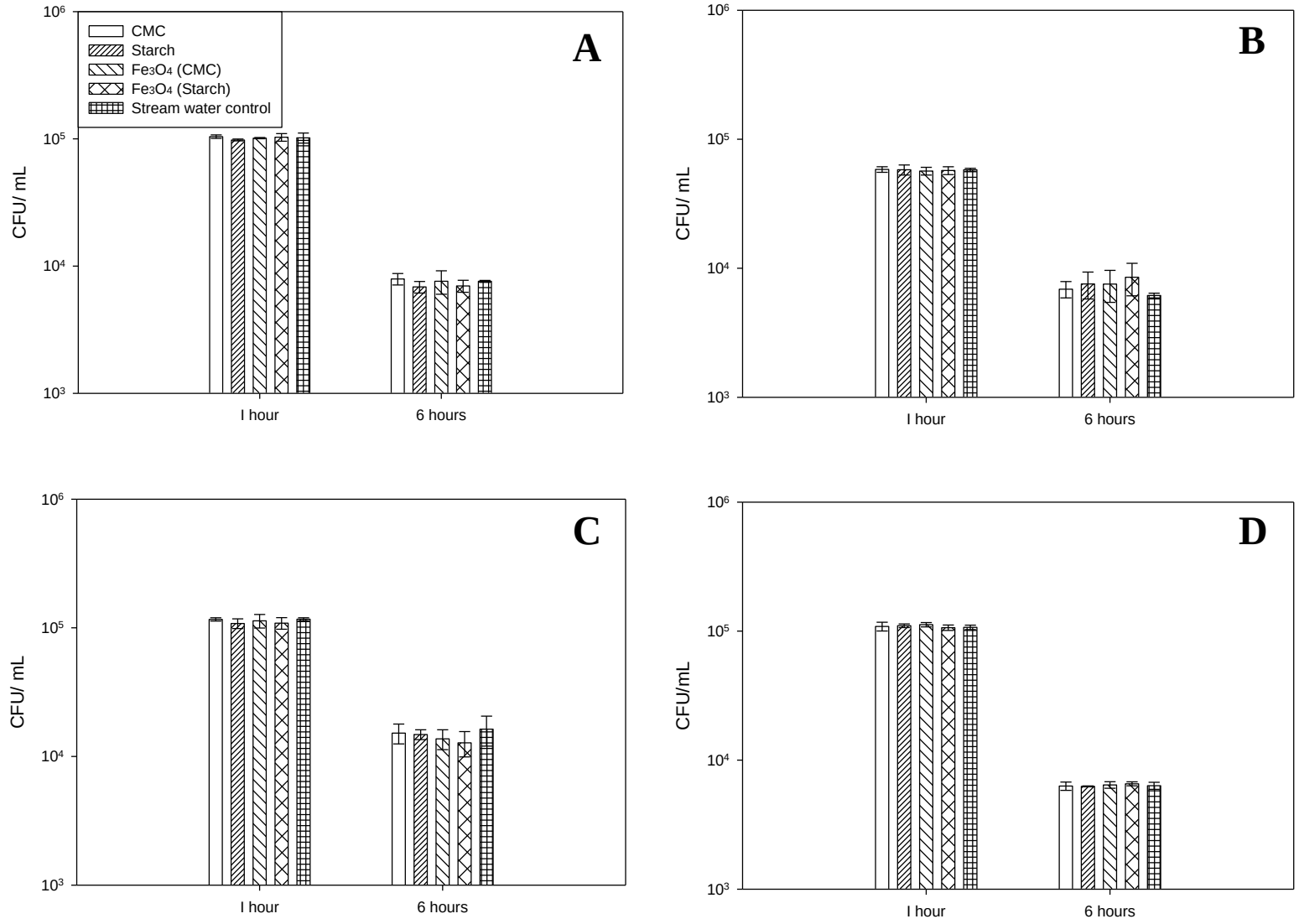
A
B
C
D
CMC
Starch
Fe3O4 (CMC)
Fe3O4 (Starch)
Stream water control
CFU/ mL
CFU/mL
10^6
10^5
10^4
10^3
I hour
6 hours

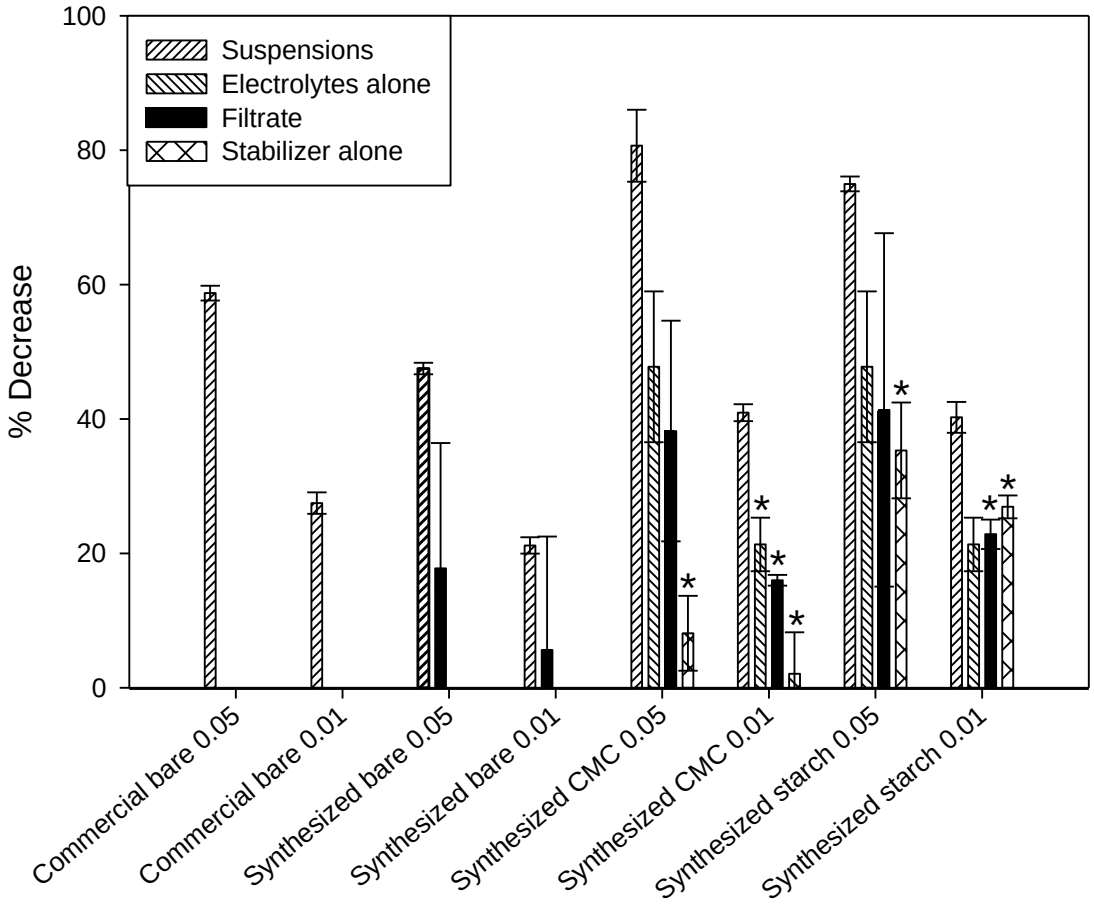
Suspensions
Electrolytes alone
Filtrate
Stabilizer alone
% Decrease
100
80
60
40
20
0
*
Commercial bare 0.05
Commercial bare 0.01
Synthesized bare 0.05
Synthesized bare 0.01
Synthesized CMC 0.05
Synthesized CMC 0.01
Synthesized starch 0.05
Synthesized starch 0.01

IV. Summary

There was no significant toxicity of magnetite nanoparticles observed across the tests performed on four species of bacteria. Cell growth was not decreased in culture media with the addition of commercial or synthesized nanoparticles, indicated by measurement of total protein and cell counts. Cell numbers in media were not decreased by the presence of the stabilizer alone, filtrate, or whole magnetite suspension and cells in stream water did not show any reduction with the addition of magnetite stabilized with either CMC or starch. However, zeta potential suggests that cells in natural water can interact with nanoparticles differently than under laboratory conditions.

SEM images supported the prediction that nanoparticles coated with CMC will interact less with cell surfaces than non-stabilized nanoparticles. It was shown that magnetite nanoparticles form large precipitates with cells and bacteria can become completely coated with magnetite nanoparticles. However, TEM showed that nanoparticles did not enter cells, suggesting internalization is not a concern for magnetite nanoparticles.

While no lethal toxicity was observed, cellular uptake of [^{3}H]thymidine was diminished dose-dependently with the addition of all four types of nanoparticles tested. CMC- or starch - stabilized nanoparticles caused the most decrease in uptake perhaps due to their small size, high reactivity, or increased dispersion. The effect observed could be attributed to background electrolytes and, to some extent, nanoparticles.

However given the discrepancy between cell counts and thymidine uptake results, more research is needed to reconcile the difference between measurements. More research is also needed to investigate the stimulatory effects of nanoparticles to cells. The effect of size could not be easily distinguished from stabilizer effect since the former depends on the latter. More study into the effect of stabilizer with constant particle size would be beneficial to understand what properties really govern bacterial toxicity. Toxicity studies should also be carried out using true environmental samples to understand the implication of nanomagnetite in the environment. Understanding the interaction of magnetite with biota outside of the laboratory setting will give more insight to the potential implications of this seemingly non-toxic nanoparticle.

Appendix 1

Table A.1. Characteristics of pond water samples collected over the study period.

	pH	EC S/m	NO3-N mg/L	NH4-N mg/L	PO4-P mg/L	Al mg/L	Ca mg/L	Cu mg/L	Fe mg/L	K mg/L	Mg mg/L	Mn mg/L	Na mg/L	P mg/L	Zn mg/L	TOC mg/L
Stream	7.5	0.002	0.581	0.169	0	0.368	19.35	0.005	0	4.915	11.23	0	2.989	0.039	0	21.12
Pond	6.3	0.1	0.717	0.095	0.033	0	10.916	0	0	1.776	4.769	0	4.113	0	0	20.9

Appendix 2

Table A.2. CMC degraders (fungi and bacteria) present after soil incubation.

Sample	Fungi (cells/g soil)	Bacteria (cells/g soil)	Total (cells/g soil)
CP Sterile 0.6 WHC	1.00E+06	3.00E+06	4.00E+06
CP sterile WHC	0	2.10E+07	2.10E+07
CP CMC 0.6 WHC	1.00E+06	2.00E+06	3.00E+06
CP CMC WHC	1.00E+06	2.00E+06	3.00E+06
GY sterile 0.6 WHC	5.00E+06	5.70E+07	6.20E+07
GY sterile WHC	1.60E+07	4.00E+06	2.00E+07
GY CMC 0.6 WHC	0	1.00E+06	1.00E+06
GY CMC WHC	1.00E+06	2.00E+06	3.00E+06

Appendix 3

Fig. A.1. Mineralization of CMC in two soils (A) Compass, and (B) Grady.

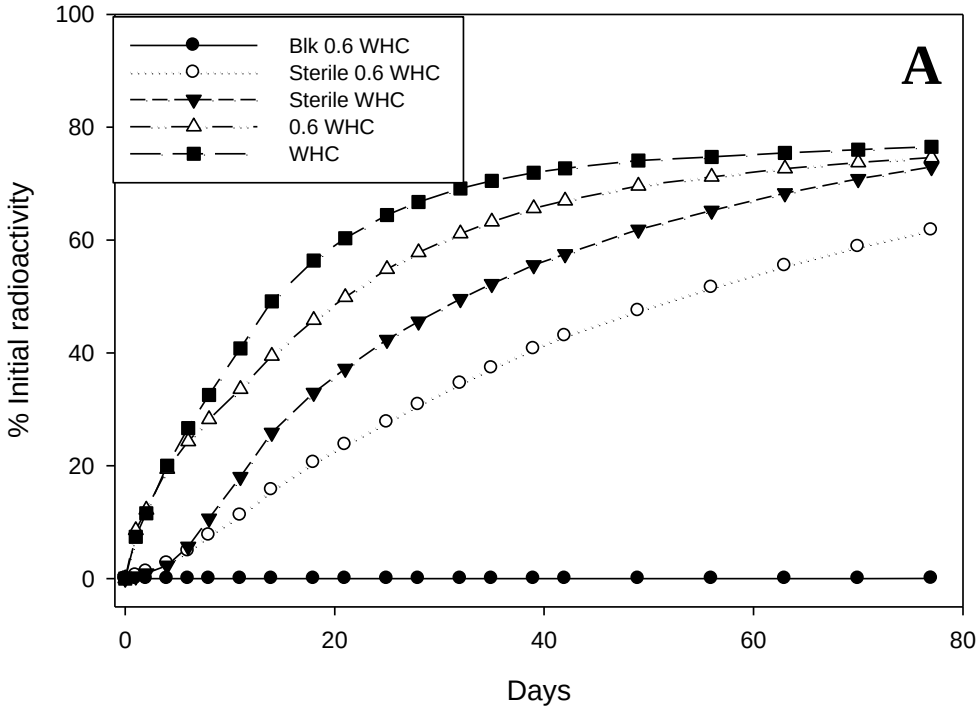

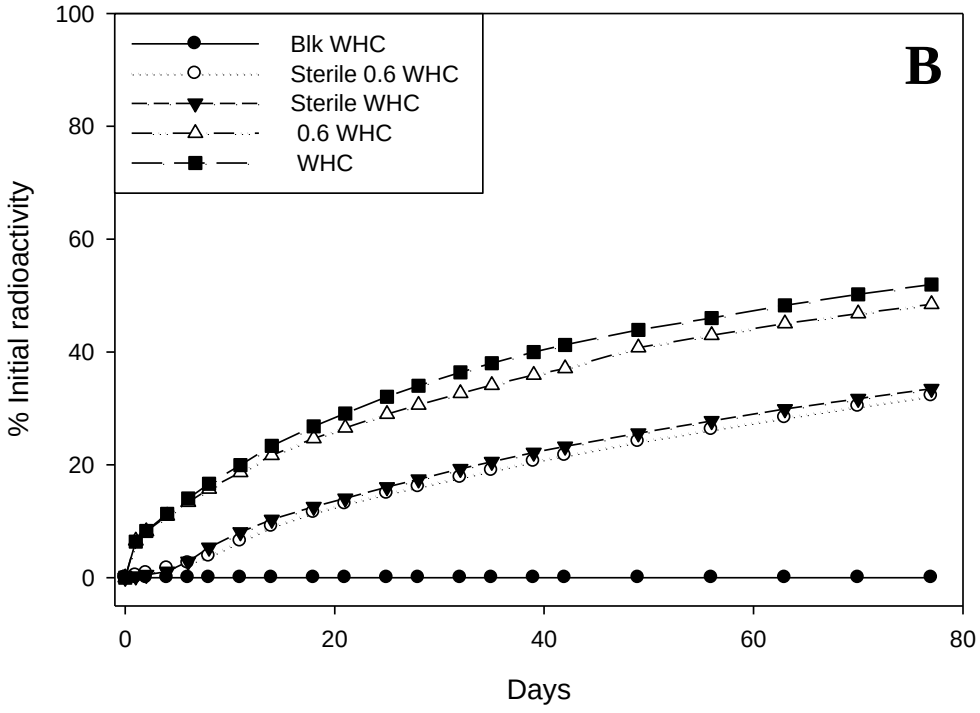

Appendix 4

Fig. A.2. Recovery of ^{14}C for two soils at different moisture contents.

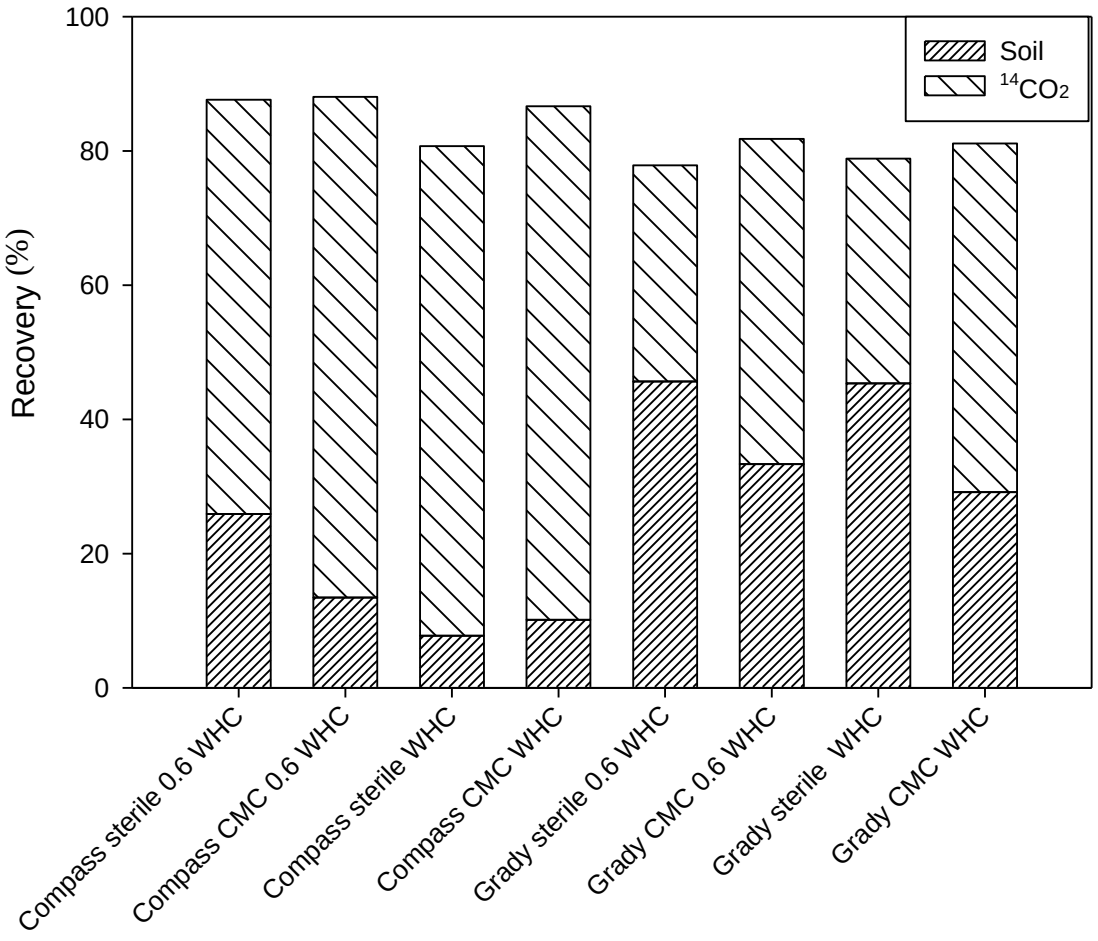

Appendix 5

Fig. A.3. Effect of bare washed magnetite on *E. coli* in stream water at 0.3, 0.6, and 1.0 g Fe/L.